

https://dspace.org/

Back analysis of previously stooped Panels to improve the safety and productivity of future stooping operations at new Denmark colliery

Gonsalves, Ricardo

2024

University of the Witwatersrand, Johannesburg

https://hdl.handle.net/10539/45609

Gonsalves, Ricardo . (2024). Back analysis of previously stooped Panels to improve the safety and productivity of future stooping operations at new Denmark colliery [Master`s dissertation, University of the Witwatersrand, Johannesburg]. WIReDSpace. https://hdl.handle.net/10539/45609

Downloaded from a DSpace repository. https://dspace.org/

School of Mining Engineering



UNIVERSITY OF THE
WITWATERSRAND,
JOHANNESBURG

BACK ANALYSIS OF PREVIOUSLY STOOPED PANELS TO IMPROVE SAFETY AND PRODUCTIVITY OF FUTURE STOOPING OPERATIONS AT NEW DENMARK COLLIERY

Ricardo Gonsalves

I declare that this research report is my own unaided work. It is being submitted for the degree of Master of Science at the University of the Witwatersrand, Johannesburg. It has not been submitted before for any degree or examination to any other university.

Johannesburg, 2024

DECLARATION

I have familiarised myself with the University of the Witwatersrand Student Academic Misconduct Policy (SAMP). I hereby declare that the work I am submitting for assessment is my original work. I affirm that I have not plagiarised, misrepresented, or colluded with any other person or source. I have properly acknowledged, cited, and referenced all the sources that I have used in my work. I also declare that I have used artificial intelligence (AI) tools only as a means of guidance. The ideas and arguments presented in my work are my original thoughts and interpretations. I acknowledge that any academic misconduct, such as plagiarism or collusion will result in serious consequences. These consequences may include a reduced grade, a fail mark, or disciplinary action according to the SAMP. The School of Mining Engineering has my consent to investigate any potential academic misconduct in my work. This investigation may include the use of similarity and AI detection software to check the originality of my work. I undertake to abide by the decision of any such investigation.



15th day of October 2024

“I can do all things through Christ who strengthens me.”

Philippians 4:13 (NKJV)

ABSTRACT

New Denmark Colliery (NDC) is a Seriti-owned underground coal mine in the Mpumalanga Province. It started stooping operations towards the end of 2018 and has since stooped 50 panels safely across all three of its shafts. NDC selected the NEVID method, which is known for its safety and success in neighbouring mines. Initially stooping panels in the 1100 block, NDC encountered challenges due to narrow panel spans, leading to limited goafing and heightened abutment stresses on surrounding pillars and infrastructure. This necessitated additional support for strategic pillars to ensure long-term stability. To address these challenges, comprehensive research was conducted, which included back-analysis of stooped panels and numerical modelling. Findings revealed that goafing was influenced more by horizontal stress concentrators, such as geological structures than panel spans. Goafing at NDC has primarily been defined by low-angle shear failures, which only extend a couple of metres into the immediate sandstone roof. This is known as partial goafing, which typically results in high abutment stresses. Since complete goafing is unlikely due to the depth below surface and the competent roof material, the high abutment stresses needed to be managed by increasing the width of the barrier pillars between panels and leaving a sufficient number of stopper pillars at the end of a stooped panel. Numerical modelling was used to validate NDC's current design strategy of stooping panels and to determine the width of new barrier pillars. The derived strategy includes an increase in barrier pillar width and stand-off distances, to ensure the long-term stability of main developments.

The current stooping strategy which was informed by comprehensive research and modelling, has proven effective in both safety and stability.

DEDICATION

This research project is dedicated to the memory of Lelanie Prinsloo who sadly passed away on the 10th of August 2021. As Seriti's Principal Rock Engineer at the time, Lelanie played a significant role in the successful implementation of the NEVID stooping method at New Denmark Colliery. Lelanie's invaluable contributions continue to resonate within the industry.

ACKNOWLEDGMENTS

I would like to express my deepest gratitude to several individuals and organisations whose support and encouragement have been instrumental in the completion of this research project.

First and foremost, I am profoundly grateful to my loving and supportive wife, whose unwavering encouragement, patience, and understanding throughout this journey have been my greatest source of strength. Your belief in me has been the cornerstone of my perseverance.

I extend my heartfelt appreciation to Professor Watson, my dedicated supervisor, for his invaluable guidance, unwavering support, and constructive feedback. His expertise, patience, and encouragement have been indispensable in shaping the direction of this research and in navigating its challenges.

I am also indebted to New Denmark Colliery for their generous financial support, which enabled the realisation of this project. Their investment in my work underscores their commitment to the advancement of knowledge and innovation in our field.

Lastly, I wish to thank all those who, directly or indirectly, contributed to this endeavour. Your support, whether moral, intellectual, or material, has been truly appreciated and has made this accomplishment possible.

Thank you all for your unwavering support and belief in me.

TABLE OF CONTENTS

DECLARATION i

ABSTRACT iii

DEDICATION v

ACKNOWLEDGMENTS vi

LIST OF FIGURES xi

LIST OF TABLES xviii

LIST OF SYMBOLS xix

1 INTRODUCTION 1

1.1 Underground Coal Mining Methods 1

1.1.1 Bord-and-pillar mining 1

1.1.2 Pillar extraction 3

1.2 Research Background 7

1.3 Justification for Research 12

1.4 Research Methods 13

1.5 Assumptions 14

2 LITERATURE REVIEW 15

2.1 Risk of Pillar Extraction 15

2.2 Factors Influencing Pillar Extraction 17

2.2.1 Pillar extraction of old workings and new panels 17

2.2.2 Geotechnical design parameters for pillar extraction 18

2.3 Advantages and Disadvantages of Goafing 43

2.3.1 Air-blasts 43
2.3.2 High gas concentrations 44
2.3.3 Groundwater 45
2.3.4 Work face stability 46
2.3.5 Surface subsidence 47
2.4 Lessons Learned from Longwall Mining at NDC 50
2.5 Pillar Extraction Methods 52
2.6 NEVID method 53
2.6.1 Stooping direction and cutting sequence: 54
2.6.2 Fenders and snooks 58
2.6.3 Stopper pillars 59
2.6.4 Pillar extraction controls 61
2.7 Numerical Modelling 65
2.7.1 Introduction 65
2.7.2 Different types of numerical models 65
2.7.3 LAMODEL 67
3 GEOLOGY OF NEW DENMARK COLLIERY 70
3.1 Stratigraphy and Geological Structures 70
3.1.1 Stratigraphy 70
3.1.2 Geological structures 73
4 STOOPING HISTORY AT NDC 78
4.1 Implementation of Stooping at NDC 78
4.1.1 1100 Block 78
4.1.2 Shosholoza stooping panels 81

4.2 NDC’s Current Stooping Strategy 85
4.2.1 Panel layout and pillar design 86
4.2.2 In-pillar cutting sequence and stooping direction 87
4.2.3 Fenders and snooks 91
4.2.4 Compartmentalising stooping panels 93
4.2.5 Stopper pillars 95
4.2.6 General stooping controls 96
5 METHODOLOGY 98
5.1 Critical Span Calculations and Underground Observations 98
5.2 Numerical Modelling 99
6 RESULTS 103
6.1 Critical Span Calculations 103
6.1.1 1100 Panels critical span calculations 103
6.1.2 Critical span calculations for planned stooping sections 105
6.2 History of Goafing in NDC Stooping Sections 106
6.2.1 Analysis of the stooping database 106
6.2.2 Discussion of individual panels where goafing occurred 110
6.3 Analysis of the Numerical Modelling 122
6.3.1 1100 Block 122
6.3.2 Shosholoza Block 138
7 DISCUSSION OF RESULTS 152
7.1 Critical Span Calculations 152
7.1.1 1100 Panels critical span calculations 152

7.1.2 Critical span calculations for planned stooping panels 153
7.1.3 Challenges with increasing the panel span 155
7.2 Goafing in NDC Stooping Sections 155
7.3 Analysis of the Numerical Modelling 161
7.3.1 1100 Block 161
7.3.2 Shosholoza Block 163
7.4 Additional Risk 166
8 CONCLUSION 168
9 RECOMMENDATIONS 172
REFERENCE LIST 174
APPENDIX A……. 182
APPENDIX B….. 183
APPENDIX C…. 184
APPENDIX D…. 185
APPENDIX E…….. 186

LIST OF FIGURES

Figure 1-1: Diagram of a bord-and-pillar panel developed by a CM..... 2

Figure 1-2: Failure of the roof in a New Denmark Colliery pillar extraction section, known as goafing. 5

Figure 1-3: Excessive scaling and slabbing of the pillar corners and ribsides (sidewalls) due to increased vertical stress. 5

Figure 1-4: Diagram of a pillar extraction panel showing the fenders and snooks formed by the NEVID-method cutting sequence. The bleeder road is formed along the periphery of the panel and is protected by taking only one cut from the adjacent in-panel pillars. 6

Figure 1-5: Locality map of New Denmark Colliery. 8

Figure 1-6: Simplified bord-and-pillar mining layout indicating the numbering of the roadways and splits. 9

Figure 1-7: NDC Mine plan indicating 1100 block where stooping was first trialled. The green represents the bords (roadways and splits) and the white areas are the barriers and in-panel pillars. 11

Figure 1-8: Excessive pillar scaling along Panel 1120 tractor road. 12

Figure 2-1: Typical self-supporting spans for various rock strata found in South African coalfields 26

Figure 2-2: Diagram indicating the relationship between mining depth and critical span for competent and weak strata 27

Figure 2-3: Comparison of Galvin's (1983) and Van der Merwe's (1995) critical span formulae for different thicknesses and depths of dolerite sills. 31

Figure 2-4: Simplified diagram illustrating the concepts of sub-critical, critical, and super-critical spans. 33

Figure 2-5: Simplified diagram of a clamped beam indicating the positions of maximum tensile and compressive stresses. 35

Figure 2-6: Simplified diagram of a cantilever beam indicating the positions of maximum tensile and compressive stresses, as well as the maximum defection and sag. 37

Figure 2-7: Model of a cross-section showing the larger extent of the tensile zone above a high extraction panel at shallower depth..... 39

Figure 2-8: Partial and full goafing of the overburden; (a) partial goafing of the overburden with the weight of the intact overburden transferred to the abutments; (b) complete goafing with the abutment stress being relieved 40

Figure 2-9: Change in the stress on the front-line pillars with an advancing face 42

Figure 2-10: Representative subsidence half-profile for South African cases. The diagram shows the relationship between maximum subsidence, tilt and strain 48

Figure 2-11: NEVID method cutting sequence from left to right..... 55

Figure 2-12: NEVID method cutting sequence with marked direction lines 56

Figure 2-13: Extraction sequence of subsequent pillars 58

Figure 2-14: Stopper pillars along the periphery and at the end of the panel 60

Figure 2-15: Positioning of breaker lines in each active intersection in a pillar extraction panel. Roof bolts are installed as breaker lines between the pillar corners 62

Figure 2-16: Timber poles placed in strategic positions as policeman sticks 63

Figure 2-17: Placement of policeman sticks before and after certain cuts are taken 64

Figure 3-1: General stratigraphic column for NDC. 71

Figure 3-2: NDC Geological Structures Plan. 75

Figure 4-1: NDC mine plan indicating the 1100 block where stooping was first trialled in Panel 1111. 79

Figure 4-2: NDC mine plan indicating Panel 1105 where the fourth fender-reducing cut was first introduced. 80

Figure 4-3: Pillars along Panel 1120 travelling road wrapped with mesh to prevent further scaling. 81

Figure 4-4: Shosholoza panels 134, 135 and 136 relative to main development, Panel 1134. 82

Figure 4-5: Panel 135 with pillar centres of 24.0 m (l) x 19.0 m (w). 83

Figure 4-6: Panel 134 with modified panel-entry configuration. 85

Figure 4-7: Panel 134 planned for stooping with pillar centres of 26.0 m (l) x 24.0 m (w). 87

Figure 4-8: NDC plan indicating the left-to-right stooping sequence of panels 040, 042 and 044..... 89

Figure 4-9: NDC stooping plan showing Panel 133 and one of its side-panels, Panel 133B..... 91

Figure 4-10: Safety factor calculations for pillar and fender stability of a standard pillar with centres of 26.0 m (l) x 24.0 m (w). 92

Figure 4-11: Stooping Panel 1135 separated from the main development, Panel 1134, with a barrier pillar of at least 50 m wide. 94

Figure 4-12: Stopper pillars left in panels 134 and 135 to protect surface structures, such as surface dams and pylons..... 96

Figure 5-1: Geology borehole logs for 1100 block and Shosholoza panels. 101

Figure 6-1: NDC mine plan indicating the position of Panel 1126 and the cross-sections along which the surface subsidence was measured. 110

Figure 6-2: Subsidence measurements above Panel 1126. 112

Figure 6-3: Eyethu goaf incident; (a) CM partially buried with only its conveyor boom visible from underneath the goaf material; (b)

thick layer of sandstone lying on top of the CM indicating that the goaf only extended about 1.5 m into the immediate roof; (c) CM successful retrieved from the goaf; (d) goaf arrested by the breaker lines with the intact policeman stick indicating stable ground on the safe side. 115

Figure 6-4: Eyethu Panel 179b with a nearby dyke to the south of it. 116

Figure 6-5: Panel 888 with nearby dyke and old longwall panels. 118

Figure 6-6: Panels 882c and 882d with nearby dyke and previously stooped panels..... 119

Figure 6-7: Panels 1001B and 1001C with multiple joints striking across them..... 120

Figure 6-8: Panel 177/5 with limited stooping ground and a fault at the end of the panel. 122

Figure 6-9: 1120 Modelling area; (a) Plan view of Panel 1120 indicating the various locations of the models; (b) northern portion virgin overburden stress model; (c) southern portion virgin overburden stress model..... 124

Figure 6-10: Stress contour plots for Panel 1120 before stooping – north to south..... 125

Figure 6-11: Stress contour plots for Panel 1120 after stooping of adjacent panels – north to south. 126

Figure 6-12: Panel 1120 pillar stress along Section 524 – northern portion 127

Figure 6-13: Panel 1120 pillar stress along Section 524 – southern portion 129

Figure 6-14: Stress contour plot for Panel 1120 before and after stooping – east to west..... 131

Figure 6-15: Panel 1120 pillar stress across Section 527. 132

Figure 6-16: Stress contour plots for Panel 1120 simulating various barrier pillar widths..... 133

Figure 6-17: Panel 1120 vertical stress conditions across barrier pillars of various widths..... 135

Figure 6-18: Shosholoza modelling area with its various cross-section locations..... 139

Figure 6-19: Stress contour plots for Panel 1134 / 135 before and after stooping..... 140

Figure 6-20: Panel 1134 / 135 pillar stress along Section 328..... 141

Figure 6-21: Stress contour plots for Panel 1134 / 134 before and after stooping..... 144

Figure 6-22: Panel 1134 / 134 pillar stress along Section 809..... 145

Figure 6-23: Panel 1134 abutment pillar – comparison of vertical stress 148

Figure 6-24: Pillar stress along Section 439 for panel-entry pillars of panels 135 and 134 – west to east..... 150

Figure 6-25: Pillar stress along Section 254 for Panel 1134 pillars – west to east. 151

Figure 7-1: The actual panel span of Panel 134 is reduced by stopper pillars 154

Figure 7-2: Goafing in areas with weak overburden compared to areas with competent overburden 160

Figure 7-3: Ideal panel-entry configuration for a secondary panel being stooped towards a main development. 165

Figure 7-4: Ideal panel-entry pillar configuration for a tertiary panel being stooped towards a secondary panel..... 166

LIST OF TABLES

Table 2-1: Typical strength and bulking properties of rock formations in South African coalfields. 24

Table 5-1: Summary of NDC mechanical rock properties. 101

Table 5-2: Modelling properties for the overburden rock and in-situ coal. 102

Table 6-1: Critical span calculations for 1100 panels. 105

Table 6-2: Critical span calculations for planned stooping panels at Central Shaft. 106

Table 6-3: NDC stooping panels where goafing was recorded and their critical span calculations 107

Table 6-4: NDC stooping panels where goafing was recorded and their possible contributing factors. 108

Table 6-5: Description of goafing in NDC stooping panels. 109

LIST OF SYMBOLS

APS	Average Pillar Stress (MPa)
C	Pillar Centre (m)
CH_4	Methane
CM	Continuous miner
CO	Carbon monoxide
D	Depth of dolerite base (m)
FOG	Fall of ground
LOM	Life of Mine
g	Gravity (9.81 m/s^2)
h	Mining height (m)
H	Mining depth (depth to floor of workings) (m)
k	Pillar bulk strength
km	Kilometre
L	Unsupported span (m)
L_c	Critical span (m)
m	Metre
MPa	Megapascal
NDC	New Denmark Colliery
w	Pillar width (m)
W	Panel width (m)
w/h	Width-to-height
SF	Safety Factor
t	Thickness of rock strata (m)
TAT	Tributary Area Theory
UCS	Uniaxial compressive strength (MPa)
ρ	Density of rock strata (kg/m^3)
σ_t	Tensile strength of rock strata (Pa/MPa)
Ø	Goaf angle measured from the vertical (°)

1 INTRODUCTION

1.1 Underground Coal Mining Methods

1.1.1 Bord-and-pillar mining

The bord-and-pillar mining method has been extensively used in underground coal mines throughout South Africa for over a century (Moolman & Canbulat, 2003). It involves leaving coal as square, rectangular or even diamond-shaped pillars to support the weight of the overburden (Van der Merwe & Madden, 2010). The bords are the openings between them, which can be subdivided into roadways and splits (Nayak & Dalai, 2010; Kgengwe, 2021a). The roadways are developed as narrow headings parallel to each other in the direction of mining. They are connected by cross headings, which are referred to as splits (Nayak & Dalai, 2010; Kgengwe, 2021a). Figure 1-1 shows a typical layout of a bord-and-pillar panel developed by a continuous miner (CM). The panel span, which is measured from one abutment to the other, is dependent on the number of roadways, bord width and size of the pillars (Nayak & Dalai, 2010; Kgengwe, 2021b).

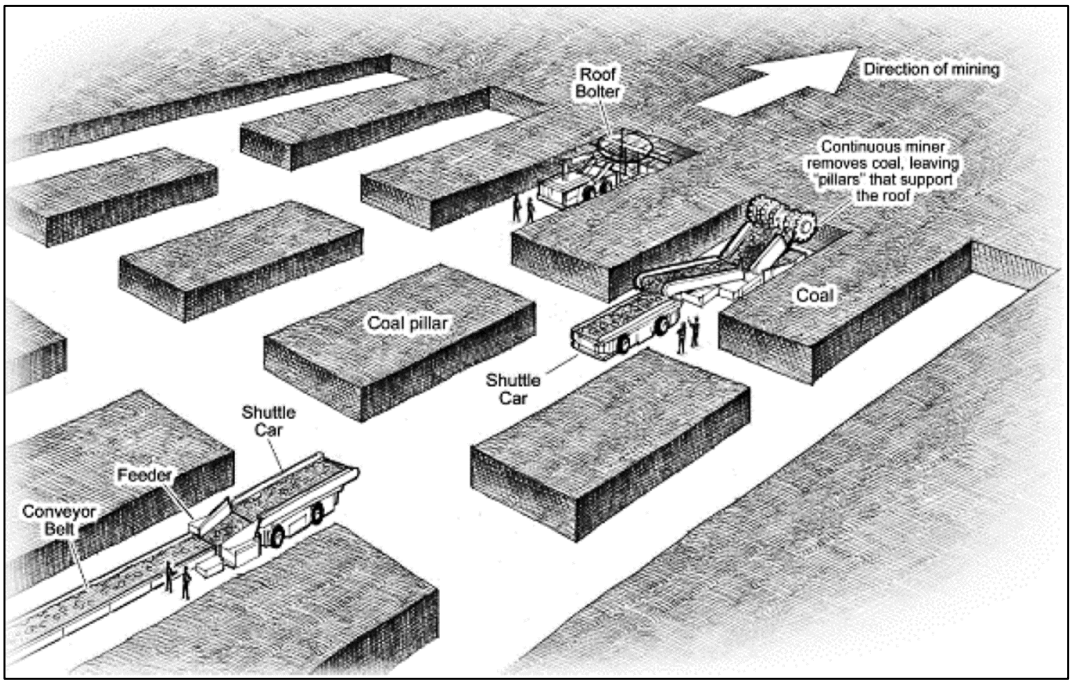


Figure 1-1: Diagram of a bord-and-pillar panel developed by a CM (Arch Coal, n.d.).

Stable pillar sizes are determined by various pillar strength formulae, general safety guidelines and legal requirements (Van der Merwe, 2006; Van der Merwe & Madden, 2010). These require pillar sizes to increase with increasing depth below the surface and mining height. The result is an ever-decreasing percentage of extraction of the coal reserve with increasing depth of mining (Van der Merwe & Madden, 2010). The percentage extraction using this method for depths ranging from 80 m to 200 m is normally in the range of 60% to 40%, respectively (Van der Merwe & Madden, 2010). Moolman & Canbulat (2003) already indicated in the early 2000s that in South Africa alone approximately 1.1 billion tonnes of potentially mineable coal were left underground and locked up in coal pillars during the period 1970 to 1997. They further estimated that this figure would

increase by about 110 million tons of coal per annum due to bord-and-pillar mining still being widely practised to this day.

1.1.2 Pillar extraction

Several studies have been done to identify suitable pillar extraction methods to safely and economically mine these coal pillars in an attempt to not only improve productivity, but also extend the life of a mine, or in some cases, even the life of a coalfield. Many of these methods, such as chequerboard, pillar splitting and the NEVID method, have over the years been trialled at mines across South Africa (Moolman & Canbulat, 2003; Van der Merwe & Madden, 2010). These trials have been met with various levels of success. Pillar extraction was, for example, predominantly confined to the comparatively thin seams and greater depths of the KwaZulu-Natal coal reserves (Fauconnier & Kersten, 1982). In the Transvaal Province, known today as Gauteng and Mpumalanga Provinces, increased extraction was mainly done in the form of top or bottom coaling in the thicker seams. Pillar robbing was also occasionally done, especially when extra production was required. Both methods resulted in roof collapses. These incidences together with the seeming abundance of easily mineable coal did not motivate mines to seriously pursue pillar extraction (Fauconnier & Kersten, 1982). Usuthu Colliery nonetheless achieved success when they introduced mechanised pillar extraction in 1969. However, few mines followed their example leaving the bord-and-pillar method as the most widely used method in these two provinces. Internationally, several pillar extraction

methods have also been developed and practiced, such as the Wongawilli (Lind, 2002b) and Old Ben (Lind, 2002b) methods in Australia, the Christmas tree method in the United States (Mark et al., 2003) and the Fish & Tail method in India (Pankaj et al., 2018).

Pillar or secondary extraction, also commonly referred to as stooping, is simply defined as a partial-to-high extraction mining method where pillars developed using the bord-and-pillar method, are partially or fully extracted on the retreat (Van der Merwe & Madden, 2010; Beukes 1989). During the development phase, the span is limited to ensure stability, for example, six to eight meters. However, during the extraction phase, the span is increased to more than a hundred meters as the pillars are extracted. This results in stress changes which are in the orders of magnitude larger than that created by bord-and-pillar development (Van der Merwe & Madden, 2010). An increased overhang and subsequent overburden failure (goafing) results in stress changes which affect the roof (Figure 1-2) and pillars (Figure 1-3).



Figure 1-2: Failure of the roof in a New Denmark Colliery pillar extraction section, known as goafing.



Figure 1-3: Excessive scaling and slabbing of the pillar corners and ribsides (sidewalls) due to increased vertical stress.

The pillars need to maintain sufficient stability of the overlying roof strata during extraction to protect personnel and machinery against regional and localised falls of ground. However, as the pillars are reduced in size during pillar extraction, they will start to lose their load-bearing capacity (Mark et al., 2003). The geotechnical design of the extraction panel and pillar

extraction method must thus cater for this. During the extraction of an individual pillar, the load of the overburden is transferred to the surrounding intact pillars. The remaining fenders and snooks as shown in Figure 1-4 provide temporary (time-dependent) support for the immediate strata (Wagner, 1981; Lind, 2002a; Van der Merwe, 1991). Figure 1-4 also shows the bleeder road, which is formed along the periphery of the stooping panel. Its main function is to ensure ventilation of the stooping panel, specifically that of the goafed area. Only one cut is taken from the in-panel pillars along the bleeder road, thus leaving most of the pillar intact to protect it (Moolman & Canbulat, 2003; Sasol Mining, n.d.).

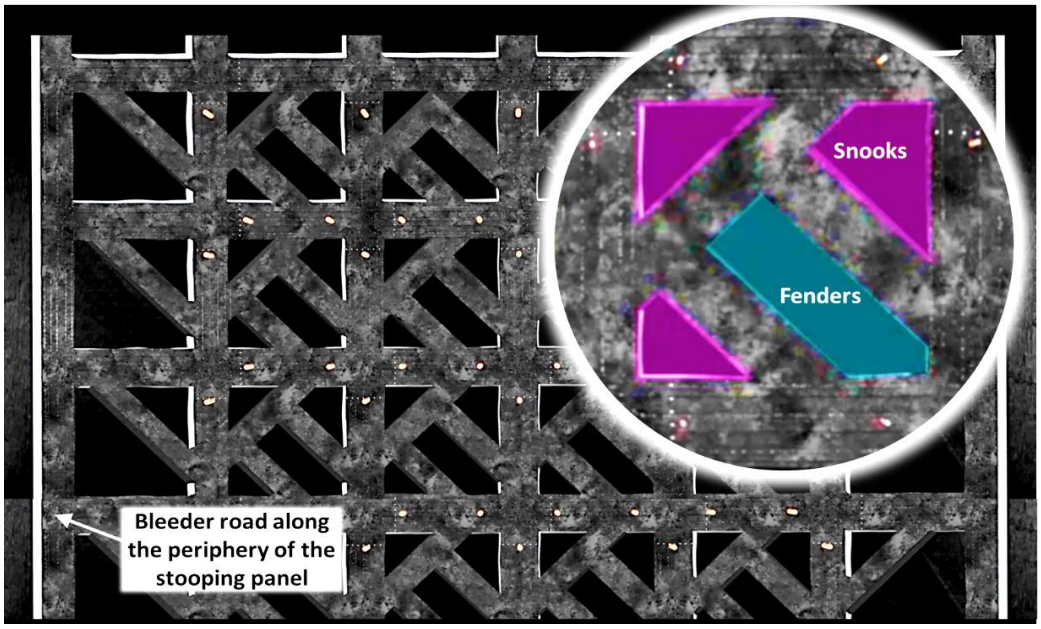


Figure 1-4: Diagram of a pillar extraction panel showing the fenders and snooks formed by the NEVID-method cutting sequence. The bleeder road is formed along the periphery of the panel and is protected by taking only one cut from the adjacent in-panel pillars (Sasol Mining, n.d.).

Once the pillar has been extracted as per the pre-approved design, and the personnel and machinery have retreated to a safe, stable area, the roof strata are encouraged to goaf. Should goafing not occur in the mined-out area, the success of the mining method is jeopardised (Wagner, 1981). It is therefore important that pillar extraction is properly designed, specifically for local geomechanical and geotechnical conditions.

1.2 Research Background

The study is based on New Denmark Colliery (NDC), which is an underground coal mine owned by Seriti Resources. Figure 1-5 shows that the mine is situated in the Highveld Coalfield, approximately 30 km north of Standerton in the Mpumalanga Province. It is contracted to supply Eskom's Tutuka Power Station with unbeneficiated thermal coal. This is achieved by mining the No. 4 coal seam at a depth ranging between 160 m and 200 m below the surface. NDC was previously well known for its longwall mining with the last longwall being decommissioned in April 2021. Its current production fleet consists of twelve CM sections using both the bord-and-pillar and stooping mining methods to extract coal at its three respective shafts.

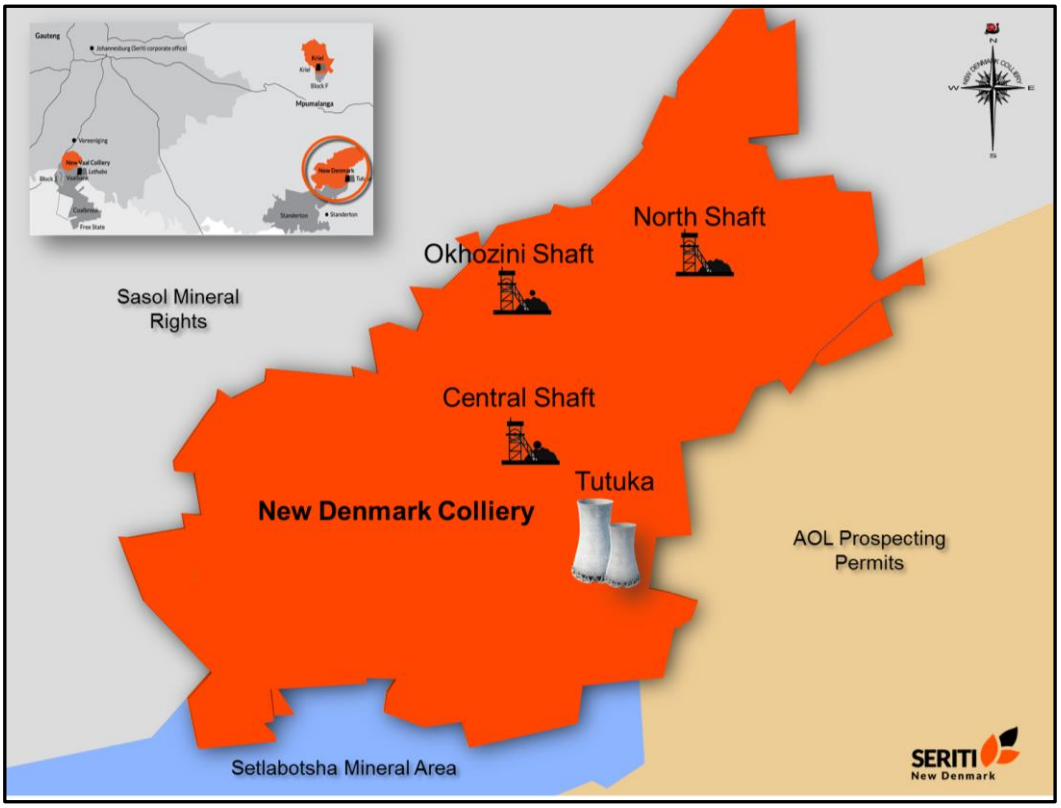


Figure 1-5: Locality map of New Denmark Colliery (Salima, 2021b).

Figure 1-6 shows that bord-and-pillar developments at NDC mainly consist of nine roadways with pillar centres of 26.0 m (length) x 24.0 m (width) (Kgengwe, 2021b). The centre roadway is called the belt road (BR), due to the section conveyor belt being positioned in it. Numbering of the roadways increases in both directions from the BR to the abutments (Kgengwe, 2021b). For instance, the first roadway to the right of BR is referred to as Road 1 Right (R1), followed by Road 2 Right (R2), Road 3 Right (R3) and Road 4 Right (R4). Similarly, on the left side, they are named Road 1 Left (L1), Road 2 Left (L2), Road 3 Left (L3) and Road 4 Left (L4). The traveling road (TR) may be positioned in either R1 or L1. Numbering of the splits

starts with Split 0 at the beginning of the panel and increases as the panel advances (Kgengwe, 2021b).

Nine roadways, or a panel span of 200 m, is the maximum span that will be mined at NDC (Malebana, 2023; Mandivheyi, 2023). Anything wider becomes impractical and inefficient as it introduces several production challenges, such as a decrease in production rate, increased away-time of the shuttle cars from the CM, and the increased risk of cable damage (Malebana, 2023; Mandivheyi, 2023).

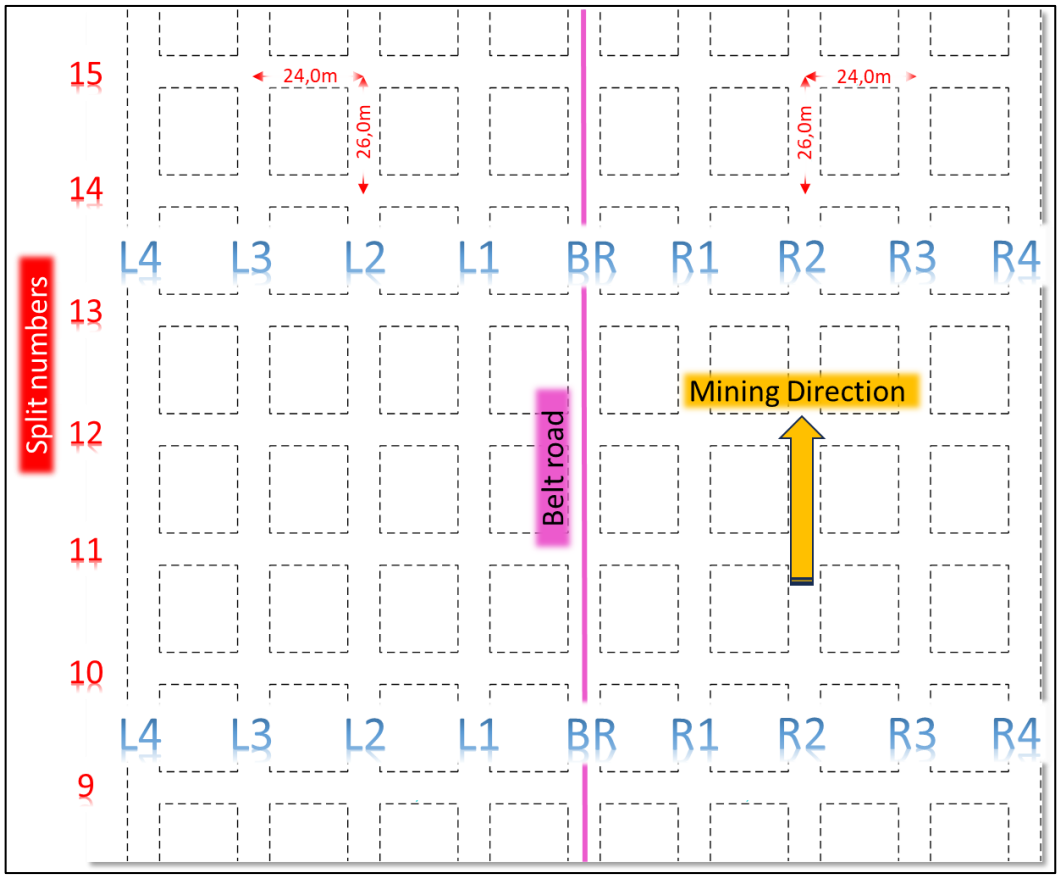


Figure 1-6: Simplified bord-and-pillar mining layout indicating the numbering of the roadways and splits.

The overburden at NDC consists of a competent sandstone beam that forms the immediate roof of the No. 4 coal seam. It is furthermore overlain by multiple competent sandstone units, of which some are interbedded with siltstone. There are also dolerite sills of variable thicknesses higher up in the strata (Wagner & Schümann, 1991; Gonsalves *et al*., 2021). The overburden thus consists of multiple thick units of competent rock material, which has the potential to span over extensive mining voids (Wagner & Schümann, 1991; Gonsalves *et al*., 2021). Even in previous longwall mining, where the panels reached an extensive span of 230 m, blasting of the roof was often necessary to initiate goafing (Prinsloo, 2019).

Stooping operations at NDC were first trialled in the 1100 block at Central Shaft (Figure 1-7). These panels were not originally designed for stooping, as their panel spans according to empirical calculations were too narrow to allow for goafing. Consequently, little goafing was recorded during and after stooping operations, which in turn resulted in the build-up of high abutment stresses on the surrounding pillars, barrier pillars and even on in-panel pillars in the surrounding panels. It was in this specific block that the stooping of multiple panels adjacent to the 1120 Main belt and travelling roads resulted in the excessive scaling of strategic pillars. These pillars as shown in Figure 1-8 consequently had to be supported to ensure the long-term stability of the panel and its associated infrastructure, which should remain stable for Life of Mine (LOM). The fact that goafing did not occur

during the pillar extraction, put the mine at risk of a late (time-dependent) goaf and an associated air-blast.

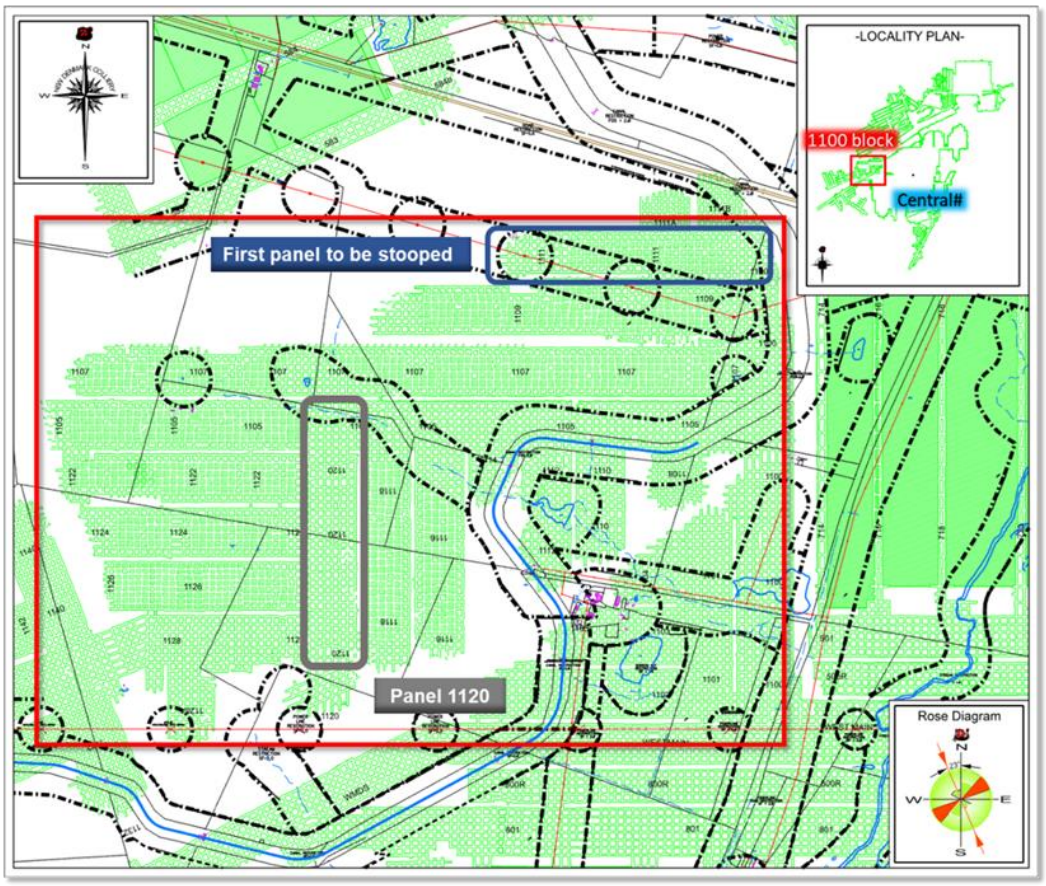


Figure 1-7: NDC Mine plan indicating 1100 block where stooping was first trialled. The green represents the bords (roadways and splits) and the white areas are the barriers and in-panel pillars.



Figure 1-8: Excessive pillar scaling along Panel 1120 tractor road.

On the contrary, Panels 179b at Okhozini Shaft, 888, 882c and 882d at North Shaft goafed consistently even though the critical span theory and calculations suggested that goafing should not have occurred. It is thought by the NDC Rock Engineering Department that there was a different stress regime due to nearby geological structures, such as dykes, faults and joints. Previously mined longwall and stooping panels may also have contributed to this changing stress regime.

1.3 Justification for Research

It is well known that goafing in pillar extraction panels would relieve the build-up of abutment stresses. The absence or variability of goafing was therefore identified as a risk at NDC since the first panels were stooped. Management became concerned that this would affect the long-term stability of the mine and that it could result in another Coalbrook disaster.

Their concerns were further exacerbated by the excessive pillar scaling in the main development, Panel 1120, after stooping on both sides of it.

In high-extraction mining methods like stooping, the level of stress and its variations primarily depend on the condition of the sill or any other stable layer in the overburden. Put simply, the design of spans should either induce failure of the overburden or ensure that stresses are transferred to barrier pillars or abutments without causing failure (Van der Merwe & Madden, 2010; Van der Merwe, 1995).

The purpose of this research was thus to validate NDC's stooping strategy or improve on it where necessary. This would be done by providing the mine with a set of guidelines that will ensure safe and effective stooping operations going forward even if no goafing occurs. It included identifying and assessing the risks of panels not goafing, the minimum width requirement for barrier pillars and safe stand-off distances of stooping panels from sensitive infrastructure.

1.4 Research Methods

A total of 50 panels have been stooped across all three shafts at NDC since the end of 2018. Several challenges have been encountered and learnings made since then. The research was done by evaluating the mine's current stooping strategy, back-analysis of the panels that have been stooped, and conducting numerical modelling on selected panels. The back-analysis of stooped panels was done by capturing relevant information in a database.

Such information, for example, included the mining parameters during development, geological conditions, stooping parameters, presence of stress concentrators and observations made during inspections.

1.5 Assumptions

No personnel were allowed to enter the goaf area due to the nature of and risks associated with stooping operations. Mine management further decided for safety reasons that no personnel were allowed to access the bleeder road for inspections of the goaf area. Consequently, no one was able to confirm whether all cuts were taken as per the stooping layout and/or inspect possible goaf areas further back in the panel.

The study was therefore based on the following assumptions:

- All cuts taken by the mining personnel were as per the rock engineer's cutting sequence and design, and as indicated on the stooping layout. The fenders and snooks left behind were similar in size to those indicated on the stooping layout.
- No goafing occurred within a specific panel if it did not goaf during stooping operations. The only way that the goafing of a panel could be confirmed after it was stooped is through subsidence measurements on the surface. This would indicate that if goafing did occur, it broke the sill and goafed to the surface.

2 LITERATURE REVIEW

2.1 Risk of Pillar Extraction

Pillar extraction has long been regarded as one of the highest-risk underground coal mining methods. Galvin (2015) reports 15 fatalities that occurred due to falls of ground (FOGs) during pillar extraction operations in New South Wales (NSW) in Australia, between 1980 to 1992. Twelve of these were associated with buried CMs as 95% of the machines at that time had on-board drivers. Mark *et al.* (1997) indicate that the United States of America (USA) experienced a similar situation between 1989 and 1996 with 25% of the 111 FOG-related fatalities being attributed to pillar extraction. This number of accidents occurred despite pillar extraction contributing only 10% of underground coal production during that period. Mark *et al.* (2003) further reported that personnel in pillar extraction panels were three times more likely to be fatally injured than those in other panels.

Although little safety statistics were found regarding ‘true’ pillar extraction operations in South Africa, it is worth mentioning the Coalbrook disaster which occurred on 21 January 1960 (Van der Merwe, 2006). In total, 437 workers lost their lives when pillars collapsed in the eastern and south-eastern portions of the mine over an area of 324 hectares. This disaster was in short attributed to the following factors:

- Secondary extraction in the form of top coaling, which not only reduced the pillar dimensions but also increased the mining height,

ultimately decreasing the pillars' width-to-height (w/h) ratios and load-bearing capacity.

- Insufficient size barrier pillars due to them being initially left too narrow to bear the weight of the overburden, or were mined smaller due to pillar robbing; and lastly
- Failure to recognize both the strengths and limitations of the overburden.

Although the pillars were mined too small, they did not exhibit any signs of being overloaded and consequent failure. This was due to a sill higher up in the overburden, which spanned across the panels and distributed the stress to the abutments (Van der Merwe, 2006). When the span reached critical proportions, it failed. The underlying, under-sized pillars were suddenly exposed to the full overburden load and failed violently (Van der Merwe, 2006).

The incident investigation revealed that the sill failure was arrested in areas where the span was restricted by solid ground. Such solid ground included the abutments or pillars that were large enough to carry the full weight of the overburden. The incident highlighted the importance of safe pillar design and leaving sufficiently large barrier pillars between panels to carry the full weight of the overburden between them. Such barrier pillars would limit failure and subsidence to a single panel in the event of pillar collapse (Van

der Merwe, 2006). Extensive research was done after this incident to prevent a recurrence of it (Van der Merwe, 2006).

Pillar extraction methods have over the years evolved through trial and error, observation and experience (Galvin, 2015). However, it was not until the mid-1990s that significant research was done on coal pillar mechanics and roof behaviour (Galvin, 2015). The research resulted in a significant improvement in safety in pillar extraction operations (Galvin, 2015).

2.2 Factors Influencing Pillar Extraction

Moolman & Canbulat (2003) indicate that several factors must be considered when planning pillar extraction. These factors include geological conditions, geotechnical design parameters, environmental conditions, surface constraints, ventilation requirements and mining methods. The research described in this report focused on the geological conditions, geotechnical design parameters and mining methods.

2.2.1 Pillar extraction of old workings and new panels

Pillar extraction can either be done in old pillar workings, or panels originally designed for it (Livingstone-Blevins & Watson, 1982; Willis & Hardman, 1997). Van der Merwe & Madden (2010) suggested that pillar extraction in old workings should optimise the given circumstances, such as panel span and pillar dimensions. However, when it is originally planned for, the panels and pillars can be designed optimally in advance and provide better control over the different factors that must be considered during pillar extraction.

Although the latter is the preferred situation, the reality, especially in South Africa, is that most old workings were not designed with pillar extraction in mind (Livingstone-Blevins & Watson, 1982; Willis & Hardman, 1997).

2.2.2 Geotechnical design parameters for pillar extraction

According to Van der Merwe & Madden (2010), pillar designs, geological conditions, stress changes and panel span are some of the most important geotechnical parameters to consider. These issues are discussed in more detail below.

Pillar designs

Proper, stable pillar designs became a focus point after the Coalbrook disaster. The aim was to scientifically determine the strength of the pillar and the loading that it was subjected to. This proved especially important for bord-and-pillar developments (Van der Merwe, 2006). Several coal pillar strength formulae have been derived since that time.

The pillar strength formula of Salamon and Munro (1967), was derived by empirical methods using statistical back-analysis on a database of 27 failed pillars and 92 intact pillars (Van der Merwe & Mathey, 2013). The derived formula is provided in Equation 2-1.

$$Strength = 7.176\ \frac{w^{0.46}}{h^{0.66}}\ (MPa) \qquad \textbf{\textit{Equation 2-1}}$$

where w = Pillar width (m)

h = Mining height (m)

7.176 = constant representing the bulk strength (including the joints) of the coal in MPa.

The squat-pillar formula was derived after Salamon (1982, as cited in Van der Merwe & Madden) realised that the original Salamon and Munro (1967) pillar strength formula underestimated the strength of very wide pillars. It indicates an increasing rate of pillar strength beyond a pillar w/h ratio of five (Van der Merwe & Madden, 2010; Van der Merwe, 2006). It is provided by Equation 2-2.

$$Strength = k\ \frac{{R_0}^b}{V^a}\left\{\frac{b}{\varepsilon}\left[\left(\frac{R}{R_0}\right)^{\varepsilon} - 1\right] + 1\right\}\ \ (MPa) \qquad \textbf{\textit{Equation 2-2}}$$

where k = 7.2 MPa; constant representing the strength of the coal pillar

R_0 = critical w/h ratio = 5.0

R = actual w/h ratio

ε = rate of strength increase = 2.5

a = constant 0.0667

b = constant 0.5933

V = pillar volume ($w_1.w_2.h$)

The assumption of the critical w/h ratio was because no pillar with a w/h ratio of greater than 3.75 had collapsed in South Africa at that time (Van der Merwe & Madden, 2010). The formula is thus typically used for deeper coal mines, such as NDC, where the w/h ratios of the pillars exceed 5.0.

The Tributary Area Theory (TAT) predicts the maximum load that each pillar is subjected to by assuming that each pillar carries the weight of the full overburden immediately above it (Van der Merwe, 2006; Van der Merwe & Madden, 2010). The assumption applies where the pillars are uniform in size and the panel width is larger than the depth to the seam (Van der Merwe, 2006; Van der Merwe & Madden, 2010). The Tributary Area Theory is given by Equation 2-3. The safety factor (SF) of the pillar can then be determined by simply dividing the pillar strength by the load that it is subjected to, as shown in Equation 2-4 (Van der Merwe, 2006; Van der Merwe & Madden, 2010).

$$Load = \frac{0.025HC_1C_2}{w_1w_2}\ (MPa) \qquad \textbf{\textit{Equation 2-3}}$$

where H = mining depth (depth to the floor of the workings) (m)

C = pillar centre distance (m)

w = pillar width (m)

0.025 = unit weight of the overburden strata (MN/m³)

$$Safety\ Factor\ (SF) = \frac{Pillar\ strength}{Pillar\ load} \qquad \textbf{\textit{Equation 2-4}}$$

A pillar with a SF of unity has a 50% probability of stability (Salamon, 1967). After careful consideration of the existing database of failed and un-failed pillars, Salamon (1967) observed that the highest concentration of un-failed pillars lay between SFs of 1.31 and 1.88. The mean SF in this range was 1.57 and no pillar failures had occurred at or above this SF in the database.

A SF of 1.6 was therefore considered safe. Salamon and Oravecz (1976) further recommended a SF of 2.0 for main developments. These recommendations have become widely accepted criteria for pillar stability in the South African coal mining industry. In pillar extraction panels, pillars are typically cut with a SF greater than 1.8 (Van der Merwe & Madden, 2010). This allows for several cuts to be taken from these pillars during extraction while leaving sufficient size snooks and fenders. The latter will maintain temporary stability in the immediate area where the cuts are being taken from the pillar (Van der Merwe & Madden, 2010).

The design of stable barrier pillars also became a focus point after the Coalbrook disaster. The Government Mining Engineer concluded that: “Mining should be carried out in panels surrounded by barriers of unmined coal of dimension which will limit subsidence to a single panel in the event of pillar collapse” (Van der Merwe, 2006). These pillars must therefore be able to carry the full load of the overburden, assuming the in-panel pillars are carrying no load. Although little research has been done to determine the strength of barrier pillars in South African coal mining, it is generally accepted that the minimum width of the barrier must be equal to that of the adjacent in-panel pillars (Van der Merwe, 2006).

Stratigraphy and geological structures

Coal seams were formed in a sedimentary environment and were overlain by multiple rock strata forming the overburden. These vary in thickness,

composition and rock mass properties. The individual rock strata, although different from each other, tend to be relatively uniform over extensive distances (Wagner & Schümann, 1991). The characteristics of the overburden will significantly determine its behaviour during pillar extraction and subsequent goafing. The strength of individual strata, for example, can vary greatly depending on the rock type and thickness of the strata (Wagner & Schümann, 1991). Overburden comprising of weak rock types will readily fail and result in more consistent goafing, whereas stronger rock types will tend to hold up and span across large distances (Van der Merwe & Madden, 2010; Wagner & Schümann, 1991).

The dominant rock formations in South African coalfields are sandstones and shales. The sandstones range in grain size from more than 1 mm (coarse-grained) to a few micrometres (fine-grained), while the shales are generally thinly bedded and often contain carbonaceous material (Wagner & Schümann, 1991). Relatively massive, fine-grained sandstone layers with a uniaxial compressive strength (UCS) ranging between 70 MPa and 120 MPa can span over tens of metres without failing. The opposite is true for thinly laminated shales of which the self-supporting spans are usually much less than 10 m in length (Wagner & Schümann, 1991).

The bulking properties of sandstone and shale also play a significant role in the behaviour of the goaf. When sandstone layers fail, they tend to break up into comparatively large blocks with many voids in between the blocks. Sandstones thus have very good bulking properties ranging between 1.3

and 1.5 (Wagner & Schümann, 1991). In contrast, shale formations tend to fail in thin slabs, resulting in tightly packed caved material with poorer bulking properties ranging between 1.1 and 1.2 (Wagner & Schümann, 1991).

Many South African coalfields are also characterised by the presence of igneous intrusions, usually of dolerite composition. These either intersected the coal seams as near-vertical dykes or intruded in between the sedimentary strata as massive sills above or below the coal seams. The dolerite dykes and sills have remarkable strength properties when unweathered, but can also be very weak in their weathered state, especially when close to the surface (Wagner & Schümann, 1991). Van der Merwe (2006) states that the material strength and stiffness of dolerite dykes and sills are much greater than that of the surrounding sedimentary rocks. Table 2-1 shows that the UCS of dolerite ranges between 180 MPa and 500 MPa (Van der Merwe, 2006) compared to a sedimentary range of between 40 MPa and 120 MPa (Wagner & Schümann, 1991). Dolerite sills, which have thicknesses of 30 m or 40 m, can consequently span over extensive distances of hundreds of metres without failing (Wagner & Schümann, 1991; Galvin, 1983). Although a sill might initially be stable and prevent subsidence from occurring, its long-term stability is questionable due to the risk of it failing over many years (Wagner & Schümann, 1991).

Table 2-1: Typical strength and bulking properties of rock formations in South African coalfields (Wagner & Schümann, 1991; Van der Merwe, 2006).

Rock Type		Uniaxial Compressive Strength (MPa)	Tensile Strength (MPa)	Bulking Factor
Sandstone	Fine	70 - 120	5	1.3 - 1.5
	Medium	50 - 70	3	
	Course	30 - 50	2	
Shale	-	40 - 80	2	1.1 - 1.2
Dolerite	-	180 - 500	10 - 14	-
Coal	-	15 - 40	1.5	1.3

The presence of geological structures, such as dykes, faults, joints, and even undulations in the strata must also be considered as they can act as horizontal stress concentrators and increase the risk of FOGs in the working area. They can alter the goafing behaviour from that which was expected for the panel (Galvin, 2015). A zone of weakness is furthermore formed at the contact area between a vertical or near-vertical dyke and the surrounding strata. The strata will tend to move along the contact area because of high-extraction mining. The effect of this is more significant when the dyke runs parallel or at very acute angles to the panel abutment (Wagner & Schümann, 1991).

Overburden strength and critical span

This research focused on determining the critical span, which is simply defined as the point at which the panel span exceeds the self-supporting span of the immediate roof beam. It is at this point that the overburden is

expected to fail in the form of goafing due to the induced tensile stresses exceeding the tensile strength of the rock strata (Galvin, 1983; Van der Merwe, 1995; Van der Merwe, 2006; Wagner & Schümann, 1991).

A self-supporting (clamped) beam is defined as a uniform unit of rock strata that is capable of spanning over a certain unsupported distance without breaking. There are several factors that determines the span of a self-supporting beam, namely the tensile strength of the rock strata, its unit weight and the thickness of the beam (Ryder & Jager, 2002; Van der Merwe & Madden, 2010; Wagner & Schümann, 1991). These factors and the relationship between them are given by Equation 2-5.

$$L = \sqrt{\frac{2(t)(\sigma_t)}{(\rho)(g)}} \quad (m) \qquad \textbf{\textit{Equation 2-5}}$$

where L = unsupported span (m)

σ_t = tensile strength of the rock strata (Pa)

ρ = density of the rock strata (kg/m^3)

g = gravitational acceleration (9.81 m/s^2)

t = thickness of the rock strata (m)

Figure 2-1 shows the typical self-supporting spans for various rock strata in the South African coalfields (Wagner & Schümann, 1991). From this diagram, a sandstone bed with a thickness of 10 m and tensile strength of 5 MPa can span over approximately 60 m. In comparison, a dolerite sill with the same thickness and higher tensile strength of 10 MPa can span up to

100 m (Wagner & Schümann, 1991). In the case of NDC where the dolerite sill has an average thickness of 40 m, it is capable to span over distances between 180 m and 200 m (Gonsalves *et al*., 2021; Wagner & Schümann, 1991).

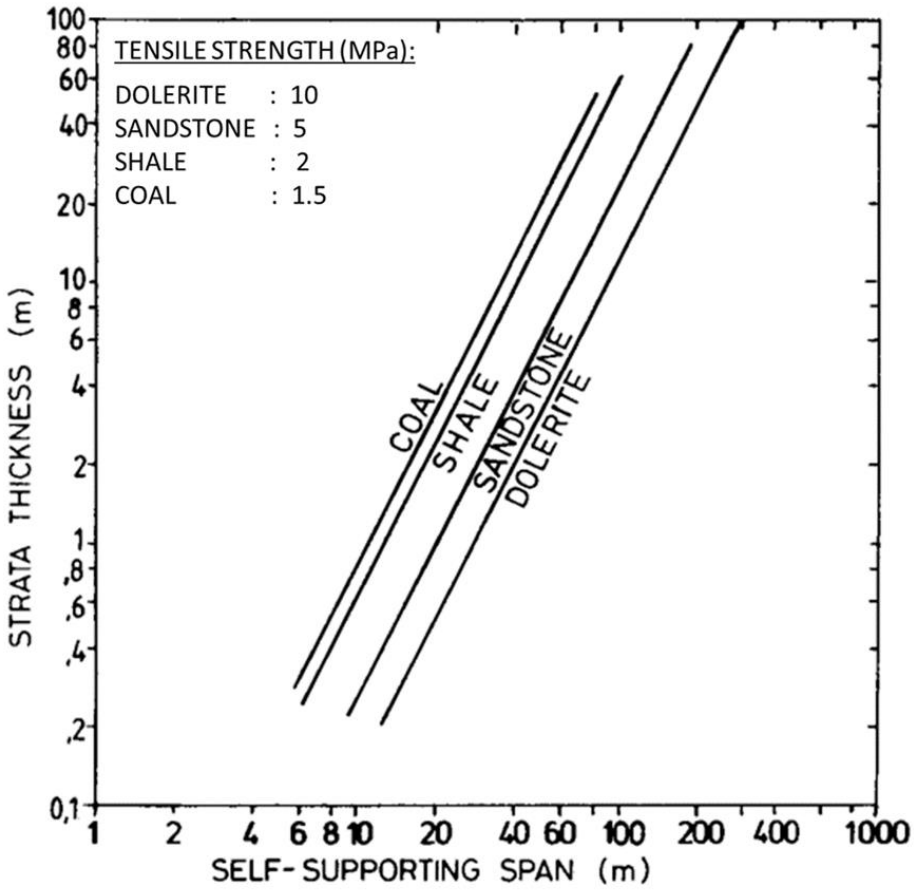


Figure 2-1: Typical self-supporting spans for various rock strata found in South African coalfields (Wagner & Schümann, 1991).

Van der Merwe & Madden (2010) derived a simple formula to determine the critical span for overburden that is without a dolerite sill and consists of incompetent strata, such as shales and mudstones. It is calculated using Equation 2-6:

$$L_c = 2H\tan(\emptyset)$$ ***Equation 2-6***

where L_c = critical mining span (m)

H = depth of mining below surface (m)

$\emptyset$ = goaf angle (°)

Van der Merwe & Madden (2010) further determined the relationship between mining depth and overburden type on critical span for situations where a dolerite sill is absent. The composition of the overburden affects the goaf angle and thereby determines the critical span. A comparison between the effects of strong sandstone and weak shale on critical span is shown in Figure 2-2.

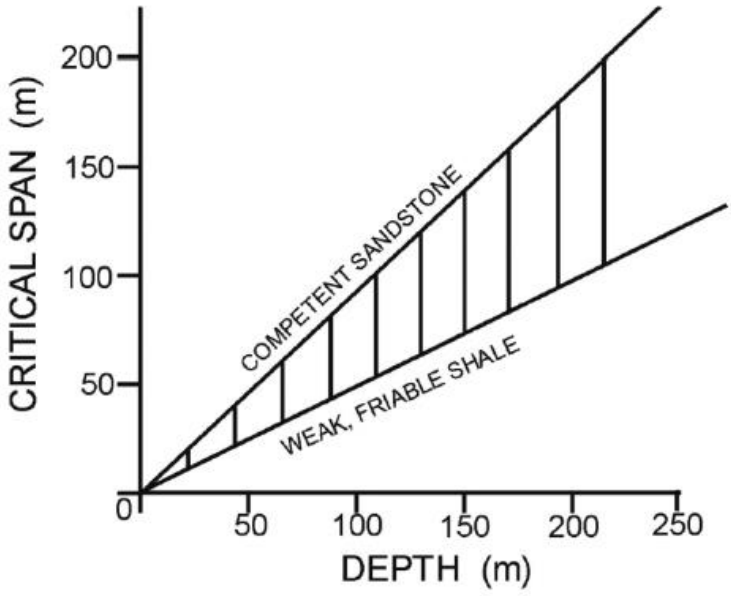


Figure 2-2: Diagram indicating the relationship between mining depth and critical span for competent and weak strata (Van der Merwe & Madden, 2010).

It was however the strength of the sill that became a focus point after the Coalbrook disaster, especially for high extraction mining methods. There are two main formulas used in the coal mining industry to determine the critical span for inducing sill failure higher up in the stratigraphy. These are:

- Galvin's (1983) 'Effective Span Elastic Thin Plate Model'; and
- Van Der Merwe's (1995) 'Critical Panel Span for Dolerite Failure'.

Galvin (1983) derived a formula to predict the minimum required panel span that will induce failure of the dolerite sill in the overlying strata. His approach was based on the elastic thin plate theory, which states that the sill will fail as several distinct plates over some time. Failure of the sill will occur at its base where the critical stress is initiated through the unsupported span of caving material underneath. His 'Effective Span Elastic Thin Plate Model' is given by Equation 2-7.

$$S_{crit} = \sqrt{1165\ t_d - 935\ \frac{t_d^2}{D_d}} + 2t_p \tan(\beta - 90) \qquad \textbf{\textit{Equation 2-7}}$$

where t_d = thickness of dolerite sills (m)

D_d = depth of base of dolerite sill below surface (m)

t_p = thickness between parting and coal seam (m)

β = caving angle of parting measured from the coal seam ahead of the working face (°)

Van der Merwe (1995) proposed a different approach to determine the critical span by assuming that the dolerite sill behaves like a beam rather than a plate. It is described as a jointed structure, thus consisting of blocks held together by cohesion and horizontal stresses. Failure of the sill will occur when the cavity that has formed beneath its base allows it to deflect to such an extent that it induces horizontal stresses in the sill itself. These will reduce the pre-existing horizontal compression until a key block at the centre of the sill can slide out under its weight. The critical span for this failure is determined using Equation 2-8.

$$L_c = 2T\sqrt{k_s + \frac{\beta}{D}} + 2(H - D)\tan(\emptyset) \qquad \textbf{Equation 2-8}$$

with

$$\beta = \frac{1.53}{\gamma_m} - 0.8 \qquad \textbf{Equation 2-9}$$

and

$$\gamma_m = 0.025\frac{D-T}{D} + 0.03\frac{T}{D} \qquad \textbf{Equation 2-10}$$

where ks = ratio of horizontal to vertical virgin stress

H = depth of mining below surface (m)

D = depth of dolerite base (m)

T = thickness of dolerite (m)

$\emptyset$ = goaf angle measured from the vertical (°)

Both are predominantly aimed at predicting the critical span required to induce the failure of the dolerite sill higher up in the strata. However, Galvin's (1983) formula was found to be ineffective in situations where the sill occurred close to the surface. Van der Merwe (1995) demonstrated this by comparing the two formulae for the critical span at the base of the sill and graphically presenting the results, as shown in Figure 2-3. The critical span as calculated by the two formulae is indicated on the vertical axis, while the horizontal axis shows a sill which progressively increases in both thickness and depth below the surface.

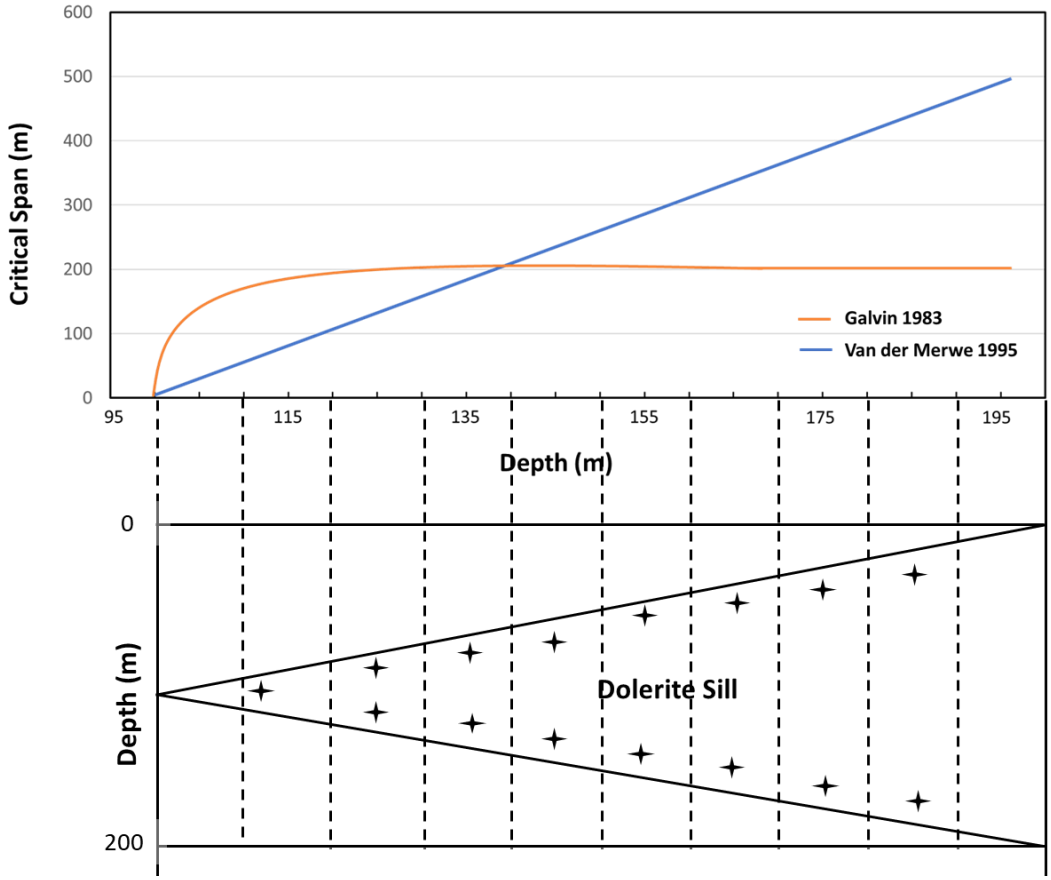
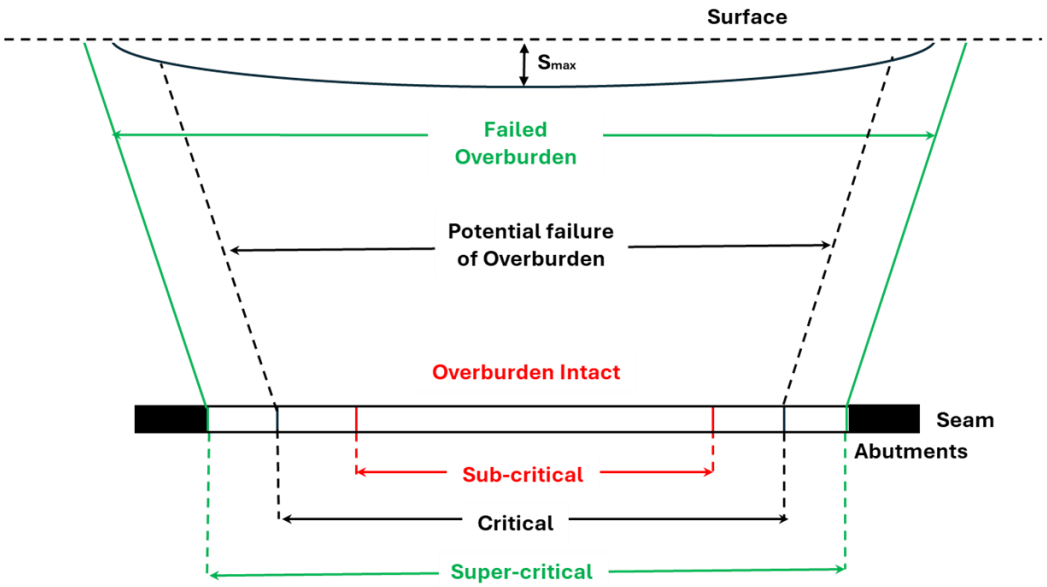


Figure 2-3: Comparison of Galvin's (1983) and Van der Merwe's (1995) critical span formulae for different thicknesses and depths of dolerite sills (van der Merwe, 1995).

Van der Merwe's (1995) critical span formula shows a continuous increase in critical span with sill thickness. The Galvin formula (1983), on the other hand, reaches a critical span at a certain point and then appears to slightly decrease with increasing sill thickness and depth. This is attributed to the fact that the Galvin formula (1983) ignores the effect of overburden loading on the critical span. In addition, the formula predicts an increase in the critical span with an increasing depth of the sill below the surface. Van der Merwe (1995) argues that the opposite is true, because as the sill depth

increases, so will the overburden load on the sill itself. Consequently, a lower critical span will be required for sills occurring at greater depths.

Van der Merwe & Madden (2010) states that ground conditions, regardless of the overburden composition, are unpredictable when the panel span falls within the critical span range. They therefore recommend that panel spans be decreased by at least 10% to fall in the sub-critical range to avoid overburden failure or be increased by 10% to fall in the super-critical range to ensure overburden failure. These concepts are shown in Figure 2-4.



Term	Description	Example
Sub-critical	• 10% less than critical span • No goafing, if panel span is less than sub-critical span • High abutment stresses	Sub-critical = 162 m
Critical	• Unsupported, panel span exceeds self-supporting span of overburden • Unpredictable goafing conditions	Critical span = 180 m
Super-critical	• 10% greater than critical span • Ensures goafing, if panel span exceeds super-critical span • Relief of abutment stresses	Super-critical = 198 m

Figure 2-4: Simplified diagram illustrating the concepts of sub-critical, critical, and super-critical spans.

Stress changes and goafing

Stress changes occur during mining, especially when high-extraction mining methods, such as pillar extraction or longwall mining, are being used. These stress changes can be much larger than those created by bord-and-pillar development (Van der Merwe & Madden, 2010). The magnitude of the stresses and change thereof is dominated by the status of the sill or any other competent layer in the overburden. In other words, spans need to be designed to fail the competent layer, or spans need to be managed to

ensure that stresses are transferred to barrier pillars or abutments without failure (Van der Merwe & Madden, 2010; Van der Merwe, 1995).

Tensile zones are created above the panel as the seam is being extracted during high-extraction mining. This is due to the vertical stresses directly above the centre of the panel being relaxed as they get transferred to the abutments (Van der Merwe & Madden, 2010; Wagner & Schümann, 1991; Ryder & Jager, 2002). The horizontal extents of these tensile zones are orientated across the panel from one abutment to the other, as well as along the length of the panel. They are predominantly governed by the panel span, W, and will increase in magnitude the wider the unsupported span becomes (Van der Merwe & Madden, 2010; Wagner & Schümann, 1991; Ryder & Jager, 2002). The stress distribution in the immediate overburden can be simply explained by comparing it to the behaviour of an unsupported, unjointed clamped beam. Figure 2-5 shows a simplified diagram of a clamped beam illustrating the positions of the maximum tensile and compressive stresses.

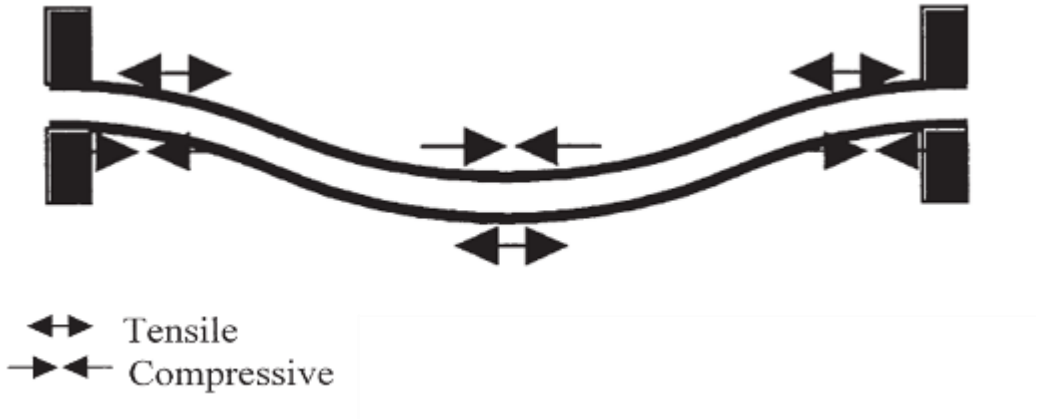


Figure 2-5: Simplified diagram of a clamped beam indicating the positions of maximum tensile and compressive stresses (Van der Merwe & Madden, 2010).

The maximum stresses occur at the edges of the beam where the compressive stresses will result in guttering, especially if the immediate overburden consists of weak, finely laminated shales (Van der Merwe & Madden, 2010; Ryder & Jager, 2002). The centre of the beam will experience the most deflection due to sag. Tensile stresses in the centre of the panel, along the bottom of the beam, will result in tensile cracks, generally orientated along the length of the panel. These tensile stresses are half the magnitude of the tensile stresses at the top (Van der Merwe & Madden, 2010; Ryder & Jager, 2002). Considering that rocks are weaker in tension than in compression, failure of the beam is expected to start at the top, at the two edges. This will not be visible due to it occurring in the immediate roof (Van der Merwe & Madden, 2010; Ryder & Jager, 2002). Tensile stresses, especially in stratified overburden also have the potential to result in bed separation between the different strata. It decouples the

immediate beam from the rest of the overburden which was assumed to be self-supporting (Ryder & Jager, 2002). The tensile zone furthermore has the potential to activate geological discontinuities in the immediate roof, such as joints, which are also commonly referred to as slips in coal mines (Ryder & Jager, 2002).

A clamped, self-supporting beam can, however, change to a cantilever beam if its continuity is disrupted by the presence of a geological structure, such as a fault, joint or even a dyke (Ryder & Jager, 2002; Van der Merwe, 2010; Wagner & Schümann, 1991). The free end of the beam is now stress free, while the stresses increase significantly at the clamped edge. Figure 2-6 shows the positions of the different stresses on the clamped side of the beam. Van der Merwe & Madden (2010) state that the tensile stress can increase six-fold at the top of the beam that is not visible. Like the clamped beam, compressive stress occurs at the bottom part of the clamped edge and will result in guttering if the beam consists of weak, finely laminated shales (Ryder & Jager, 2002; Van der Merwe, 2010). The magnitude of both the tensile and compressive stresses are highest at the clamped edge, from where it will decrease in the direction of the free end.

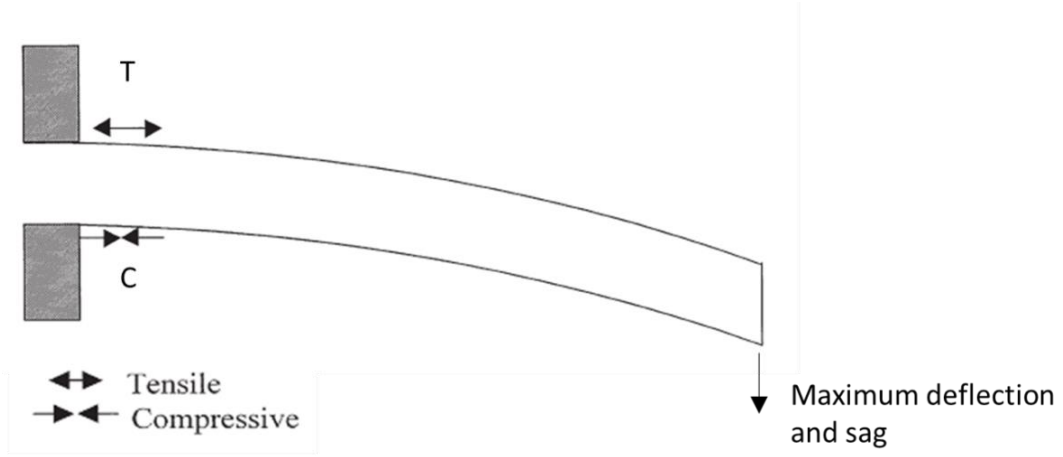


Figure 2-6: Simplified diagram of a cantilever beam indicating the positions of maximum tensile and compressive stresses, as well as the maximum defection and sag (Van der Merwe & Madden, 2010).

The stress changes induced by a cantilever beam are two-fold. There is the horizontal component, namely the tensile and compressive stresses along the beam, and the vertical component (Ryder & Jager, 2002; Wagner & Schümann, 1991). The latter is caused by the deflection and sag of the free end due to gravity and the weight of the beam itself. A cantilever beam can be formed over a small, localised area such as over a bord or an intersection. In such an instance, the free end of the beam will be supported by anchoring it into the overlying strata with roof bolts (Van der Merwe & Madden, 2010). When the cantilever beam is formed over a larger area, such as a panel, the weight of the beam will have to be supported by the pillars underneath. This will increase the vertical stress that they are exposed to and may be seen in the form of pillar scaling (Wagner & Schümann, 1991; Van der Merwe & Madden, 2010). The deflection and sag

of a cantilever beam will also induce tensile stress where the beam separates from the overlying strata (Ryder & Jager, 2002).

The vertical extent of the tensile zones is a function of the ratio of mining depth, H, to the panel span, W (Van der Merwe & Madden, 2010; Wagner & Schümann, 1991; Ryder & Jager, 2002). The *H/W* ratio is large for extraction panels at great depth. It results in small tensile zones, which explains why extensive caving in deep-level gold mines is limited (Van der Merwe & Madden, 2010; Wagner & Schümann, 1991). However, as the *H/W* ratio decreases, the overburden above high extraction panels will increasingly come into tension (Van der Merwe & Madden, 2010; Wagner & Schümann, 1991). This is typical of shallower coal mines. Studies have shown that at depths equal to the span, approximately 35% of the overburden rock is in tension. Due to rock being weak in tension, the overburden will readily fail, especially if it consists of weak rock types. This is likely to result in subsidence on the surface or even the formation of sinkholes if the workings are sufficiently shallow enough (Van der Merwe & Madden, 2010). Van der Merwe & Madden (2010) illustrate this concept with an elastic numerical modelling plot obtained with the Examine2D software (Rocscience, 2003). Figure 2-7 compares the vertical extent of the tensile zone above a 200 m wide, high extraction panel at depths of 50 m and 200 m below the surface.

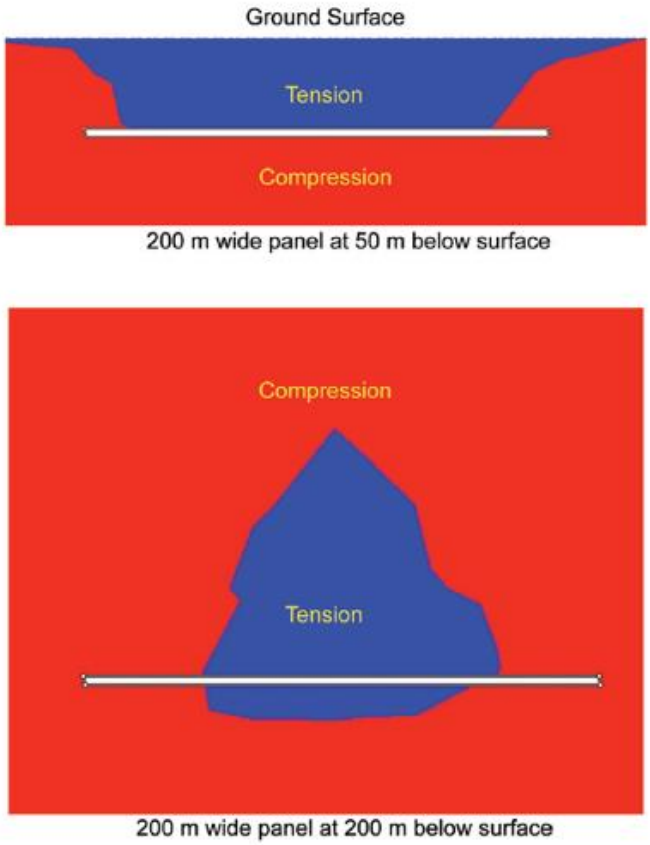


Figure 2-7: Model of a cross-section showing the larger extent of the tensile zone above a high extraction panel at shallower depth (Van der Merwe & Madden, 2010).

Van der Merwe & Madden (2010) distinguishes between partial (small) and complete (major) goafing (Figure 2-8). Partial goafing occurs when only minor falls occur in the mined-out area, thus extending a limited distance into the immediate roof depending on the roof lithology. The bulk of the overburden material, including the sill, remains intact (Figure 2-8 (a)). If the overburden consists of weaker, thinly laminated shales, progressive goafing will occur until the sill is reached. In this situation, high vertical stresses are transferred to the barrier pillars and working faces. The magnitude of these

stresses is predominantly determined by the span, mining depth and the position of the dolerite sill in the overburden (Galvin, 1983; Van der Merwe, 1995). It is important to note that the increased abutment stresses are usually due to the weight of the sill and the material above the sill (Van der Merwe & Madden, 2010).

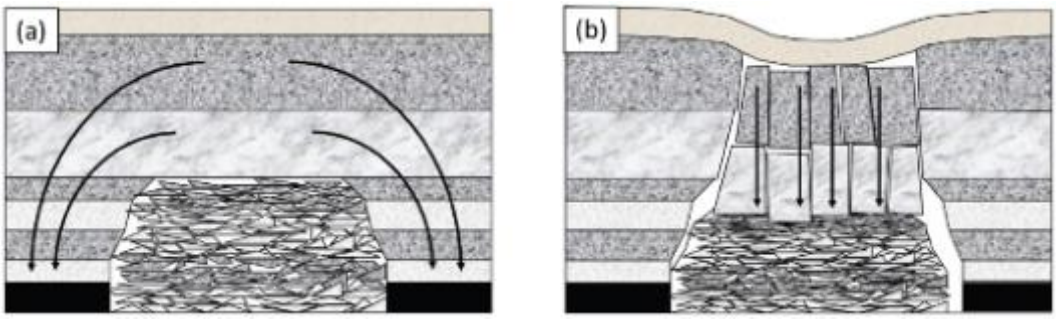


Figure 2-8: Partial and full goafing of the overburden; (a) partial goafing of the overburden with the weight of the intact overburden transferred to the abutments; (b) complete goafing with the abutment stress being relieved (Van der Merwe & Madden, 2010).

If the overburden consists of mainly sandstone formations, these will start to fail once the mining span exceeds their critical, self-supporting spans. As the sandstone material progressively goafs, it will quickly bulk and gradually fill the void created by seam extraction. Once this point is reached, the failed sandstone blocks will start to resist further goafing (Wagner & Schümann, 1991). The resistance will be initially low but increase rapidly as the goaf material becomes more and more compressed by the weight of the overlying strata. Ultimately, a point of equilibrium is reached where the resistance of the failed, but compressed, sandstone equals the weight of

the overburden strata (Wagner & Schümann, 1991). This scenario is still considered partial goafing due to the sill remaining intact; however, significantly less stress is transferred to the abutments.

Complete goafing occurs when the panel span is sufficient to induce failure of the sill. Figure 2-8 (b) shows that the overburden fails and extends up to the surface where it results in subsidence. It is at this point that the load of the overburden rests on the goaf itself and the high abutment stresses on the face and abutments are relieved (Van der Merwe & Madden, 2010). The varying stress environment of a pillar extraction panel can be divided into three phases, as shown in Figure 2-9.

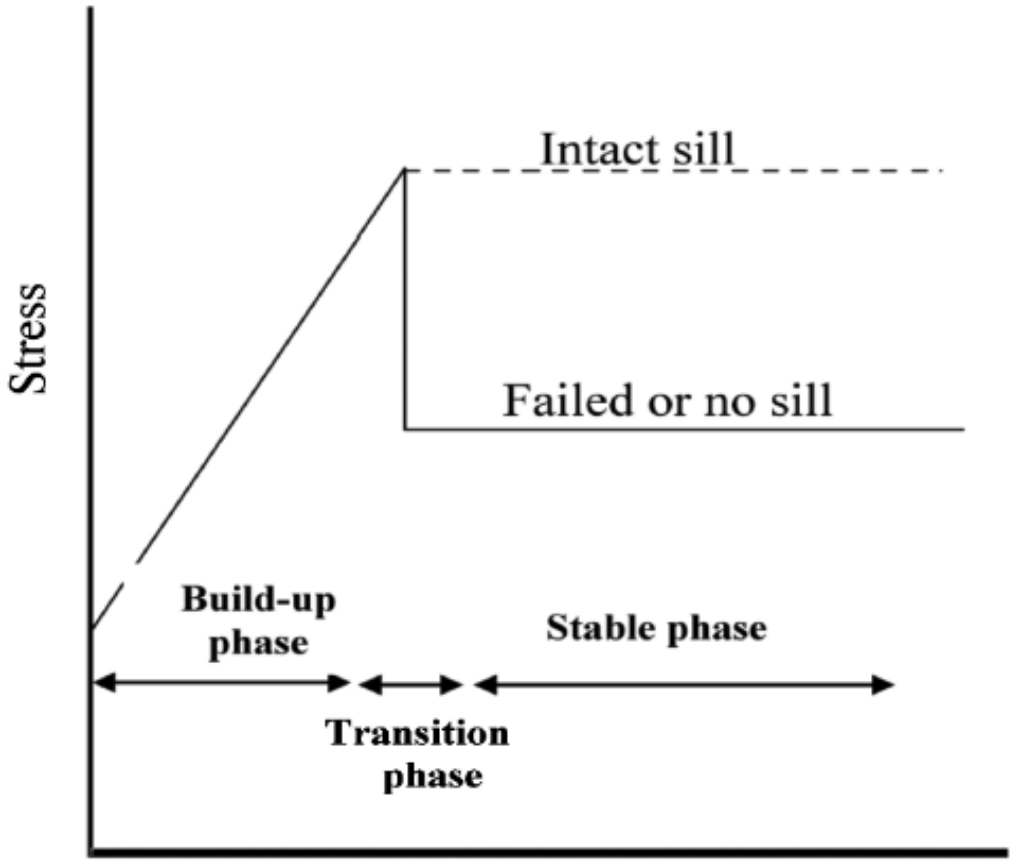


Figure 2-9: Change in the stress on the front-line pillars with an advancing face (Van der Merwe & Madden, 2010).

The build-up phase consists of the pillar and overburden stress initially being at the same low level as during development. It will increase as the face advances with pillar extraction due to each successive pillar being subjected to a higher stress than the previous one. This will continue until a critical point is reached during the transition phase when the advance is equal to the mining depth, or the panel span (van der Merwe & Madden, 2010). In the event of the overburden consisting of weak rock types, it will most likely goaf after which there will be a stress relief, especially on the in-panel pillars. If the overburden remains intact due to it consisting of

competent rock types, the stress levels will remain high. The rate of increase will however be reduced until it stabilises (Van der Merwe & Madden, 2010). This is known as the stable phase and generally occurs when the face advance is about twice that of the panel span (Van der Merwe & Madden, 2010). The stress levels for a panel with weak overburden, as indicated above, will have been relieved after the initial goaf and will be more consistent for the remainder of the panel. It will remain at lower stress levels, even though periodic stress build-ups may occur as the overburden hangs up from time to time (Van der Merwe & Madden, 2010). A panel with competent overburden will continue to exhibit the effects of high-stress levels, such as excessive scaling on the barrier and in-panel pillars (Van der Merwe & Madden, 2010).

2.3 Advantages and Disadvantages of Goafing

Goafing is desired in a high extraction panel as it brings stress relief to the abutments and surrounding pillars. It is important to note that there are also several disadvantages and hazards associated with goafing. These include air-blasts, gas concentrations and water inflow (Galvin, 1983). In addition, the risk to the immediate safety of mining personnel and surface subsidence, or even sinkholes is increased if the workings are shallow enough (Wagner & Schümann, 1991).

2.3.1 Air-blasts

Air-blasts or wind-blasts occur due to a displacement of the air in the mined-out area when there is a sudden collapse or goaf of the roof material. The

air in the mined-out area is displaced at high velocity towards the direction of the working area. It has the potential to throw people, turn equipment into projectiles and blow out ventilation structures, such as walls and brattices. The magnitude and severity of the air-blast depends on the mining height and extent of the goaf area, in other words over how many splits did the goaf hang up before coming down. Frequent goafing, extending over small areas, is thus preferred as it will reduce the magnitude and severity of an air-blast (Lind, 2002a; Gonsalves, 2021).

2.3.2 High gas concentrations

The build-up of noxious and/or flammable gasses, such as carbon monoxide (CO) and methane (CH_4), can potentially occur during goafing, especially if the stability of the bleeder road is compromised. These gasses can be released from the continuous cracking, scaling and crushing of the fenders and snooks left in the goaf area, or even the barrier pillars. The gasses can also result from the goaf itself when it breaks into overlying gas-bearing layers (Moolman & Canbulat, 2003; Plaistowe *et al*., 1989). There is the risk of an air-blast blowing such hazardous gasses into the working area in the event of goafing (Lind, 2002a).

Plaistowe *et al*. (1989) also warn that during progressive goafing of the overlying strata, a ‘dome effect’ may be formed along the centre of the panel being extracted. Methane can accumulate in such a cavity and will not necessarily be cleared by the normal ventilation current. Rocks falling during

the progressive goafing process can ignite the methane through frictional heating.

Several controls can be implemented to manage the hazards and risks mentioned above, such as:

- Sufficiently ventilating the working face and goaf area;
- Stabilising the bleeder road through proper design of the pillars along it and only allowing certain cuts to be taken from them;
- Regular inspections of the bleeder road by authorized and competent mining personnel;
- Methane drainage holes drilled from the surface at regular intervals to intersect and drain any pockets of methane in the goaf area; and
- Continuous monitoring of methane, carbon monoxide and airflow velocities through installed air monitoring equipment in the intake and return of the bleeder road.

2.3.3 Groundwater

Groundwater is often contained in aquifers above the sill. It is minimally affected in areas where the sill remains intact. However, in areas where the sill fails due to its critical span being exceeded, the underground water reservoir is often locally drained. This has several consequences, which include the drying up of wells on the surface to the management of increased water quantities in the underground working areas (Van der

Merwe, 1995). In the event of wells drying up on the surface, the mine will be held responsible and will have to supply water to whoever was using it. Water accumulating in the underground workings is also contaminated through the mining equipment, as well as through the chemical and biological processes when it is exposed to various minerals. This water must be pumped and treated as it cannot simply be discharged into the environment (Moolman & Canbulat, 2003). This is a costly exercise which increases the production costs.

2.3.4 Work face stability

Designing the panels to goaf, or not to goaf, during pillar extraction, may also largely be determined by mine management's risk appetite, specifically referring to the risk on the working face. Although pillar extraction is done on the retreat, this is not entirely accurate for the working face (Mark *et al.*, 2003). Pillars are extracted by several cuts being taken towards the goaf area, thus in the opposite direction to the panel retreat. Where panels are designed to goaf, the working face is exposed to falls of ground by progressively removing ground support from the area. Over the years, this specific risk has been reduced by the introduction of remote-controlled CMs and even Mobile Breaker Line Supports (MBLS), or Mobile Roof Supports (MRS) (Galvin, 2015; Mark *et al.*, 2003). Safety on the working face has also become reliant on the awareness of the operators and their response to signs of imminent goafing. These include bending or cracking policeman sticks, bumping and cracking noises from the goaf area, increased water

seepage from the roof, triggered roof monitoring devices and excessive pillar scaling and spalling (Galvin, 2015).

2.3.5 Surface subsidence

Surface subsidence over high extraction panels is induced by goafing of the overburden, the magnitude of which is determined by the mining height, depth below the surface and bulking factor of the caved material (Plaistowe *et al*., 1989; Wagner & Schümann, 1991). The maximum recorded surface subsidence is the best understood and most readily measured subsidence parameter. It was found to be slightly less than half the mining height in the majority of South African cases for high extraction mining (Van der Merwe & Madden, 2010; Wagner & Schümann, 1991). However, according to studies done by Wagner & Schümann (1991), other subsidence parameters, such as tilt and strain, play a more significant role in the damage of surface structures. Figure 2-10 shows the relationship between maximum subsidence, tilt and strain. The maximum subsidence is expected to occur in the centre of the mined-out panel and tends to decrease in magnitude towards the edges. Tilt is defined as the parameter that determines the visibility of a subsidence trough with the naked eye. It is at its maximum over the position where half of the maximum subsidence occurs. The strain, which can also be referred to as deformation, is tensile over the edges of the mined-out area, but changes to compression towards the centre of the trough (Van der Merwe & Madden, 2010; Wagner & Schümann, 1991).

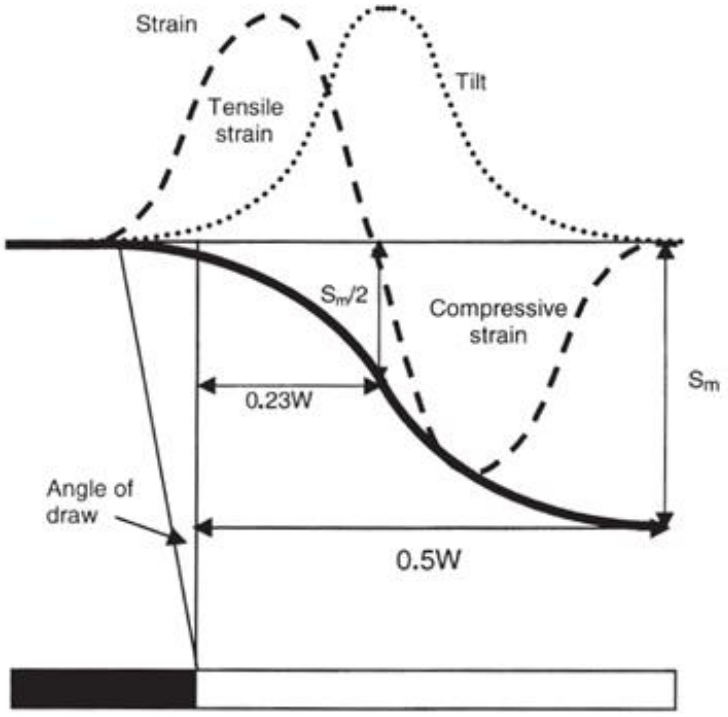


Figure 2-10: Representative subsidence half-profile for South African cases. The diagram shows the relationship between maximum subsidence, tilt and strain (Van der Merwe & Madden, 2010).

The negative impact of surface subsidence, with its associated tilt and strain, is a function of two main factors, namely the nature of the use of the surface and the severity of the induced subsidence (Van der Merwe & Madden, 2010). Wagner & Schümann (1991) concluded from several South African case studies that structural damage to, for example, roads and buildings could in general be controlled and was well within the range of repairs. Such structures could be maintained in an operational condition during undermining provided that proper precautions are taken. It is nonetheless important to note that certain surface structures will be more

sensitive to subsidence than others, such as a gas pipeline compared to a gravel road. The general approach today is that high extraction mining methods are avoided underneath sensitive surface structures and water bodies by leaving exclusion or restriction zones underneath them. In the case of pillar extraction, several pillars will be left intact to maintain the stability of the overburden in that specific area (Moolman & Canbulat, 2003).

In the event of undermining agricultural land, the induced tilt may alter drainage patterns of surface water, whereas subsidence may cause ponding rendering the affected land unusable. In such an event, the farmer will be compensated and the mine responsible for the rehabilitation of the affected area (Van der Merwe & Madden, 2010). Several steps need to be taken by mine management before high-extraction mining commences. These include:

- Identifying all the surface structures, as well as agricultural activities, that may be affected by subsidence; and
- Engaging and communicating with all the relevant stakeholders, such as the owners/custodians of the surface and the structures, as well as the Department of Mineral Resources and Energy (DMRE) has to grant permission for the undermining of the identified surface structures (Van der Merwe & Madden, 2010).

There is no clear-cut preference for either inducing goafing or preventing it when considering the abovementioned advantages and disadvantages.

Each mine's management team will decide based on an assessment of their mine's conditions. Whatever the decision may be, the situation must be controlled to achieve the desired effects in terms of underground stress, groundwater and surface subsidence. Identifying all the hazards and risks and implementing the correct controls can only be effectively done if the conditions under which goafing will occur can be accurately predicted (Van der Merwe & Madden, 2010).

2.4 Lessons Learned from Longwall Mining at NDC

Since pillar extraction had not previously been done at NDC, the previous longwall mining was reviewed to provide information on critical spans and rock behaviour. As mentioned in the introduction, NDC was previously well known for its longwall mining with it being extensively implemented at all three shafts. It contributed to the bulk of the mine's coal production. The last longwall was nonetheless decommissioned in April 2021 due to ageing equipment and the presence of multiple dolerite dykes hampering production. Much experience and understanding were gained over the years, especially about high extraction mining and its effects on the surrounding and overlying ground conditions.

Longwall mining, as with pillar extraction, was characterized by an increase in vertical and horizontal stress as the longwall face mined away from its face line or start-up position, as it was also referred to. The stress continued to increase until a critical point was reached where the overburden goafed and the stress was released. This normally happened when the face

advance was about one and a half times the panel span. If the overburden hung up and the face advance was greater than the panel span, the stress merely stabilised at the high level. This high stress was then transferred to the abutments, which were formed by the face and inter-panel pillars of the chain roads (Van der Merwe & Madden, 2010).

NDC's longwall panels were typically 230 m wide and separated by chain roads consisting of three roadway panels. These formed the main- and tailgates of the respective panels. The first goaf in NDC longwall panels generally occurred after approximately 30 m to 45 m of advance. This was partial goafing (Figure 2-8 (a)) and was estimated to extend about 1 m to 2 m into the roof, thus only breaking into the overlying sandstone (Prinsloo, 2019). During this stage, the chain road pillars, which were designed as crush pillars, would remain under high vertical stress resulting in excessive pillar scaling. The tailgate, which is the chain road between the active longwall panel and the previous one, would also exhibit significant floor heave due to the high-stress conditions (Prinsloo, 2019).

Failure of the sill, and thus complete goafing (Figure 2-8 (b)), would only be achieved much later with frequent and continuous goafing as the longwall face continued to advance away from its start-up position (Prinsloo, 2019). Goafing would progressively extend deeper into the overburden until it reached the sill and exceeded its critical span. It is only then that the overburden would have completely goafed and resulted in surface subsidence. It was at this point that the load of the overburden rested on the

goaf itself and the high abutment stresses on the face and inter-panel pillars were relieved. The Survey Department measured the subsidence to be typically in the range of 0.6 m to 0.8 m (Salima, 2021a).

Although goafing naturally occurred in the longwall panel, the first goaf would only occur after about 30 m to 45 m of advance. The collapse of this amount of roof material, even though it extended to a maximum height of 2 m into the roof, resulted in a significant air-blast (Prinsloo, 2019). This posed a serious risk to the safety of the longwall mining personnel and equipment in the section, as well as the ventilation structures, such as walls and brattices. To reduce the magnitude of the air-blast and the associated risks, goafing would be initiated through blasting. This was achieved through pre-drilling the blast holes in the face line and allowing the longwall to advance approximately 9 m before they were charged with explosives and the immediate roof blasted (Prinsloo, 2019). The advantages of this exercise were that it first of all enhanced goafing, but limited the size of the initial goaf and the associated air-blast. The blasted material lying on the floor furthermore acted as a cushion for the initial goaf, thus further limiting the impact of the goaf and associated air-blast (Prinsloo, 2019).

2.5 Pillar Extraction Methods

Wagner (1981) stated that pillar extraction mining methods offer several advantages compared to longwall mining. These include more flexibility regarding geological disturbances, such as the presence of dykes, as well as lower capital costs. Pillar extraction methods make maximum use of the

load-bearing capacity of coal, thereby avoiding the need for powerful artificial roof support, which is characteristic of longwall mining (Wagner, 1981). He further states that pillar extraction does not only have the potential to supplement longwall mining but can replace it completely in several instances (Wagner, 1981).

As previously mentioned, there are several pillar extraction methods which have been trialled and implemented with various levels of success in South Africa, as well as in the rest of the world. These include but are not limited to the chequerboard, pillar splitting, Usutu, Christmas tree, Old Ben, Wongawilli and the NEVID methods (Moolman & Canbulat, 2003). The selection of a pillar extraction method will mainly be determined by the geological conditions and mining methods of a mine (Moolman & Canbulat, 2003).

2.6 NEVID method

NDC selected the NEVID method as its preferred pillar extraction method due to its success in the surrounding Sasol and Exxaro mines, namely Bosjesspruit and Matla collieries. The NEVID method, at that stage, had already proven itself to be one of the safest and most successful pillar extraction methods. It is also a fairly adaptable method which can be applied in most circumstances, especially in deeper coal mines with mining depths greater than 150 m (Moolman & Canbulat, 2003). The research therefore focused exclusively on the NEVID method because it has been firmly entrenched as the secondary mining method at NDC.

The NEVID method, which is a variant of pillar splitting, is classified as a partial extraction method due to the fenders and snooks being left behind (Figure 1-5). It was developed by Sasol Mining at their Bosjesspruit Colliery and named after the two people who developed it, Neels Joubert and David Postma (Moolman & Canbulat, 2003; Van der Merwe & Madden, 2010). Moolman & Canbulat (2003) describe it as one of the best pillar extraction methods, with its success predominantly attributed to its cutting sequence and consistency of the snooks and fenders left behind.

2.6.1 Stooping direction and cutting sequence:

The typical layout for the NEVID method consists of seven roadways with 28 m pillar centres, although this may vary from one mine to another. The in-pillar cutting sequence for each pillar, as well as the extraction sequence of the panel, ensures maximum protection of the CM at all times. This is achieved by always leaving a solid pillar or the strongest possible remaining snook adjacent to it (Moolman & Canbulat, 2003). Figure 2-11 shows the cutting sequence for a panel with an extraction direction from left to right.

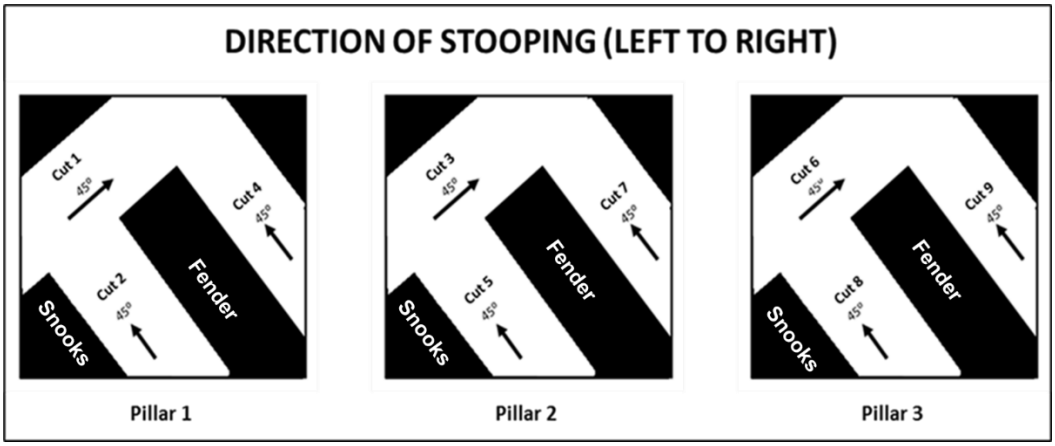


Figure 2-11: NEVID method cutting sequence from left to right (Van der Merwe & Madden, 2010).

The CM will start by taking cuts 1 and 2 on Pillar 1, after which it will move to the adjacent pillar to take Cut 3. While Cut 3 is being taken on Pillar 2, the remaining portion of Pillar 1 maintains stability of the intersection. The CM will then return to Pillar 1 to take the final cut from it. The remaining portion of Pillar 2 maintains stability of the intersection while Cut 4 is being taken on Pillar 1. The sequence is such that only one large intersection is created per pillar, namely between cuts 3 and 4, as well as between cuts 6 and 7 for the next two pillars. The CM will spend very little time in these enlarged intersections, thus minimizing its exposure to localised FOGs. The sequence will repeat itself until all the pillars in that specific split are cut (Van der Merwe & Madden, 2010).

Figure 2-12 shows that all cuts are taken at 45° to the original pillar sidewalls and that each cut consists of two lifts. Direction lines will be marked on the roof and the pillar before any cut is taken from it. They are marked on the

right-hand side of the first lift to be made by the CM, namely the “a”-lift. These assist the CM operator to easily control the cutting direction from a safe position (Moolman & Canbulat, 2003).

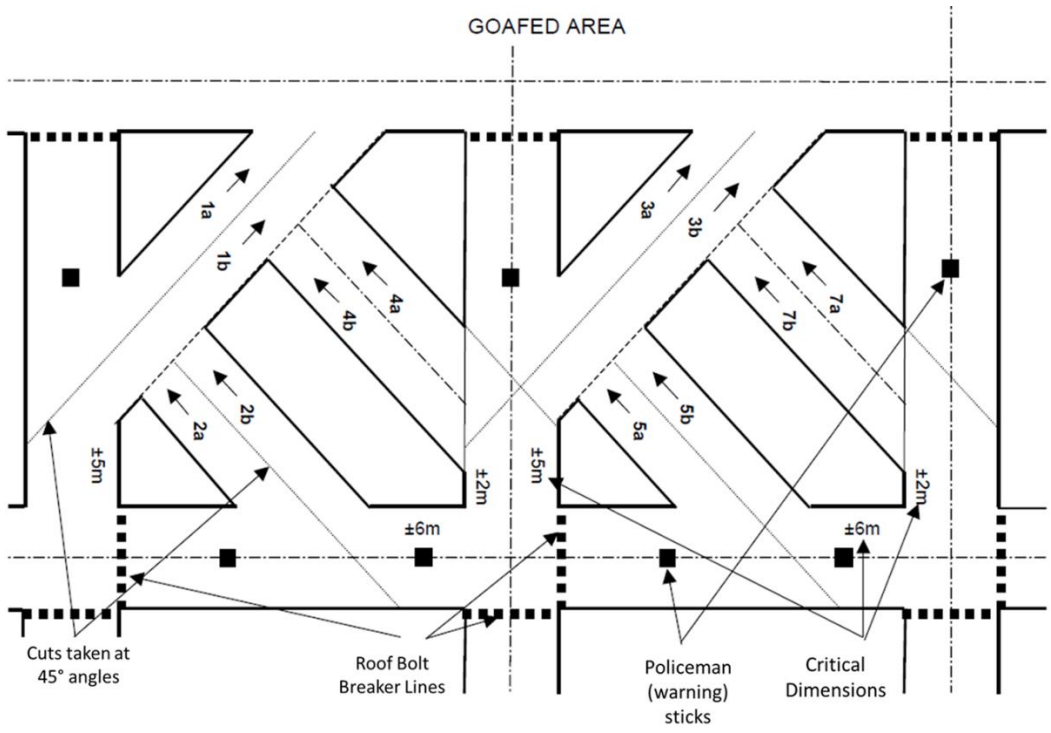


Figure 2-12: NEVID method cutting sequence with marked direction lines (Moolman & Canbulat, 2003).

The “a”-lift must always be cut through before the “b”-lift, due to it being shorter. It allows the CM to break through into the return air side of the pillar in the shortest possible time. This establishes through-ventilation, which improves dust removal and methane drainage, thus further enhancing safe extraction (Moolman & Canbulat, 2003). Several more benefits are associated with the cutting sequence and the angle of the cuts at 45°, namely:

- Goafing and localized FOGs on the working face is an inherent risk of pillar extraction operations. In the event of an imminent goaf, it is critical that all personnel are evacuated, and machines pulled out of the working face as quickly as possible. The 45° cutting angles provide for the fastest possible retreat of the CM should conditions dictate it (Moolman & Canbulat, 2003; Van der Merwe & Madden, 2010);
- It further improves the vision of the CM operator, which in turn allows him/her to have better control over the CM and the cuts being taken without being exposed to high-risk areas (Moolman & Canbulat, 2003; Van der Merwe & Madden, 2010); and
- Improved cutting and direction control also provide for greater consistency of the snooks and fenders, thus making the goafing pattern more predictable (Moolman & Canbulat, 2003; Van der Merwe & Madden, 2010).

The extraction direction of subsequent pillars is generally from left to right, thus against ventilation, and retreating as row after row of pillars are cut as shown in Figure 2-13 (Moolman & Canbulat, 2003; Van der Merwe & Madden, 2010). The pillars are numbered to ensure that each pillar is cut according to the sequence indicated on the approved stooping plan. The direction of ventilation and the configuration of the cable arm on the CM may however necessitate a change in the extraction direction, e.g. from right to left (Gonsalves, 2021).

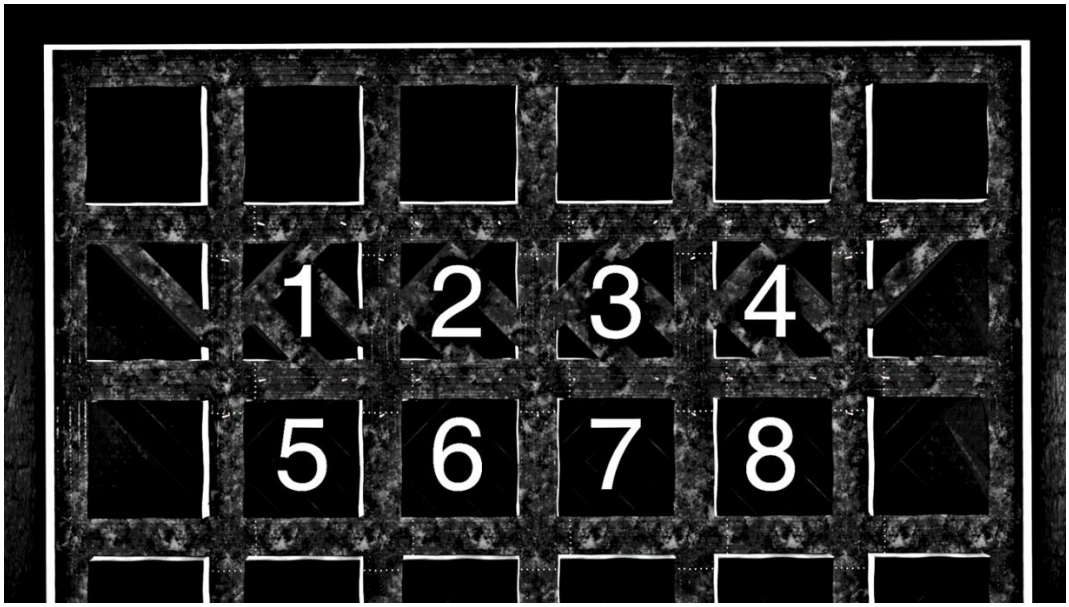


Figure 2-13: Extraction sequence of subsequent pillars (Sasol Mining, n.d.).

2.6.2 Fenders and snooks

Fenders and snooks are remnants of coal left behind during pillar extraction operations (Figure 1-4). The snooks, which are coloured purple, are the smaller pillar corners, while the fenders, coloured blue, are the larger strips of coal in the centre of the pillar. Their purpose is to maintain temporary stability of the roof in the specific work area where cutting operations are taking place (Van der Merwe & Madden, 2010; Sasol Mining, n.d.).

Van der Merwe & Madden (2010) found that snooks with a SF of 1 will remain stable for a couple of days. Those with a SF ranging between 0.6 to 0.8 should be stable for a couple of hours, while at 0.4 they should fail almost instantaneously. This was determined using elastic pseudo-three-dimensional boundary element modelling software for pillar extraction panels with a competent sandstone roof at a mining depth of 120 m. Van

der Merwe & Madden's (2010) findings should only be used as a guideline for determining the ideal snook and fender sizes, as there will be some variation from mine to mine due to the different mining parameters and ground conditions.

Snooks and fenders that are left too small may result in premature failure of these remnant pillars or of the roof in the working area. If they are left too large on the other hand, they will remain intact and prevent goafing (Van der Merwe & Madden, 2010). It is therefore essential that they be cut according to the design (Sasol Mining, n.d.).

2.6.3 Stopper pillars

Stopper pillars are defined as pillars that are either left completely intact or pillars from which only selected cuts are taken. They are left in strategic positions for several reasons which include the following:

- To compartmentalise goafing and reduce the associated air-blast risk, especially if a goaf has been hanging up for two or more splits. A stopper pillar will then be left on the third split to stop a potential goaf at that point (Moolman & Canbulat, 2003).
- To protect the bleeder road along the periphery of the panel for ventilation purposes (Figure 2-14). Generally, only 10 m cuts will be taken into the sides of these pillars, thus leaving much of the pillar intact (Sasol Mining, n.d.).

- To mitigate the impact of pillar extraction and its associated high abutment stresses on surrounding panels. Two rows of stopper pillars, for example, will be left at the end of a pillar extraction panel where it branches from a secondary or even a main panel (Van der Merwe & Madden, 2010).
- To prevent cutting of a pillar that was either left too small due to offline mining or is affected by one or more geological discontinuities making it unsafe to cut; and/or
- To protect sensitive surface structures (Gonsalves, 2021).

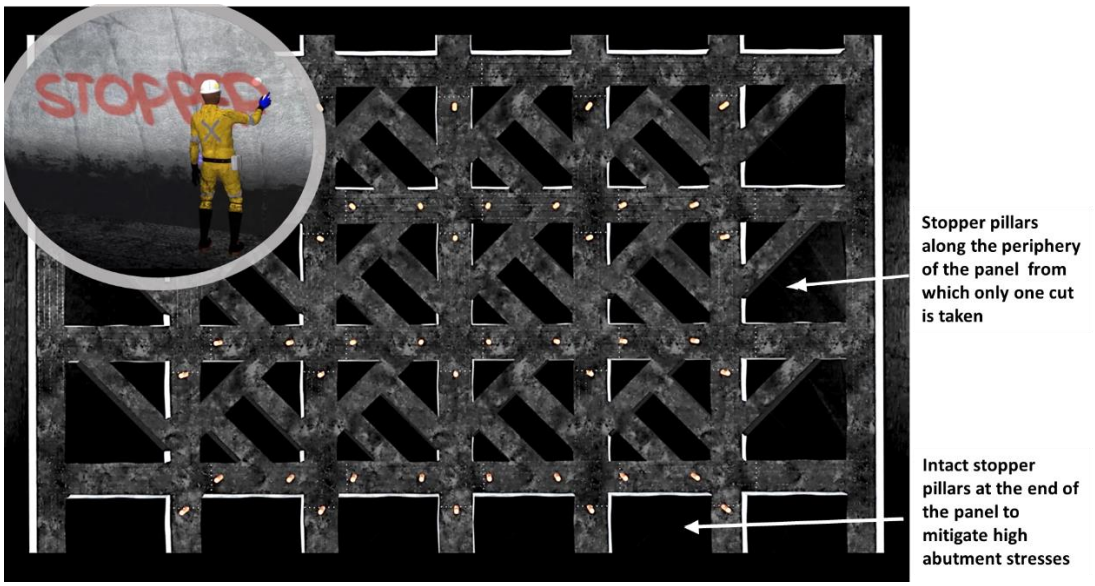


Figure 2-14: Stopper pillars along the periphery and at the end of the panel (Sasol Mining, n.d.).

The frequency and positioning of stopper pillars will vary from one mine to another based on the mining parameters and ground conditions. They must

be indicated on a plan and marked accordingly underground to ensure that they are left as per the design (Sasol Mining, n.d.).

2.6.4 Pillar extraction controls

Several controls are implemented in a pillar extraction panel to ensure safe extraction. These include the cutting sequence, as well as the size of the fenders and snooks. In addition, breaker lines (Figure 2-15), policeman sticks (Figure 2-16) and the visual inspections, which are done by the responsible face boss and CM operator in the section.

Breaker lines

A breaker line is defined as a row or rows of either roof bolts or timber props installed across the bord width between two pillars. Its function is to prevent the goaf from extending into the working area by arresting the planned displacement of roof strata at that point (Van der Merwe & Madden, 2010). It also forms a clear demarcation line between the goaf and the working area. It is therefore viewed as a critical control for stooping operations and must be installed according to standard.

The use of roof bolts for breaker lines has predominantly replaced timber props in modern-day stooping operations due to the numerous advantages associated with them. These include the fact that they can be installed during development, which means that people are not exposed to the goaf during the installation process, as is the case with timber props. They can furthermore be installed with relative ease and are not dependent on the

mining height (Van der Merwe & Madden, 2010). They will be installed in all the roadways leading from the active stooping intersection (Sasol Mining, n.d.; Gonsalves, 2021). The position of these breaker lines, when the stooping direction is from left to right, is shown in Figure 2-15.

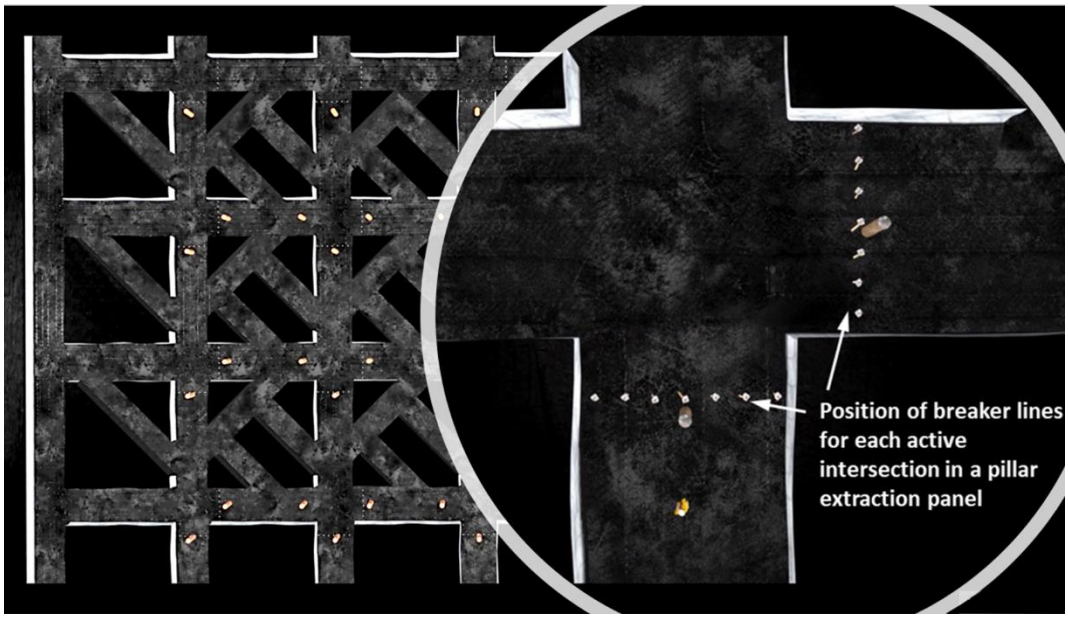


Figure 2-15: Positioning of breaker lines in each active intersection in a pillar extraction panel. Roof bolts are installed as breaker lines between the pillar corners (Sasol Mining, n.d.).

Monitoring

Monitoring for an impending goaf in a pillar extraction panel is critical for the safety of the mining personnel and the safeguarding of the machinery and equipment. It is achieved using policeman sticks and extensometers or closure-meters in all intersections. These are supplemented by observations made by the face boss and CM operator before and during cutting operations (Gonsalves, 2021).

Policeman sticks, as shown in Figure 2-16, are timber poles placed in strategic positions before and after certain cuts are taken. They will warn the face boss and CM operator of an impending goaf when they start to bend and crack due to the weight of the sagging overburden (Moolman & Canbulat, 2003; Gonsalves, 2021). They must be installed according to the sequence shown in Figure 2-17.

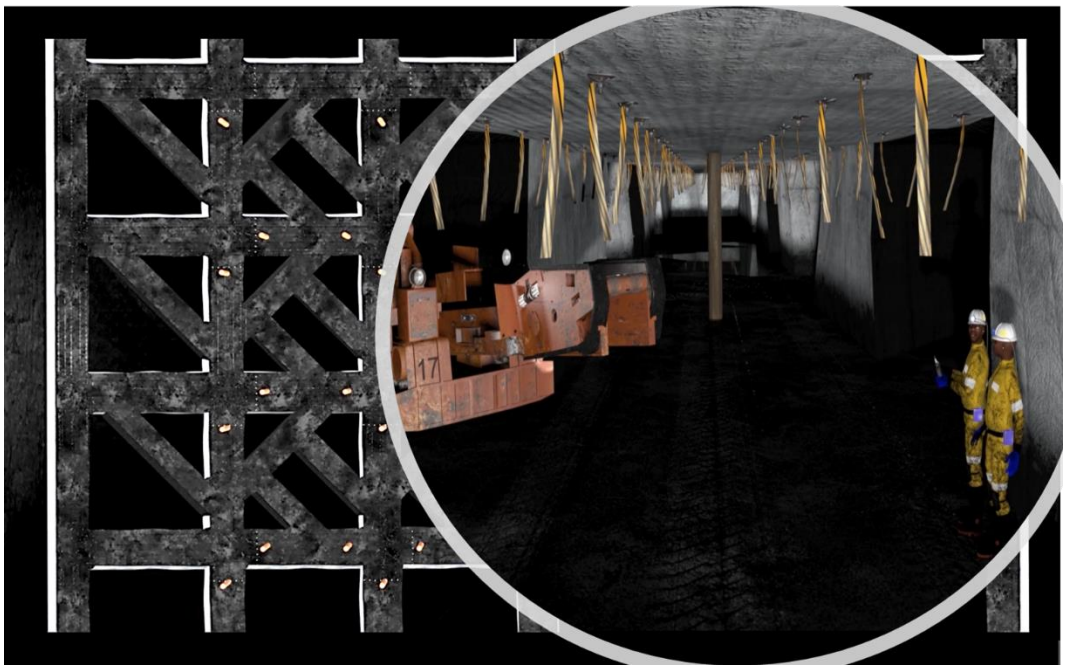


Figure 2-16: Timber poles placed in strategic positions as policeman sticks (Sasol Mining, n.d.).

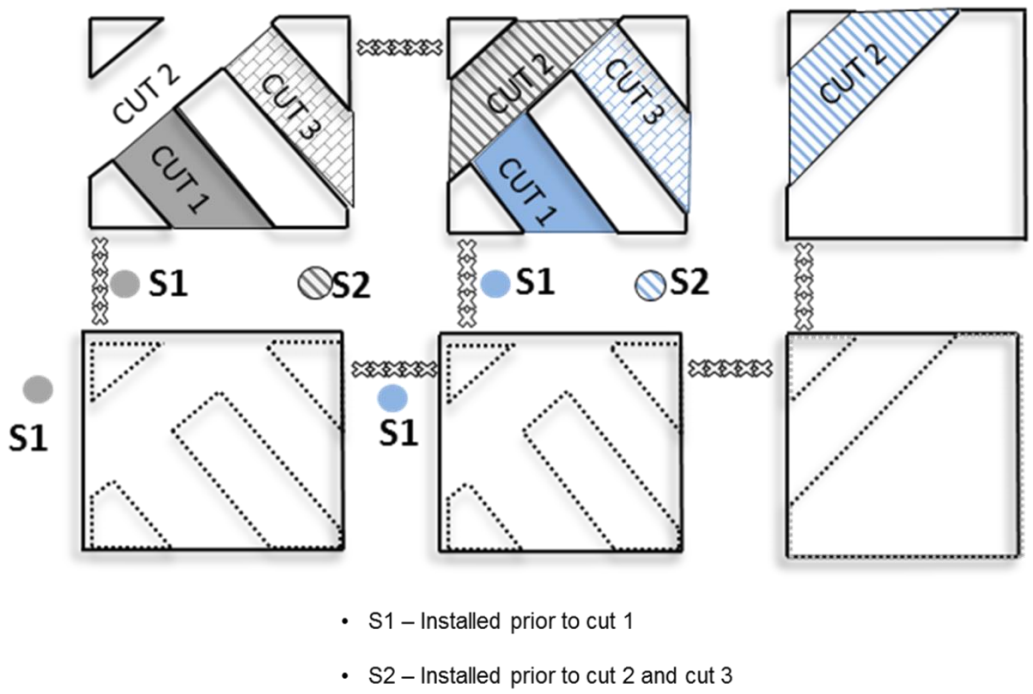


Figure 2-17: Placement of policeman sticks before and after certain cuts are taken (Gonsalves, 2021).

Roof monitoring devices, also known as telltales (extensometers), are installed in each intersection to monitor the stability of the roof while working in the intersection. The type and length of the roof monitoring devices will differ from one mine to another based on the general depth of failure.

Awareness of the ground conditions, especially the change thereof as more and more pillars are extracted, is key to safe pillar extraction operations. The responsible face boss and CM operator must ensure that all the required controls are in place before any pillar extraction commences. They also need to check for telltale signs of an imminent goaf, which include the following: bending or cracking policeman sticks, bumping and cracking noises from the goaf area, increased water seepage from the roof, triggered

roof monitoring devices and excessive pillar scaling and spalling (Gonsalves, 2021).

2.7 Numerical Modelling

2.7.1 Introduction

A model is an attempt to replicate reality for various purposes, such as prediction or gaining fundamental understanding. Modellers can adjust the model's features, allowing them to safely explore different mining scenarios and their potential outcomes in a safe, risk-free manner (Van der Merwe & Madden, 2010). With the advent of computers, numerical models have emerged as the most powerful type, capable of simulating complex geometries and interactions based on established physical laws (Van der Merwe & Madden, 2010).

2.7.2 Different types of numerical models

All models are composed of different elements that are interconnected to form a simulated geometry. There are two main approaches to achieve this. The first involves modelling the rock mass where mining takes place, with openings representing the excavations – this method is called 'finite element' modelling. The second approach models the outline of the excavations, with the space between the boundaries representing the rock environment – these are known as 'boundary element' models (Van der Merwe & Madden, 2010).

Finite element models offer the advantage of assigning different properties to the rock mass at almost any point. However, they require significantly longer computation times compared to boundary element models. For many years, mainframe computers were needed to run these models (Van der Merwe & Madden, 2010). Some examples of numerical modelling software packages using the finite element method are RS_2 and RS_3.

Boundary element models, on the other hand, are favoured for their simplicity in setup and faster execution. Although they may not always provide the same level of precision as finite element models, their accuracy is generally sufficient for most mining applications (Van der Merwe & Madden, 2010; Jansen van Vuuren & De Beer, 2022a). Some examples of numerical modelling software packages using the boundary element method are Map3D and LAMODEL.

A compromise between the two is the discrete element model, which treats the rock mass as a collection of individual blocks of any shape. Each block functions as a mini boundary element, connected to neighbouring blocks through user-defined friction and cohesion. These models closely represent a real rock mass composed of fragmented material, unlike other models that simulate joints or faults by softening the rock mass (Van der Merwe & Madden, 2010).

Hybrid models also exist, combining both boundary and finite element techniques. While they offer the benefits of both types, they are more

complex and not as user-friendly for non-expert modellers (Van der Merwe & Madden, 2010).

2.7.3 LAMODEL

LAMODEL v.3.0.2 (West Virginia University, 2013, as cited in Jansen van Vuuren & De Beer, 2022a) was chosen as the preferred numerical modelling software for this research project. It is an elastic pseudo-3D boundary-element programme used to simulate and calculate the vertical stress and displacements in stratified, laminated, sedimentary deposits, at the seam level. It uses the displacement-discontinuity variation of the boundary-element method with a simplified laminated overburden model. Due to its formulation, it was able to analyse large areas quickly and effectively (Jansen van Vuuren & De Beer, 2022a).

LAMODEL is different from other boundary-element modelling software in that it applies a laminated overburden model (LAMODEL) as opposed to a homogeneous, elastic overburden model. The laminated overburden model has been found to provide more realistic stress and displacement calculations, particularly with layered sedimentary geology that is associated with coal deposits. The software also has the capability to apply the effect of a variable topography. Most importantly, it can simulate coal pillars as per the original mine plan, i.e. as the pillars are formed. It can therefore simulate the effect of variable sizes of pillars that is the result of offline mining, which is a common occurrence in mechanised mining (Jansen van Vuuren & De Beer, 2022a).

The ‘nonsense in, nonsense out’ (NINO) principle also applies to LAMODEL, as it does to any other numerical modelling software. It implies that one should be aware of the limitations to the output accuracy of a specific numerical modelling software. In any event, a model merely results in a quantified answer to a question about loads or displacements based on the quality of the input parameters and setup of the model. A well setup model by an experienced modeller with good quality input parameters will result in more accurate results, whereas the opposite is also true. It is nonetheless critical to understand the limitations of the software and use sound engineering judgement to analyse the results and predict whether failure will occur (Van der Merwe & Madden, 2010). Some of LAMODEL’s limitations are listed below:

- Linear-elastic modelling – the induced stress load can easily be over or underestimated as the element does not yield, but continues to absorb load, beyond its actual capability (Jansen van Vuuren & De Beer, 2022a).
- Although different material properties can be assigned to different layers in the overburden, each layer is still considered to be continuous, homogeneous and isotropic (Jansen van Vuuren & De Beer, 2022a).
- Only one rock-type/layer can be modelled at a time. If the focus point, for example in a coal mine, is on the coal pillars, one would not be

able to see the influence of stress on the roof and floor (Jansen van Vuuren & De Beer, 2022a).

- The setup of the model, specifically that of the pillar dimensions and layout, will be based on the latest Survey measurements and plans and will not consider any pillar scaling that might have taken place since development (Jansen van Vuuren & De Beer, 2022a).

3 GEOLOGY OF NEW DENMARK COLLIERY

3.1 Stratigraphy and Geological Structures

The geological setting, stratigraphy and the presence of geological structures are some of the most important factors to consider for the planning of stooping sections and the prediction of goafing. It is therefore essential to have a good overview of these.

3.1.1 Stratigraphy

NDC's lease area lies within the Highveld Coalfield. It is underlain by the coal-bearing Vryheid Formation of the Ecca Group, which in turn overlies the Dwyka Group. Both the Ecca and Dwyka groups form part of the Karoo Supergroup, which was deposited on a glacially sculpted pre-Karoo basement (Gonsalves *et al*., 2021). Figure 3-1 shows the general stratigraphic column for NDC. This research will focus extensively on the No. 4 coal seam, as well as the strata forming its floor and roof. It is the only seam of economic interest.

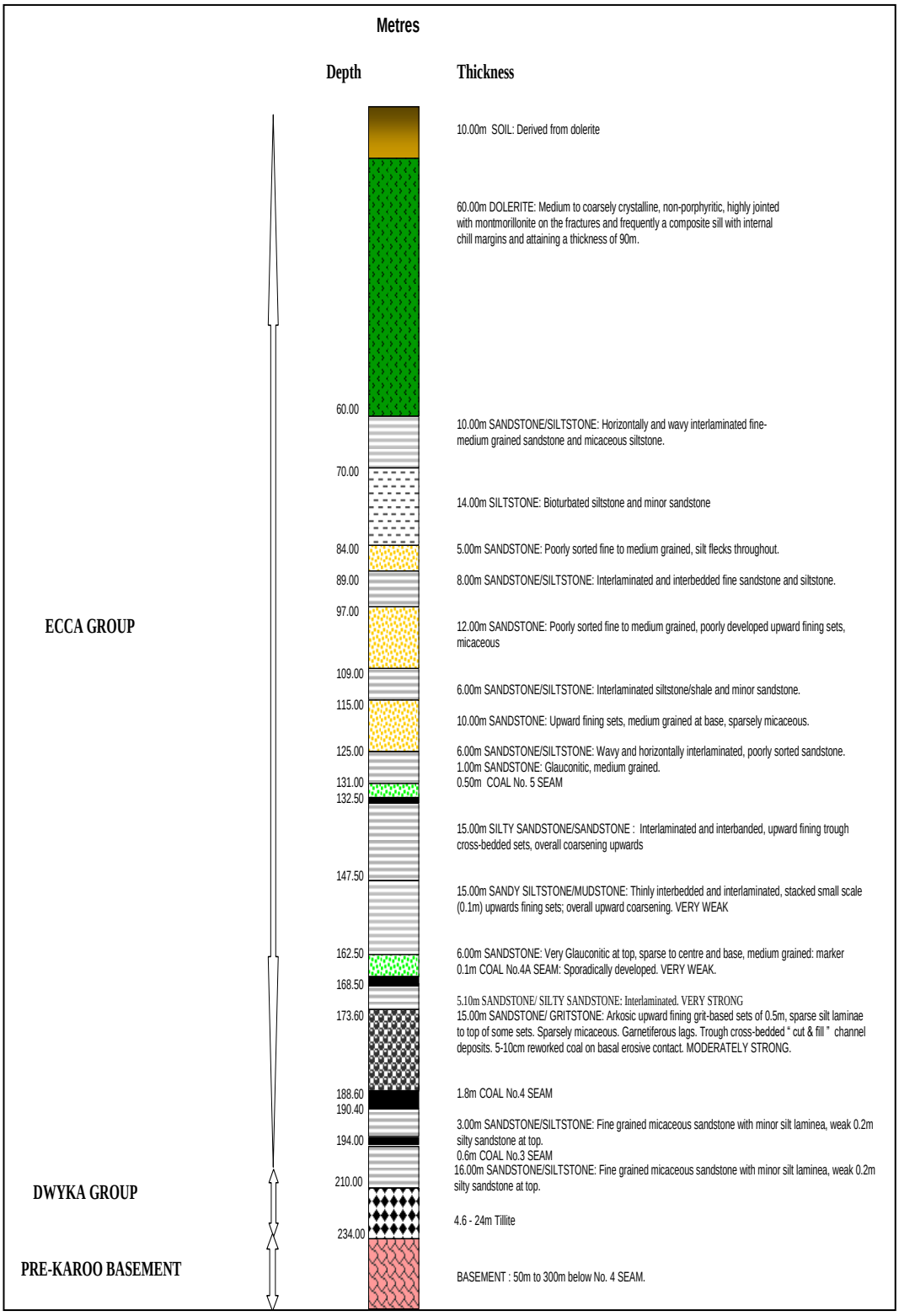


Figure 3-1: General stratigraphic column for NDC (Sibiya, 2021).

No. 4 coal seam

The No. 4 coal seam has an average thickness of 1.85 m and ranges from a minimum of 1.50 m to a maximum of 2.70 m. It is mined at an average depth of 200 m below the surface, with a minimum mining depth of 140 m to a maximum of 280 m below the surface (Gonsalves *et al*., 2021).

No. 4 coal seam - roof

The immediate roof of the No. 4 seam generally consists of a relatively competent, medium-to-coarse-grained sandstone and gritstone. It ranges in thickness from 15 m to 20 m and consists of vertically stacked cross-bedded sets which decrease upwards in scale and grain size. This unit is generally able to bridge over large unsupported spans (Gonsalves *et al*., 2021).

A few areas have nonetheless been identified where the immediate roof consists of fine-grained, interlaminated sandstone and siltstone. These finer-grained sediments represent quieter depositional areas within the original braided river environment. The roof type of fine-grained interlaminated sandstone and siltstone is relatively small in extent and occurs randomly. The micaceous interface between the sandstone and siltstone increases the propensity for roof failure, however, is still managed by the normal systematic support (Gonsalves *et al*., 2021).

Three sills of various thicknesses are also present higher up in the stratigraphy. These add to the competency of the roof when doing partial or full extraction. They will be discussed in more detail under Section 3.1.2.

No. 4 coal seam - floor

The immediate floor of the No. 4 seam generally consists of a 3 m to 5 m thick sequence of upward coarsening sandy siltstone or bioturbated silty sandstone (Gonsalves *et al*., 2021). Four different rock types have been identified as the No. 4 seam immediate floor across the lease area. These are listed below:

- Dark grey, carbonaceous and micaceous siltstone;
- Medium to dark brown, highly micaceous silty sandstone;
- Pale brown, micaceous and slightly silty sandstone; and
- Pale greyish white, fine-to-medium-grained sandstone.

Mining experience at NDC has established that over much of the area, the first two floor types are the most common (Gonsalves *et al*, 2021; Sibiya, 2019). They are highly susceptible to weathering in areas with water accumulation and readily fail in areas affected by high horizontal stress due to their weak strength properties (Sibiya, 2019). Floor heave is often observed in the tailgates of mined-out longwall panels and return ways of stooped panels (Prinsloo, 2019).

3.1.2 Geological structures

Faults, dykes and sills are the three main geological structures found across the NDC lease area. As previously mentioned, these structures act as stress concentrators and can increase the risk of FOGs in the working area. They can also alter the goafing behaviour from that what is expected for the panel

(Galvin, 2015). Figure 3-2 indicates the most recent structural plan for NDC as compiled by the NDC Geology Department.

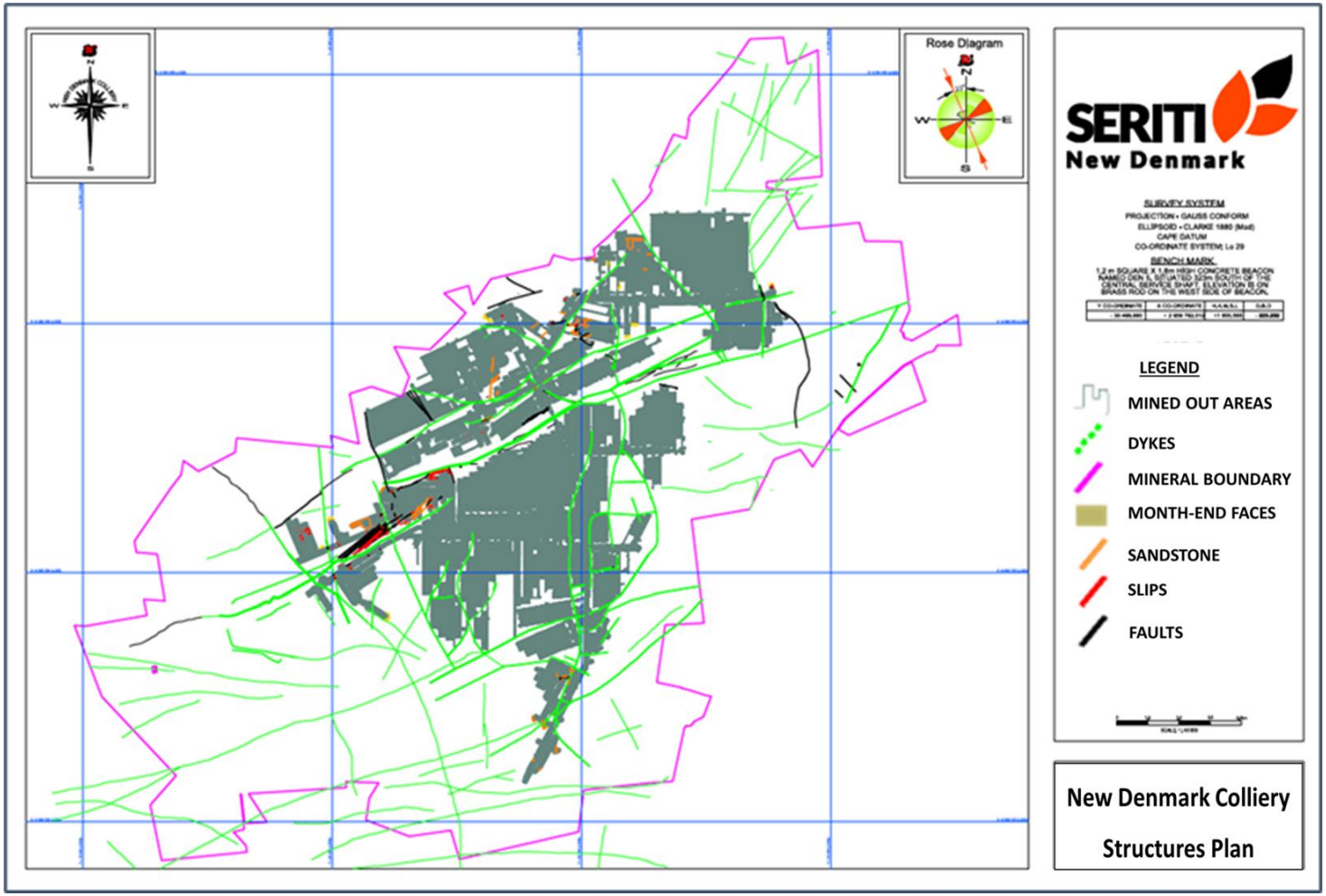


Figure 3-2: NDC Geological Structures Plan (Sibiya, 2022).

Dykes

Two types of dykes occur across the NDC lease area, namely, Type A and Type B. Type A dykes have a northerly to northwest strike direction and range in thickness from 0.5 m to 4.5 m. The width of devolatilisation associated with these intrusions is approximately twice the width of the intrusions (Gonsalves *et al*., 2021). Type B dykes vary in thickness from 9 m to 70 m and have a common east-to-northeast strike direction. The extent of devolatilisation of the coal seam averages three times the width of the dyke (Gonsalves *et al*., 2021).

Aeromagnetic surveys have also identified numerous linear features that could represent dykes. These are indicated on the structural plan as stipple green lines. They are only confirmed as dykes and consequently changed to solid green lines on the plan when they are intersected by in-seam underground long-hole (horizontal) drilling, surface directional drilling and mining itself (Gonsalves *et al*., 2021).

Dykes pose a significant risk to mining. Over and above the safety risks, loss of coal due to burning and/or devolatilisation and delays to production may be substantial. Disturbance of the ground along the dyke may include friable ribsides, slabbing of the immediate sandstone roof and the presence of multiple, sympathetic joint planes. The presence and extent of such ground conditions varies from dyke to dyke (Gonsalves *et al*., 2021).

Sills

There are three correlatable dolerite sills present in the NDC area, which are distinguished by thickness and appearance. The first sill, non-porphyritic in texture, named B4, has an average thickness of 30 m. This sill occurs just beneath the topographic surface. It is the oldest of the three sills and has mostly been weathered away in low-lying areas. It is relatively flat and consists of fine-to-medium crystalline olivine-rich dolerite (Gonsalves *et al*., 2021). The second sill, denoted B8, is porphyritic in texture and has an average thickness of 32 m. The sill occurs just below the B4 sill, it is the youngest of the three sills and is also weathered away in low-lying areas. The upper fragmented portion of these sills is one of the water aquifers in the area. Goafing of these sills may lead to large amounts of water flowing into the underground workings (Gonsalves *et al*., 2021).

The third sill is named B6. It is porphyritic in texture and ranges in thickness from 0.2 m to 4.0 m. It is older than the B8 sill and often transgresses various stratigraphic units, including the No. 4 coal seam. Available borehole data indicates that this sill lies well above the No. 4 coal seam in most areas of the NDC lease area, but transgresses into the No. 4 coal seam in several areas. A variable displacement is associated with the B6 sill intrusion where it transgresses the No. 4 coal seam. Where this B6 sill is near the No. 4 coal seam it has caused extensive burning and poor roof conditions (Gonsalves *et al*., 2021).

4 STOOPING HISTORY AT NDC

4.1 Implementation of Stooping at NDC

In 2017, NDC management started to investigate stooping as an alternative high-extraction mining method due to the challenges faced with longwall mining. NDC started stooping towards the end of 2018 using the NEVID stooping method as previously mentioned. Panel 1111 was the first panel to be stooped even though the original mining was not designed for it. It was viewed as a trial to determine the feasibility of stooping at NDC.

4.1.1 1100 Block

Stooping operations at NDC started with Panel 1111 in the 1100 block at Central Shaft (Figure 4-1). It was soon followed by the stooping of panels 1126, 1124, 1122, 1109, a portion of 1105, 1118, 1116 and lastly 1107. These were old panels and not initially planned and consequently designed for stooping. The NEVID method had to be adjusted according to the prevailing mining parameters, for example, in Panel 1126 only two cuts were taken on smaller pillars as opposed to the normal three cuts per pillar. The panels were also too narrow to induce goafing and as a result, minimal goafing occurred in these panels. All stooping controls were nonetheless implemented.

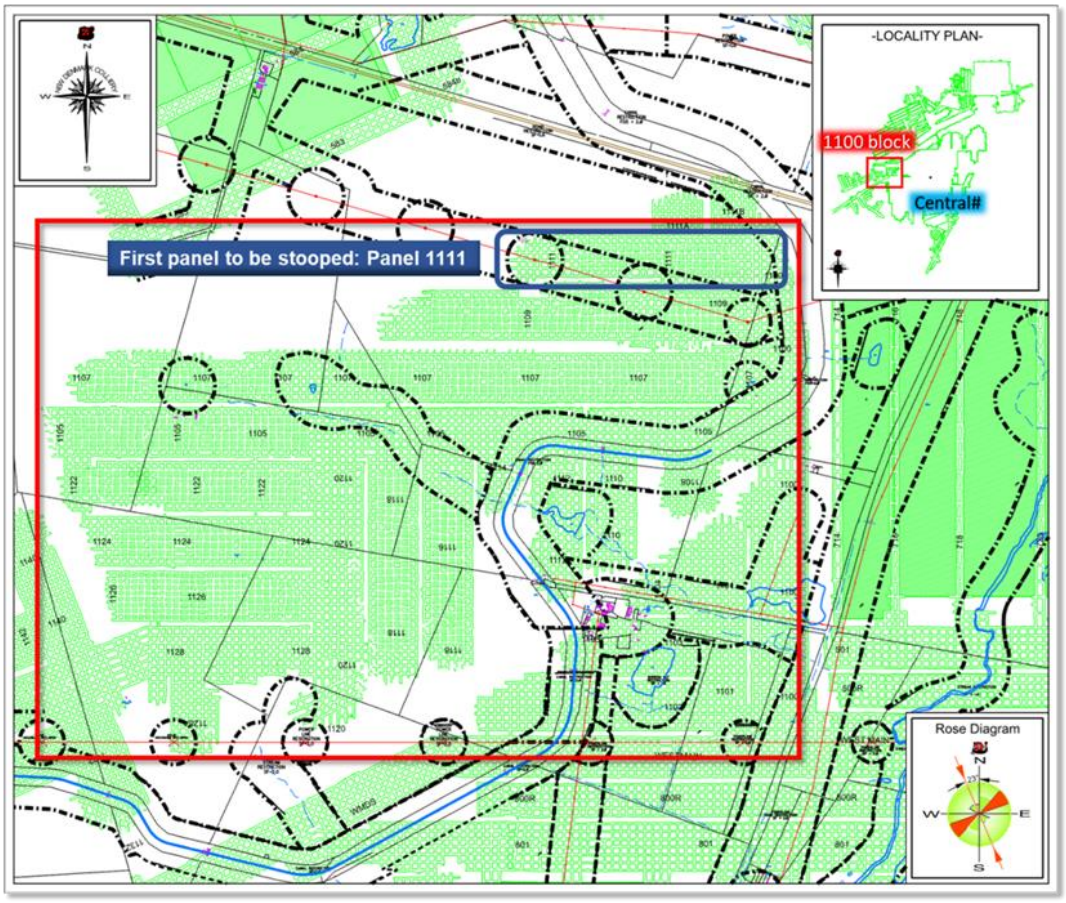


Figure 4-1: NDC mine plan indicating the 1100 block where stooping was first trialled in Panel 1111.

The fourth fender-reducing cut, as applied at Matla Colliery, was introduced by the on-site rock engineer once he realised that goafing was unlikely. This was a 5 m deep cut into the fender once the third cut had been taken on the pillar as shown in Figure 4-2. The CM would take this cut before tramming out of the active intersection and taking Cut 2 on the following pillar. The idea was to enhance production and attempt to induce goafing by reducing the sizes of the fenders left behind. The proposal was initially met with resistance from the mining department and as a result not consistently taken.

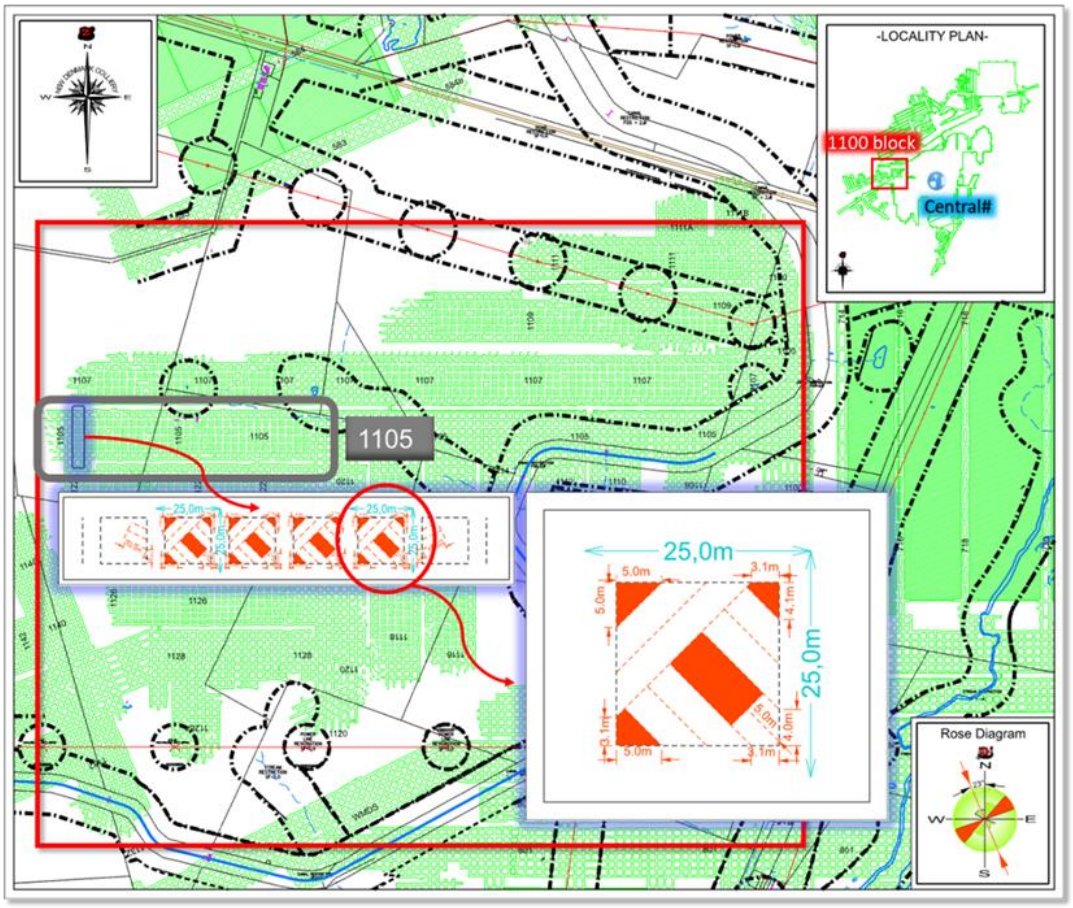


Figure 4-2: NDC mine plan indicating Panel 1105 where the fourth fender-reducing cut was first introduced.

The stooping of panels perpendicular and parallel to the main development, Panel 1120, later proved to be a costly exercise. The induced high stress from the surrounding panels caused excessive scaling of the pillars along the 1120 Main belt and travelling roads (Figure 1-8). Upon investigation, the condition of the pillars was attributed to the induced high stress exacerbating deterioration of pillars already affected by layer-bound joints. These pillars consequently had to be wrapped with mesh, as seen in Figure 4-3, to prevent further scaling and maintain long-term stability.



Figure 4-3: Pillars along Panel 1120 travelling road wrapped with mesh to prevent further scaling.

Stooping of the 1100 panels was nevertheless considered as a success as it proved that stooping could be safely done at NDC. Apart from the valuable lessons learned, it contributed approximately 890 thousand tons of coal to NDC's production.

4.1.2 Shosholoza stooping panels

Shosholoza Section started stooping soon after the stooping of the 1100 panels began. Figure 4-4 shows the layout of these panels relative to the main development, Panel 1134.

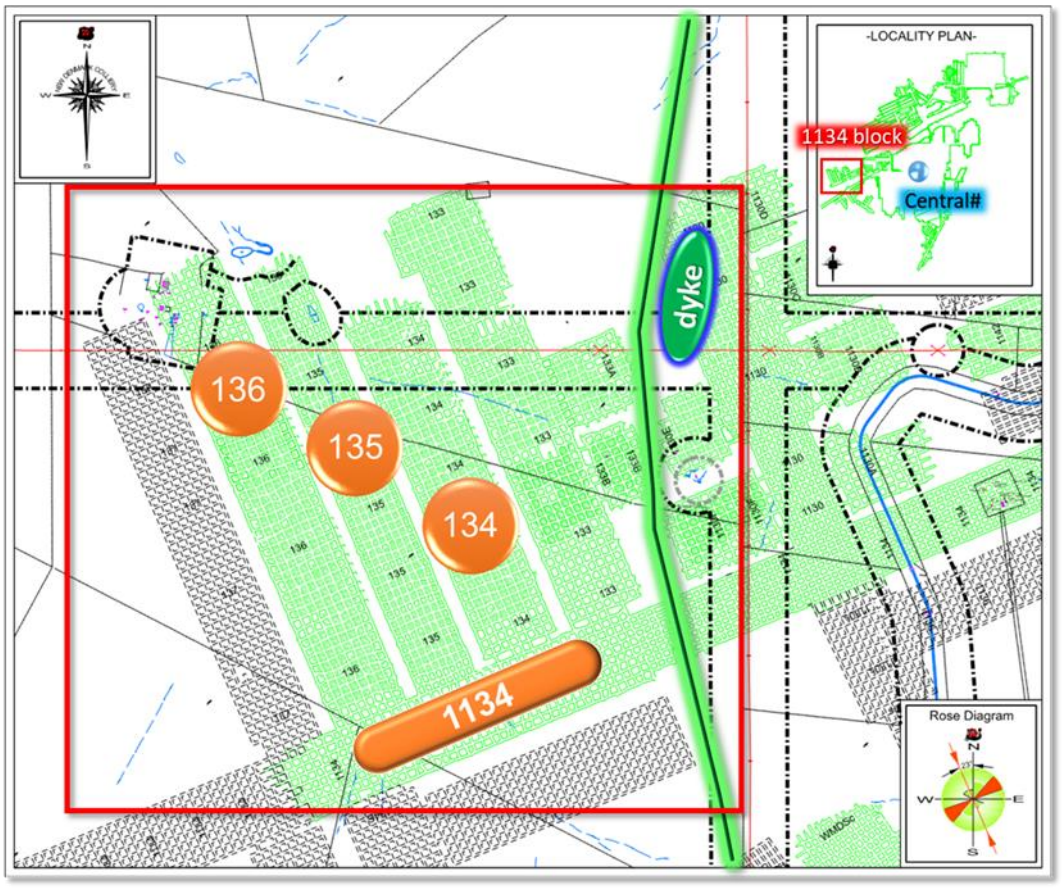


Figure 4-4: Shosholoza panels 134, 135 and 136 relative to main development, Panel 1134.

Development of Panel 135 had already begun before stooping operations in the 1100 panels. It was thus not initially planned for stooping, hence, its narrower pillar dimensions and consequently panel span compared to the two adjacent panels, 134 and 136. Management soon changed their minds when stooping proved to be successful in the 1100 panels. However, a couple of changes had to be made to the NEVID method due to the smaller pillar sizes and ventilation direction. The ventilation was from left to right, which meant that stooping had to be done in an opposite direction from how it was normally done. Consequently, the in-pillar cutting sequence and

positioning of the breaker lines had to be a mirror image of a normal stooping panel as shown in Figure 4-5. The three in-pillar cuts furthermore had to be fitted into two different-sized pillars with centres of 28.0 m (length) x 19.0 m (width) and 24.0 m (length) x 19.0 m (width).

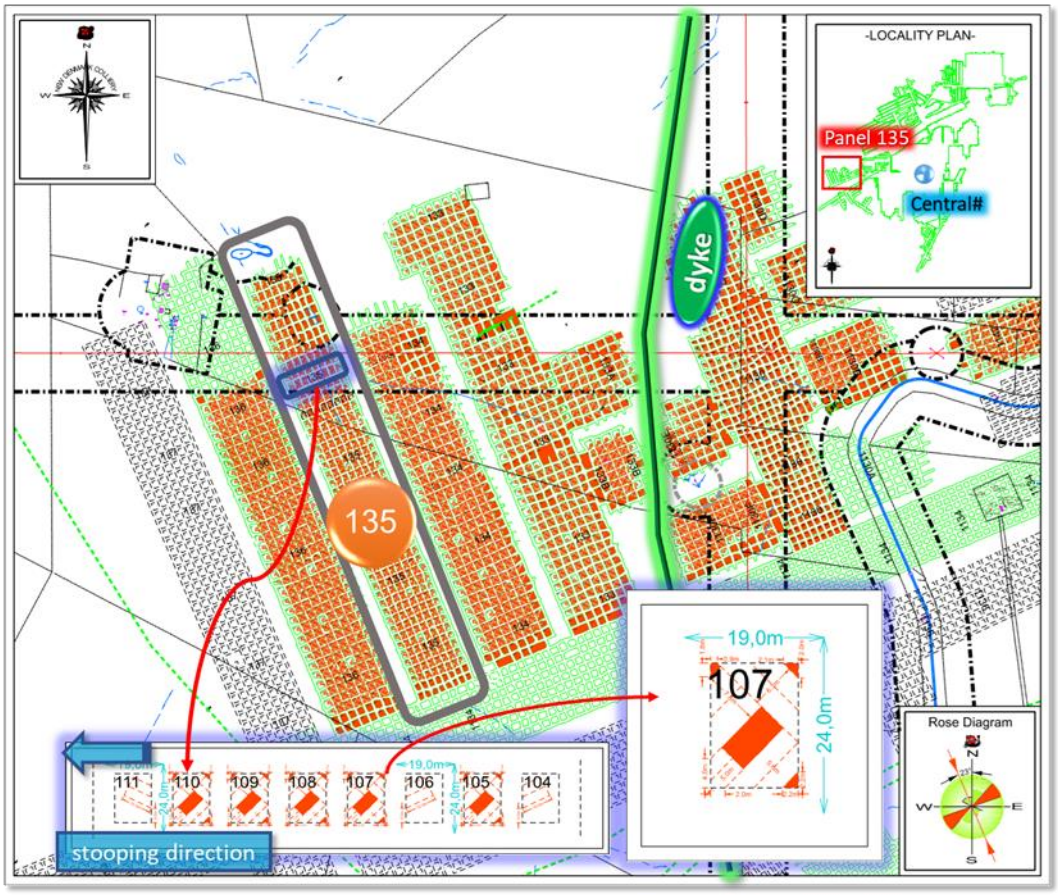


Figure 4-5: Panel 135 with pillar centres of 24.0 m (l) x 19.0 m (w).

Panels 136, 134 and most recently 133 were developed and stooped afterwards. They were planned for stooping, hence, their pillar centres were increased to 26.0 m (length) x 24.0 m (width). This was found to be the ideal pillar dimension for NDC as it provided a sufficient SF of more than two

during development and allowed for the three cuts during stooping. The SF was calculated using the squat-pillar formula as given by Equation 2-2.

Shosholoza Section had already developed and stooped panels 135 and 136 when the excessive pillar scaling was detected in Panel 1120. In response, the on-site rock engineer made a slight change to the design and layout of the pillars at the start of the panel as seen in Figure 4-6. These were large panel-entry pillars, as commonly referred to on the mine. Their pillar centres were 26.0 m (length) x 40.8 m (wide). Their function was to minimise the impact of the high abutment stress from the stooped panel onto the main development. The layout further ensured that there were limited entries into the stooping panel making access control and sealing of the panel at the end easier (Gonsalves, 2023). This layout was then applied to all other panels planned for stooping.

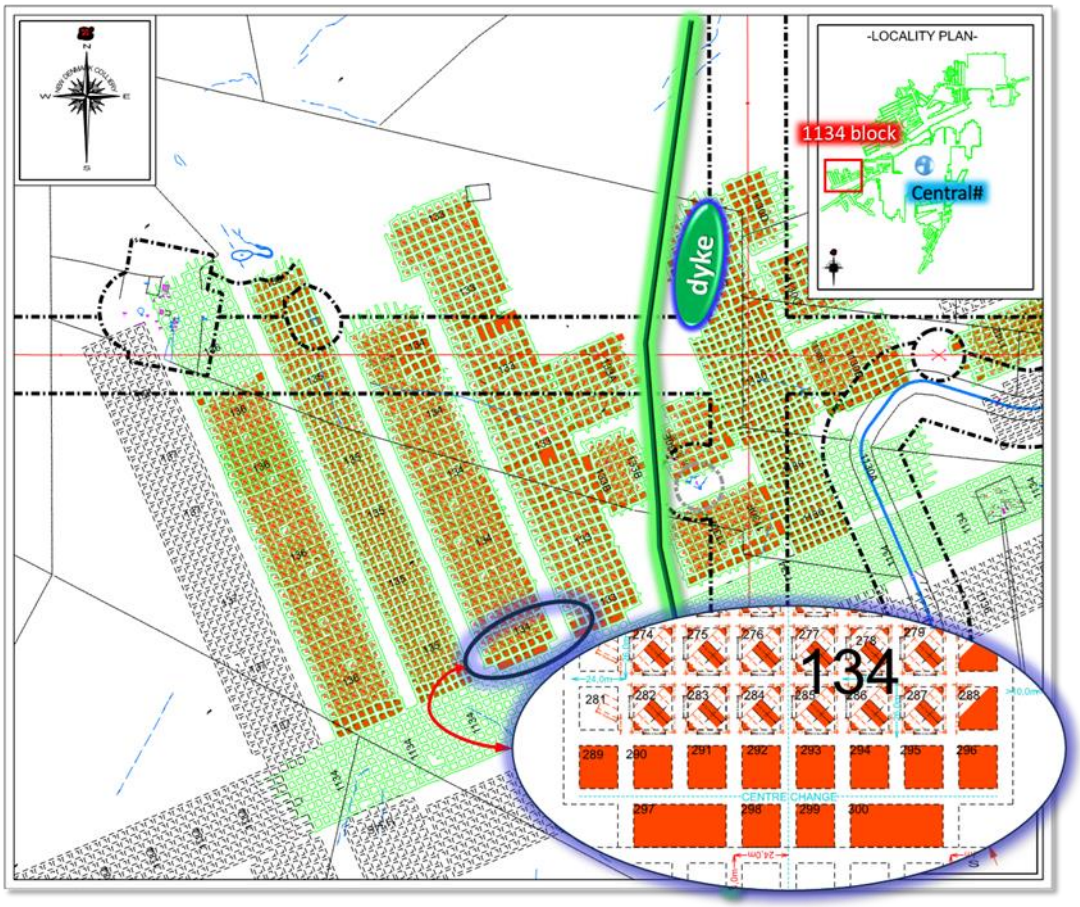


Figure 4-6: Panel 134 with modified panel-entry configuration.

4.2 NDC's Current Stooping Strategy

Stooping has been well entrenched at NDC with a total of 50 panels safely stooped up to date across all three shafts. It is responsible for about 30% of NDC's annual coal production. Much experience has been gained and several lessons learned since it was first trialled in Panel 1111 (Figure 4-1). These lessons have been used to improve NDC's stooping strategy over the last five years. The NEVID method and its associated controls have throughout remained the core of this strategy.

4.2.1 Panel layout and pillar design

Most panels that are planned for stooping typically consist of nine roadways with pillar centres of 26.0 m (length) x 24.0 m (width) as indicated in Figure 4-7. It allows for the three cuts per pillar to be taken as per the conventional NEVID method. The fourth fender-reducing cut is included but is to be taken at the discretion of the face boss and/or CM operator. They will only take the cut if it is safe to do so and there are no signs of an imminent goaf, e.g., the surrounding policeman sticks are all intact. The percentage area extraction per pillar will be approximately 50% during development and increase to 80% during stooping. The fourth fender-reducing cut will increase this percentage by another 3-5% if it is taken.

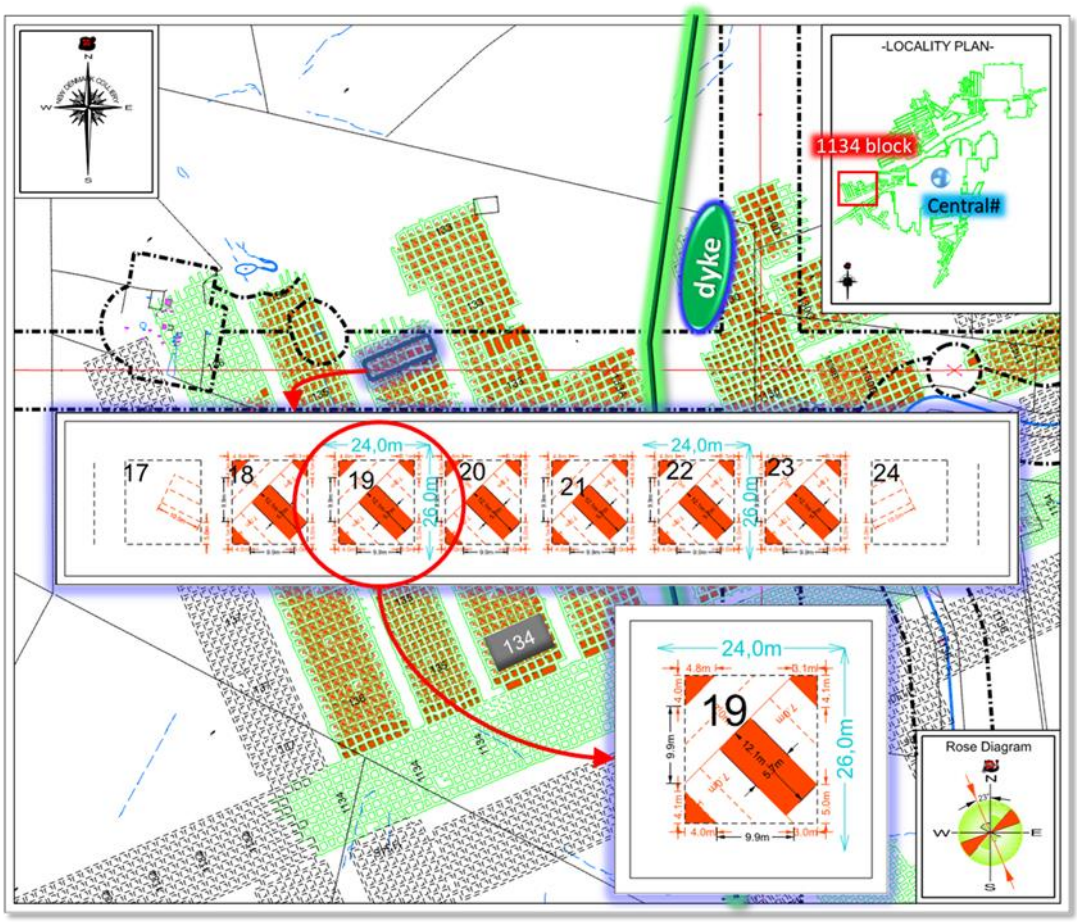


Figure 4-7: Panel 134 planned for stooping with pillar centres of 26.0 m (l) x 24.0 m (w).

4.2.2 In-pillar cutting sequence and stooping direction

The in-pillar cutting sequence and stooping direction are as per the NEVID method shown in Figures 2-11, 2-12 and 2-13. The ventilation is typically from right to left which means that the stooping direction within the panel will be from left to right, thus against ventilation. There are, however, rare occasions where the ventilation is in the opposite direction as was the case with Shosholoza Panel 135. In these panels, the ventilation flows from left to right which means that the stooping direction is from right to left. The stooping strategy, principles and controls remain the same, except that the

in-pillar cutting sequence and positioning of the breaker lines are mirror images of those in the normal stooping panels.

It is furthermore considered good practice that the stooping of adjacent panels be done according to such a sequence that a section will always stoop away from a previously stooped panel (Van der Merwe & Madden, 2010). Adjacent panels will thus be stooped in the same direction as that of the previous panel which is generally from left to right. The opposite applies for panels where the in-pillar cutting direction is from right to left. Figure 4-8 shows the sequence in which panels 040, 042 and 044 were developed and stooped by Simunye Section as an example. The in-pillar cutting sequence for these panels was from left to right, thus against ventilation. As a result, the panels were also developed and stooped in sequence from left to right.

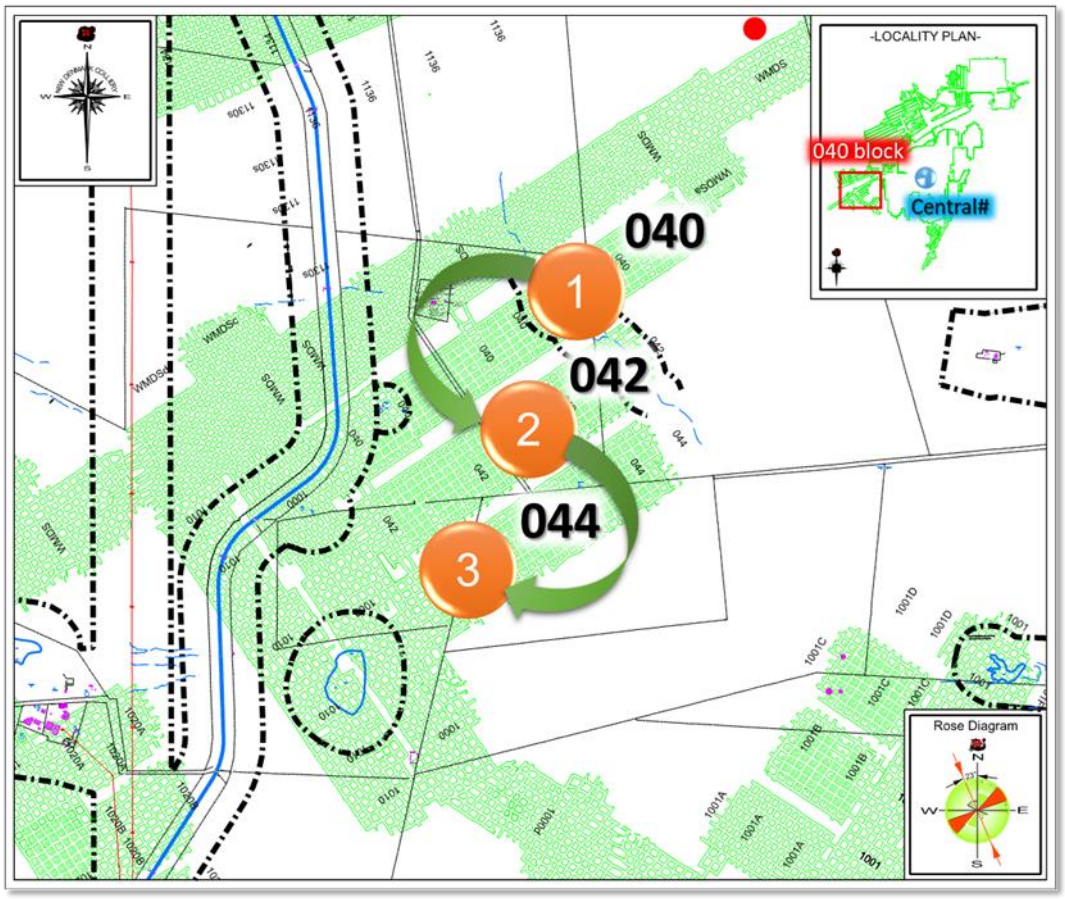


Figure 4-8: NDC plan indicating the left-to-right stooping sequence of panels 040, 042 and 044.

It is not always possible to mine according to good practice, especially when a panel forms a dog-leg with the main panel. In such an instance, Van der Merwe & Madden (2010) have suggested that one or more rows of stopper pillars be left at the end of the dog-leg panel to mitigate its increased stress from affecting the main panel. An example of this can be seen in Figure 4-9 where Panel 133 has two side-panels 133a and 133b.

Panel 133 was developed to the end of the panel and stooped back up to the planned position of Panel 133a. Panel 133a was thereafter developed and stooped back, leaving one row of stopper pillars between it and Panel 133. Stooping then resumed in Panel 133, but the in-pillar cutting sequence was in the direction of the recently stooped Panel 133a. The same sequence applied to the development and stooping of Panel 133b. Although it is not considered good practice to stoop in the direction of a previously stooped panel, the stooping operations were completed successfully due to a pre-mining risk assessment and putting the necessary controls in place, such as the row of stopper pillars between the main and side-panels.

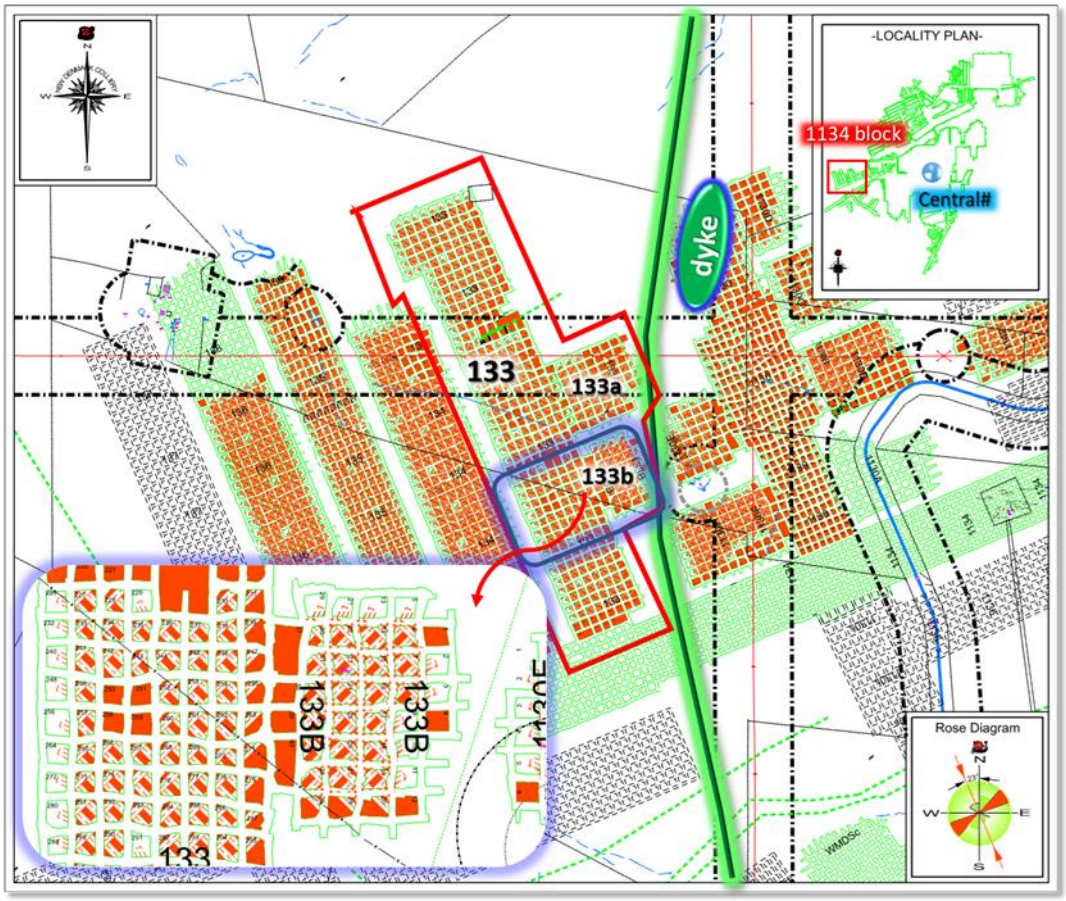


Figure 4-9: NDC stooping plan showing Panel 133 and one of its side-panels, Panel 133B.

4.2.3 Fenders and snooks

Fenders and snooks are left behind to ensure temporary stability of the working area. Snooks at NDC are, however, not considered for stability due to them generally being reduced in size by excessive pillar scaling during stooping. The focus is thus mainly on the fenders to maintain stability of the immediate working area. Figure 4-10 shows the dimensions of a stable fender: 12.1 m (length) x 5.7 m (width). These dimensions provide for an effective w/h ratio of more than 3.5 and a SF ranging between 0.5 to 0.9, even after the fourth fender-reducing cut has been taken from it. The SF is

calculated using the Salamon & Munro formula as given by Equation 2-1. Although this is not the ideal pillar strength formula for NDC, it is merely used as an indication of the fender's stability. Pillar designs for NDC, as previously mentioned, are determined using the squat-pillar formula due to the w/h ratio requirement of the pillars at the depth of mining. These pillars have a w/h ratio exceeding five. Since fenders have a w/h ratio of less than five, the squat-pillar formula cannot be used for them. Figure 4-10 also shows the mining parameters and pillar design calculations of the panel planned for stooping. It furthermore shows the position, sequence and dimensions of the cuts to be taken from each pillar during stooping.

Development	
Panel	133
Average Mining Depth (m)	163.62
Average Mining Height (m)	1.98
Average Bord Width (m)	7.26
Pillar Centers (m)	26.0 (l) x 24.0 (w)
Pillar Dimensions (m)	18.8 (l) x 16.8 (w)
Safety Factor (S&M) ***Eq 2-1***	2.10
Safety Factor (Squat) ***Eq 2-3***	2.61
w/h ratio (effective)	8.87
% Areal Extraction	49.38

Stooping	
Fender Dimensions (m)	12.1 (l) x 5.7 (w)
Fender w/h ratio (effective)	3.87
Fender Safety Factor (S&M) ***Eq 2-1***	0.81

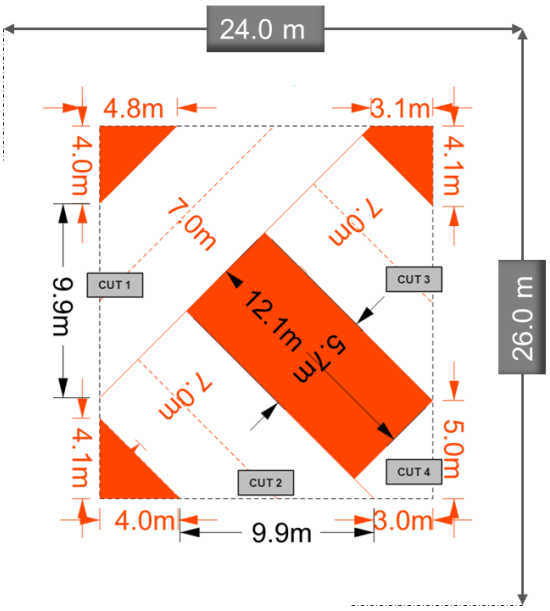


Figure 4-10: Safety factor calculations for pillar and fender stability of a standard pillar with centres of 26.0 m (l) x 24.0 m (w).

4.2.4 Compartmentalising stooping panels

Barrier pillars are left in place to compartmentalise stooping panels. These pillars are continuous with a minimum width of 17.0 m which is equal to the width of the in-panel pillars. However, these pillars often have a width equal to that of the in-panel pillars' centre distance, i.e. pillar width plus the 7.2 m bord width.

In the event of a production panel, which is planned for stooping, being orientated parallel to a main development, the barrier pillar width will be increased to a minimum of 50.0 m as shown in Figure 4-11 (Van der Merwe & Madden, 2010). Panel 1135, which is yet to be developed and stooped, will be separated from the main development, Panel 1134, by a barrier pillar with a minimum width of 50 m. This size barrier pillar will prevent any detrimental stress interactions with the adjacent stooped panel and ensure long-term stability of the main development.

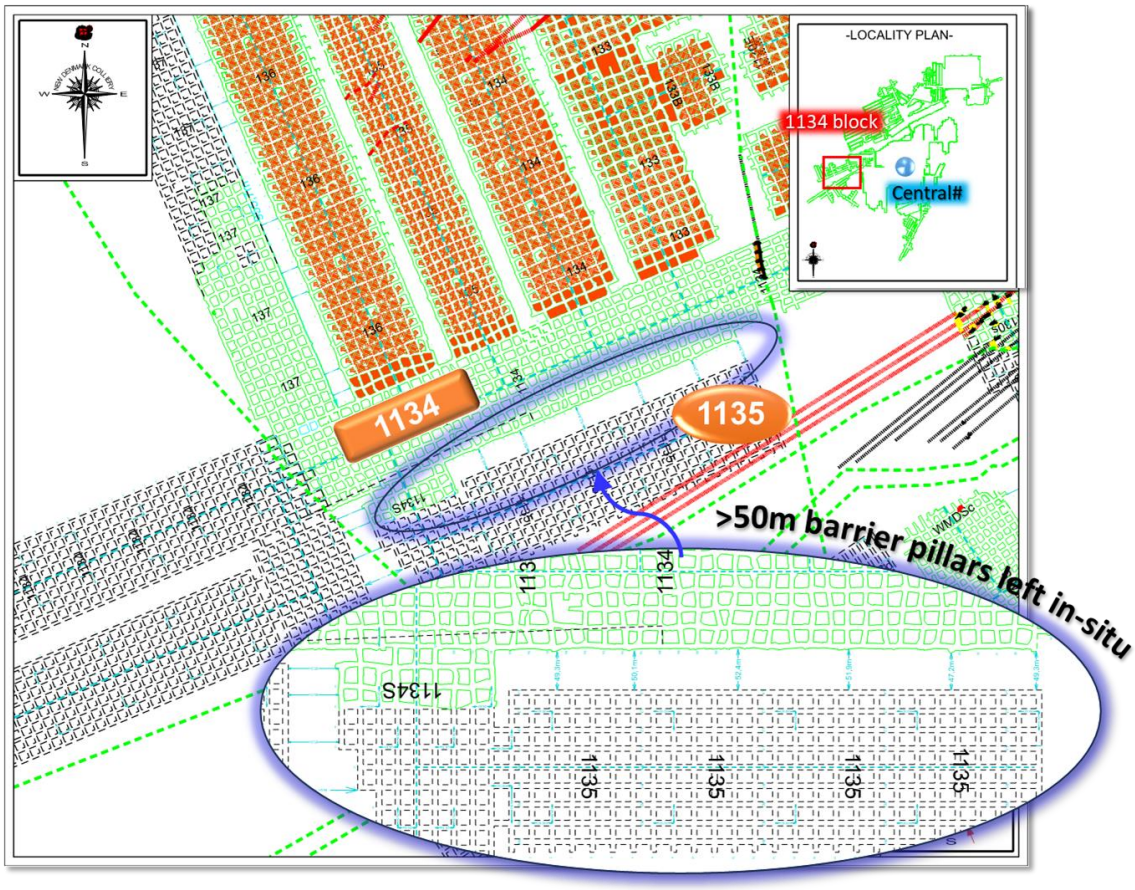


Figure 4-11: Stooping Panel 1135 separated from the main development, Panel 1134, with a barrier pillar of at least 50 m wide.

The compartmentalisation of panels is furthermore achieved by leaving a row or more of stopper pillars at the beginning of a development panel, or the end of a stooping panel, depending on how one views it. Two large panel-entry pillars are also left between splits 0 and 1 (Figure 4-6).

4.2.5 Stopper pillars

Stopper pillars are strategically left for several reasons, which include the following:

- *To protect the bleeder road*. Only one cut is taken into these pillars along the perimeter of the panel. The depth of these cuts may vary from 10 m cubby cuts, which are normally taken on the return side, to full cuts on the pillars along the intake side of the bleeder road. These predominantly intact pillars along the bleeder road reduces the panel span to an effective span, which is measured between these pillars.

- *To compartmentalise goafing*. This is done especially if the goaf hangs up for two or more splits. A stopper pillar will then be left every third to fourth split. It may either be completely left intact or have only one cut taken from it, generally the bottom diagonal cut.

- *To protect sensitive surface structures*. Intact pillars are left in a 100 m radius around the specific surface structure that must be protected. It may be reduced by the rock engineer depending on the sensitivity of the surface structure. This reduced distance is determined by dividing the mining depth by 2.7 (Van der Merwe & Madden, 2010). Figure 4-12 shows an example of where stopper pillars have been left intact to protect a surface dam and powerline pylons above panels 135 and 134, respectively.

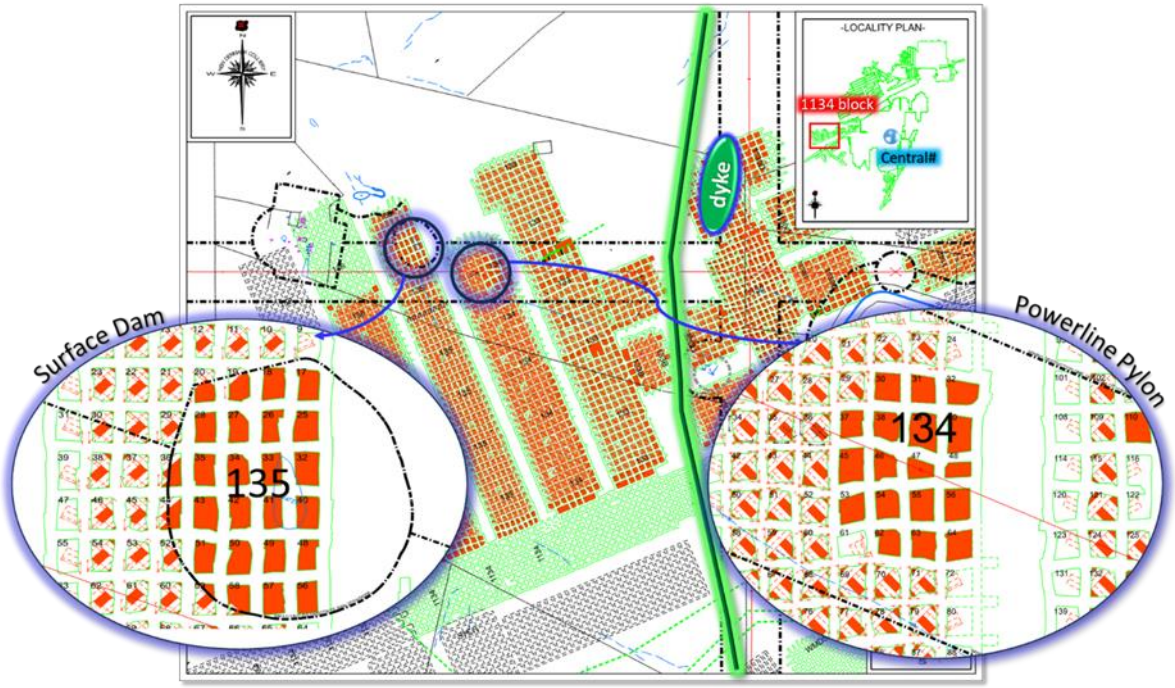


Figure 4-12: Stopper pillars left in panels 134 and 135 to protect surface structures, such as surface dams and pylons.

4.2.6 General stooping controls

Breaker lines are installed in all roadways leading from the active intersection (Figure 2-15). A breaker line consists of six 1.5 m long roof bolts installed with full column resin. These roof bolts are spaced 1 m apart from one another, one to two metres from the pillar corner (Sasol Mining, n.d.; Gonsalves, 2021). Although the standard for breaker lines was initially adopted from Sasol Mining, it has been proven effective in NDC ground conditions. This has been done with the blasting of drive chambers where 1.5 m long roof bolts have been successfully used as breaker lines. No back break has been reported to extend beyond the breaker lines.

Monitoring consists of policeman sticks, installed as per the pattern indicated in Figures 2-16 and 2-17. The policeman sticks are supplemented with 2 m long roof monitoring devices (extensometers), which are installed in the centre of each intersection (Gonsalves, 2021). Visual inspections are done by the face boss and CM operator at the start of each shift and throughout the shift as the different cuts are taken.

5 METHODOLOGY

5.1 Critical Span Calculations and Underground Observations

Back-analysis of the mine's stooping database was used to identify common factors that either directly caused goafing or contributed to it. It included lessons learned from the 50 panels stooped to date. The following information for each stooping panel was recorded in the database:

- Mining parameters during development, for example, depth below the surface, pillar dimensions, seam height, panel width, pillar safety factors and w/h ratios.
- Geological conditions, such as roof composition and thickness, as well as the presence of geological structures.
- Stooping parameters, for example, critical span to induce goafing, cutting sequence and direction, snooks and fender dimensions, fender safety factors and w/h ratios.
- Panel orientation relative to the major horizontal stress direction, as well as the presence of nearby horizontal stress concentrators, such as dykes and mined-out longwall panels.
- Anticipated goafing based on the actual and effective panel span.
- Actual versus predicted goafing.
- Subsidence recorded on the surface.
- Implemented stooping controls and their effectiveness.

- Notes made of important occurrences during inspections while stooping the panel; and
- Safety incidents, for example, trapped machinery due to goafing, or air-blasts injuring personnel and/or damaging equipment.

5.2 Numerical Modelling

Two stooped areas were identified for numerical modelling analysis, namely the 1100 block and the Shosholoza panels. The 1100 block was selected due to the excessive pillar scaling of the 1120 Main belt and travelling roads, while the Shosholoza panels were selected due to the changes made to them during stooping. These changes were a result of the observations and learnings made in the 1100 block. Numerical modelling analysis of these stooped areas was done using LAMODEL v.3.0.2. The purpose of the analysis was to determine the following:

- The stress regimes to which the pillars within the stooped panels were exposed to before and after pillar extraction.
- The extent of the stress around single and multiple stooped panels.
- The ideal barrier pillar width between panels, as well as the impact of the larger panel-entry pillars as those introduced in Panel 134; and
- The safe stand-off distance between stooped panels and sensitive structures.

Table 5-1 shows a summary of the mechanical rock properties for NDC. These were derived from numerous geotechnical tests that were historically done across the NDC lease area. They represent the dolerite sill in the overburden, immediate sandstone roof, No. 4 coal seam and its immediate floor. The amount of dolerite contained within the overburden was also taken into consideration due to the significant effect that it has on the overburden stiffness. This is due to its strength and Elastic Modulus (Young's Modulus) being substantially higher than that of the surrounding sedimentary overburden strata (Jansen van Vuuren & De Beer, 2022a). As an example of this, Figure 5-1 shows two borehole logs specifically for the 1100 block (NDC3131) and Shosholoza (NDC3151) panels. The dolerite sill makes up approximately 32% of the overburden in the 1100 block, and about 10% in the Shosholoza panels. These borehole logs represent the immediate areas of the panels in which they had been drilled, but it is known that the presence and thickness of the sill not only varies from one panel to another, but even within a specific panel. A statistical analysis of the geology borehole data was therefore done to determine the frequency distribution of the dolerite in the overburden stratigraphy. It was found that the overburden comprises on average 20% dolerite. Table 5-2 shows the rest of the overburden rock and in-situ coal modelling properties.

Table 5-1: Summary of NDC mechanical rock properties.

	Average	Min.	Max.	Std. Dev.	CoV *
Dolerite UCS (MPa)	205.2	99.1	428.1	111.3	0.54
Dolerite YM (GPa) (Tan @ 50 % UCS)	67.1	15.9	99.1	32.2	0.48
Dolerite PR (Tangent @ 50 % UCS)	0.29	0.25	0.38	0.04	0.14
Dolerite Relative Density (t/m³)	2.84	2.49	3.00	0.21	0.08
Sandstone UCS (MPa)	77.4	35.1	235.8	29.5	0.38
Sandstone YM (GPa) (Tan @ 50 %)	19.1	5.4	61.6	7.9	0.42
Sandstone PR (Tangent @ 50 % UCS)	0.39	0.17	0.65	0.08	0.20
Sandstone Relative Density (t/m³)	2.43	2.22	3.28	0.11	0.05
Coal UCS (MPa)	32.4	18.8	49.2	12.135	0.37
Siltstone UCS (MPa)	81.8	28.0	126.5	20.7	0.25
Overburden (20 % DOL) UCS (MPa)	**102.9**				
Overburden (20 % DOL) YM (GPa)	**28.7**				
Overburden (20 % DOL) PR	**0.37**				
Overburden (20 % DOL) Relative Density (t/m³)	**2.508**				

* *The **coefficient of variation** (CoV) is a measure of relative event dispersion that is equal to the ratio between the standard deviation and the mean.*

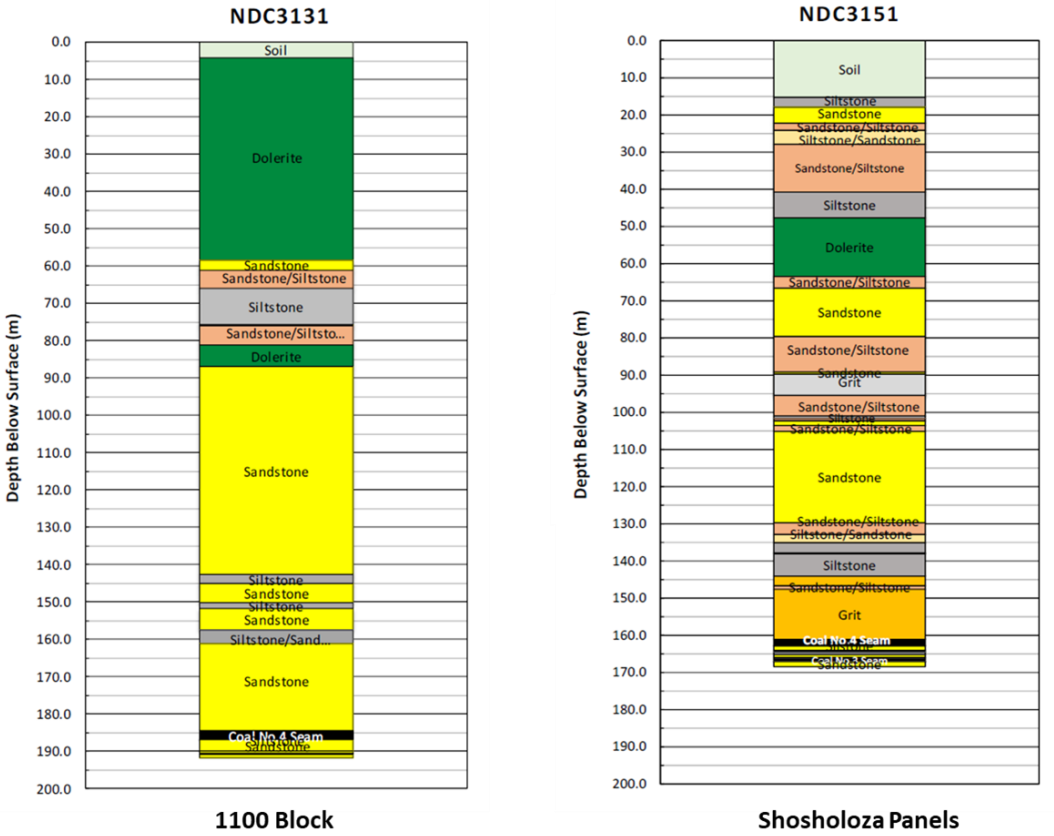


Figure 5-1: Geology borehole logs for 1100 block and Shosholoza panels.

Table 5-2: Modelling properties for the overburden rock and in-situ coal.

Design Parameters	Value	Comments
Overburden Poisson's Ratio	0.37	Relatively lower; lower than the 0.3 value used for the coal deformation but based on the actual rock properties.
Overburden Elastic/Young's Modulus (GPa)	28.7	Relatively high, but based on the actual rock properties.
Element width (m)	0.5	-
Lamination/bedding thickness (m)	25.0	This lamination thickness is debatable but provides approximately eight laminations (layers) within the overburden strata. It also stiffens the immediate roof strata, in order to simulate the immediate roof layer (sandstone) in excess of 20 m.
Vertical stress gradient (Mpa/m)	0.0251	Based on the combined relative density, assuming at least 20 % dolerite within the overburden rock mass.
In-situ coal Elastic/Young's Modulus (GPa)	4.0	Slightly higher than the generally accepted value of 3.9 GPa as a South African industry norm.
In-situ coal strength (MPa)	6.2	More conservative compared to the in-situ strength applied in the Squat Pillar formula of 7.2 MPa.
Mining height (m)	-	Equal to the thickness of the No. 4 coal seam. As per the geological borehole logs for the specific area to be modelled.
Average mining depth (m)	-	Measured up to the No. 4 coal seam floor. As per the geological borehole logs for the specific area to be modelled.
Bord width (m)	7.2 & 7.0	7.2 m for pillar development and 7.0 m for the snooks and fenders. However, as the pillars in the model are set up according to the actual mine plan pillar offsets, this parameter is only applicable to the determinist calculations.
Displacement convergence limit (m)	0.000001	To ensure sufficient convergence within the model.

It is essential to note that due to the linear-elastic material properties of the panel pillars used in the simulation, the vertical stress load could easily have been over or underestimated as the element does not yield, but continues to absorb load, beyond its actual capability. This is an inherent flaw of any linear-elastic model or simulation as the strata behaviour in a stooping panel is not linear-elastic. However, applying a linear-elastic model is significantly quicker and within acceptable accuracy levels, providing a useful and quick means of comparison, if the stresses are within the elastic limit of the material being simulated (Jansen van Vuuren & De Beer, 2002a).

6 RESULTS

6.1 Critical Span Calculations

6.1.1 1100 Panels critical span calculations

Table 6-1 shows a summary of the critical span calculations for the 1100 block panels to induce both failure of the sandstone layer forming the immediate roof, as well as the sill higher up in the overburden. These spans were calculated using equations 6-1 (Van der Merwe & Madden, 2010) and 6-2 (Van der Merwe, 1995), respectively. Both equations have been repeated for the reader's convenience:

- $L_c = 2H\tan(\emptyset)$ ***Equation 6-1***

- $L_c = 2T\sqrt{k_s + \frac{\beta}{D}} + 2(H - D)\tan(\emptyset)$ ***Equation 6-2***

with

$\beta = \frac{1.53}{\gamma_m} - 0.8$ ***Equation 6-3***

and

$\gamma_m = 0.025\frac{D-T}{D} + 0.03\frac{T}{D}$ ***Equation 6-4***

where ks = ratio of horizontal to vertical virgin stress

H = depth of mining below surface (m)

D = depth of dolerite base (m)

T = thickness of dolerite (m)

∅ = goaf angle measured from the vertical (°)

The calculations considered the average mining depth of the panels, thicknesses of the immediate sandstone layer and the dolerite sill, as well as their respective positions in the overburden. The complete table of calculations can be seen in Appendix A.

The first column of Table 6-1 shows the various panels that were stooped in the 1100 block. This is followed by the actual span for each panel, which is simply measured across the panel from one abutment to the other. The effective span of the panel is the reduced span measured between the predominantly intact pillars along the perimeter of the panel. The function of these pillars is to protect the bleeder road, which is required for ventilation. It is this effective span which is compared to the critical span calculations for both failure (goafing) of the immediate roof, as well as goafing of the overburden all the way to surface, in which case it would break the sill. It was also compared to both the sub-critical span (to avoid goafing) and super-critical span (to ensure goafing) calculations for both the immediate roof and sill higher up in the stratigraphy.

Table 6-1: Critical span calculations for 1100 panels.

Area/ Block	Panels	Actual Panel span (m)	Effective Panel span (m)	Critical span for immediate roof (m) (Eq 6-1)	Sub-critical span for immediate roof (m)	Super-critical span for immediate roof (m)	Critical span for sill (m) (Eq 6-2)	Sub-critical span for sill (m)	Super-critical span for sill (m)
1100 Block	1111	158.00	108.00	180.88	162.79	198.97	319.34	287.41	351.27
	1126	160.60	110.60	182.12	163.91	200.33	299.89	269.91	329.88
	1124	158.00	108.00	180.47	162.42	198.51	290.63	261.57	319.70
	1122	158.00	108.00	180.50	162.45	198.54	294.32	264.89	323.75
	1109	182.00	132.00	179.23	161.30	197.15	319.26	287.33	351.19
	1105	158.00	108.00	171.85	154.67	189.04	266.39	239.75	293.03
	1107	158.00	108.00	179.50	161.55	197.45	305.98	275.38	336.58
	1118	158.00	108.00	186.12	167.51	204.73	305.95	275.35	336.54
	1116	158.00	108.00	175.83	158.25	193.42	263.15	236.83	289.46
	1142	160.00	122.00	-	-	-	-	-	-
Average		**160.86**	**112.06**	**179.61**	**161.65**	**197.57**	**296.10**	**266.49**	**325.71**
Min		**158.00**	**108.00**	**171.85**	**154.67**	**189.04**	**263.15**	**236.83**	**289.46**
Max		**182.00**	**132.00**	**186.12**	**167.51**	**204.73**	**319.34**	**287.41**	**351.27**

It is well known that goafing of the overburden would bring relief to the abutment stresses, especially if it were to take place up to the surface. The effective span of a panel was therefore colour-coded red if it fell below the sub-critical span, yellow if it ranged between the sub-critical and super-critical, and green if it exceeded the super-critical span.

6.1.2 Critical span calculations for planned stooping sections

Table 6-2 shows a summary of the critical span calculations for all the Central Shaft panels that were developed and stooped after the 1100 block and Panel 135 were completed. These panels were specifically planned for stooping; hence, they consisted of nine roadways with pillar centres of 26.0 m (length) x 24.0 m (width). Similar to Tabel 6-1 above, Table 6-2 further shows the actual span and effective span of each panel, and how they compare to the critical span calculations for both the immediate

sandstone roof and sill higher up in the stratigraphy. The complete table of calculations can be seen in Appendix B.

Table 6-2: Critical span calculations for planned stooping panels at Central Shaft.

Area/ Block	Panels	Actual Panel span (m)	Effective Panel span (m)	Critical span for immediate roof (m) (Eq 6-1)	Sub-critical span for immediate roof (m)	Super-critical span for immediate roof (m)	Critical span for sill (m) (Eq 6-2)	Sub-critical span for sill (m)	Super-critical span for sill (m)
1134 / Shosholoza Block	135	160.00	122.00	149.84	134.86	164.82	144.90	130.41	159.40
	136	200.00	152.00	152.54	137.29	167.79	146.40	131.76	161.04
	134	200.00	152.00	150.53	135.48	165.59	142.13	127.92	156.34
	133	200.00	152.00	153.07	137.76	168.38	135.31	121.78	148.84
	133A	200.00	152.00	148.44	133.60	163.29	141.10	126.99	155.21
	133B	200.00	152.00	153.14	137.83	168.46	173.25	155.93	190.58
1130 / Mmabatho Block	1130	200.00	152.00	156.40	140.76	172.04	-	-	-
	1130B	200.00	152.00	160.01	144.01	176.01	135.76	122.19	149.34
	1130C	200.00	152.00	159.08	143.17	174.99	197.72	177.95	217.49
	1130D	200.00	72.00	156.77	141.10	172.45	171.05	153.94	188.15
	1130E	200.00	152.00	151.62	136.46	166.78	-	-	-
	1130F	200.00	152.00	156.01	140.40	171.61	-	-	-
1001 / Simunye Block	1001B	200.00	152.00	153.12	137.81	168.44	112.95	101.66	124.25
	1001C	200.00	152.00	152.95	137.65	168.24	113.01	101.71	124.31
Average		**197.14**	**144.14**	**153.82**	**138.44**	**169.21**	**146.69**	**132.02**	**161.36**
Min		**160.00**	**72.00**	**148.44**	**133.60**	**163.29**	**112.95**	**101.66**	**124.25**
Max		**200.00**	**152.00**	**160.01**	**144.01**	**176.01**	**197.72**	**177.95**	**217.49**

6.2 History of Goafing in NDC Stooping Sections

6.2.1 Analysis of the stooping database

Analysis of the stooping database showed that goafing was recorded in only 13 of the 50 panels stooped at NDC. Table 6-3 shows the panels where goafing occurred and their critical span calculations for the immediate sandstone roof as well as the sill higher up in the stratigraphy. The complete table can be seen in Appendix C.

Table 6-3: NDC stooping panels where goafing was recorded and their critical span calculations.

No.	Location		Critical Span Calculations						
	Panels	Section	Effective Panel span (m)	Critical span for immediate roof (m) (Eq 6-1)	Sub-critical span for immediate roof (m)	Super-critical span for immediate roof (m)	Critical span for sill (m) (Eq 6-2)	Sub-critical span for sill (m)	Super-critical span for sill (m)
1	1126	Siyanqoba	110.60	182.12	163.91	200.33	299.89	269.91	329.88
2	135	Shosholoza	122.00	149.84	134.86	164.82	144.90	130.41	159.40
3	040	Simunye	122.00	152.00	136.80	167.20	128.51	115.66	141.36
4	042	Simunye	140.00	153.44	138.10	168.79	118.67	106.81	130.54
5	179b	Eyethu	139.00	153.21	137.88	168.53	181.14	163.03	199.25
6	888	Lesedi	127.00	171.73	154.56	188.90	273.47	246.12	300.82
7	887	Lesedi	79.00	153.21	137.88	168.53	181.14	163.03	199.25
8	882c	Inyanda	127.00	173.58	156.22	190.93	266.98	240.28	293.67
9	882d	Inyanda	152.00	178.20	160.38	196.02	293.61	264.25	322.97
10	1001B	Simunye	152.00	153.12	137.81	168.44	112.95	101.66	124.25
11	1001C	Simunye	152.00	152.95	137.65	168.24	113.01	101.71	124.31
12	177/5	Thubelisha	80.00	148.50	133.65	163.35	176.37	158.73	194.01
13	177/6	Thubelisha	104.00	148.50	133.65	163.35	176.37	158.73	194.01
		Average	**123.58**	**159.26**	**143.33**	**175.19**	**189.77**	**170.79**	**208.75**
		Min	**79.00**	**148.50**	**133.65**	**163.35**	**112.95**	**101.66**	**124.25**
		Max	**152.00**	**182.12**	**163.91**	**200.33**	**299.89**	**269.91**	**329.88**

Table 6-4 indicates the potential contributing factors that might have enhanced goafing in these panels. It includes the presence of geological structures and nearby stooped or longwall panels. It also considers the orientation of the panel and the strike of the geological structures relative to the regional major horizontal stress (σ_{1H}) as indicated by the Rose diagram. The regional major horizontal stress is considered a contributing factor to goafing when it aligns with the induced horizontal stress caused by the geological structures.

Table 6-4: NDC stooping panels where goafing was recorded and their possible contributing factors.

No.	Location			Goaf - contributing factors					
	Panels	Shaft	Section	Critical span (m)	Presence of geological structures / poor roof conditions	Adjacent longwall/ stooped panels	Fourth Fender reducing cut	Panel orientation w.r.t regional major horizontal stress ($\sigma 1_H$)	Orientation of geological structures w.r.t regional major horizontal stress ($\sigma 1_H$)
1	1126	Central	Siyanqoba	Sub-critical	Faults	Stooping	No	Oblique	Parallel
2	135	Central	Shosholoza	Sub-critical	Slips/joints	No	No	Parallel	Perpendicular
3	040	Central	Simunye	Sub-critical	None	No	Yes	Perpendicular	NA
4	042	Central	Simunye	Critical	None	Stooping	Yes	Perpendicular	NA
5	179b	Okhozini	Eyethu	Critical	Dykes	NA	Yes	Perpendicular	Perpendicular
6	888	North	Lesedi	Sub-critical	Dykes	Longwall	Yes	Oblique	Perpendicular
7	887	North	Lesedi	Sub-critical	Dykes	Stooping	Yes	Oblique	Perpendicular
8	882c	North	Inyanda	Sub-critical	Dykes	Stooping	Yes	Oblique	Perpendicular
9	882d	North	Inyanda	Sub-critical	Dykes	Stooping	Yes	Oblique	Perpendicular
10	1001b	Central	Simunye	Critical	Slips/joints	No	Yes	Oblique	Oblique
11	1001c	Central	Simunye	Critical	Slips/joints	Stooping	Yes	Oblique	Oblique
12	177/5	Okhozini	Thubelisha	Sub-critical	Faults	No	Yes	Perpendicular	Oblique
13	177/6	Okhozini	Thubelisha	Sub-critical	Faults	Stooping	Yes	Perpendicular	Oblique

Table 6-5 shows the typical observations that were made during the inspections of each goaf. It includes the position of the goaf in the panel, the estimated depth of goafing into the immediate roof, the estimated goaf angle and any measured surface subsidence.

Table 6-5: Description of goafing in NDC stooping panels.

No.	Location			Goaf Description				
	Panels	Shaft	Section	Affected roadways	Estimated depth of goafing (m)	Estimated goaf angle (degrees)	Goaf Description	Surface Subsidence (m)
1	1126	Central	Siyanqoba	-	To surface	-	Slabs of sandstone, sharp edges, 10 – 30 cm in thickness	0.3
2	135	Central	Shosholoza	R3; L3	1.5 - 2.0	22 - 25	Slabs of sandstone, sharp edges, 10 – 30 cm in thickness	No
				BR - R1				No
				L1 - R3				No
				L2 - R1				No
3	040	Central	Simunye	L2 - R1	0.3 - 2.0	22 - 25	Slabs of sandstone, sharp edges, 10 – 30 cm in thickness	No
				R2 - R3				No
4	042	Central	Simunye	BR - R2	0.3 - 2.0	22 - 25	Slabs of sandstone, sharp edges, 10 – 30 cm in thickness	No
				L1 - R1	0.3 - 2.0			No
5	179b	Okhozini	Eyethu	L2 - R2	1.5 - 2.0	22 - 25	Slabs of sandstone, sharp edges, 10 – 30 cm in thickness	No
6	888	North	Lesedi	L2 - R2	1.5 - 2.0	22 - 25	Slabs of sandstone, sharp edges, 10 – 30 cm in thickness	No
7	887	North	Lesedi	BR - L2	1.5 - 2.0	22 - 25		No
8	882c	North	Inyanda	BR - R3	1.5 - 2.0	22 - 25	Slabs of sandstone, sharp edges, 10 – 30 cm in thickness	No
9	882d	North	Inyanda	L1 - R1	1.5 - 2.0	22 - 25		No
10	1001b	Central	Simunye	L1 - R2	1.5 - 2.0	22 - 25	Slabs of sandstone, sharp edges, 10 – 30 cm in thickness	No
11	1001c	Central	Simunye	L2 - L3	1.5 - 2.0	22 - 25		No
				L1 - R3				No
12	177/5	Okhozini	Thubelisha	L1 - R1	1.5 - 2.0	22 - 25	Slabs of sandstone, sharp edges, 10 – 30 cm in thickness	No
13	177/6	Okhozini	Thubelisha	L1 - R1	1.5 - 2.0	22 - 25		No

6.2.2 Discussion of individual panels where goafing occurred

Panel 1126

Goafing in Panel 1126 (Figure 6-1) has been confirmed even though no goafing occurred while stooping the 1100 panels. Complaints were received in 2023 from a farmer owning the surface rights above Panel 1126. He reported subsidence, which resulted in ponding of water rendering the affected land unusable.

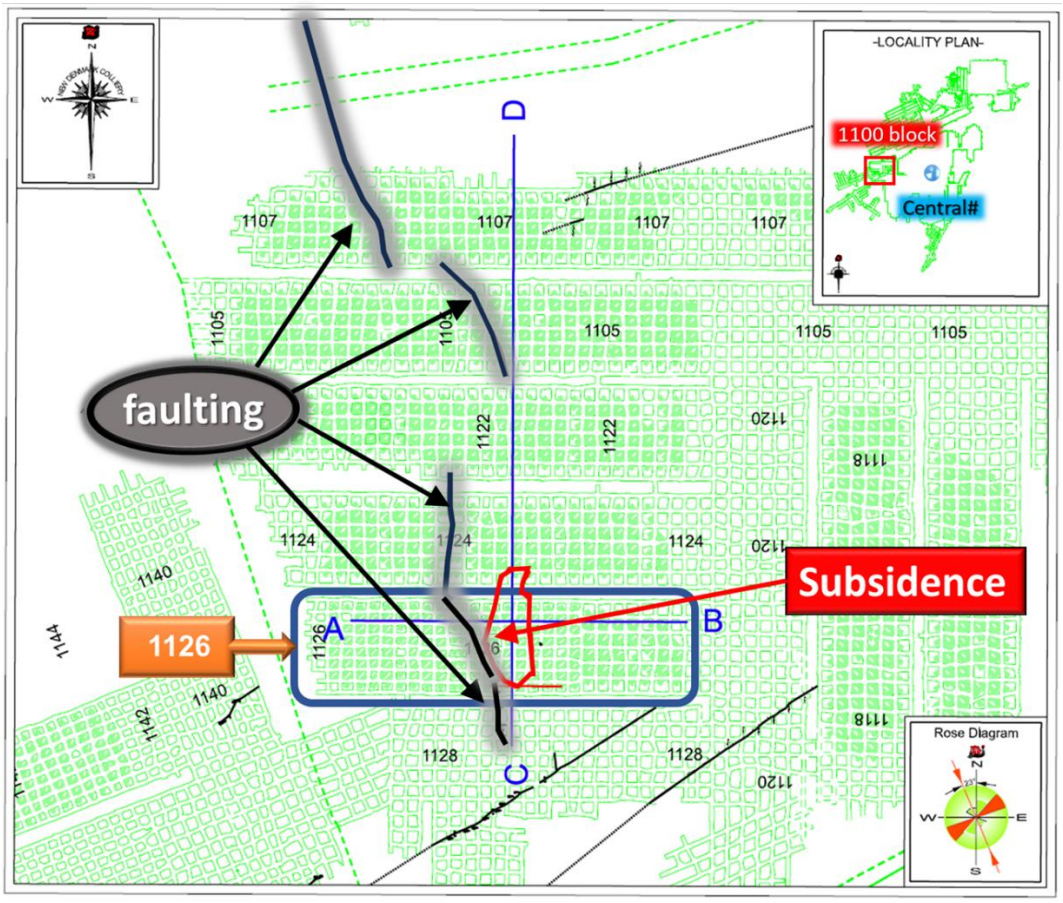


Figure 6-1: NDC mine plan indicating the position of Panel 1126 and the cross-sections along which the surface subsidence was measured.

Figure 6-2 shows the cross-sections of the subsidence measurements above Panel 1126. From Figure 6-1, Cross-section A'-B' represents the measurements taken along the length of Panel 1126 in east-west orientation. It shows that the subsidence occurs above the centre of the panel, just east of the position of the fault.

The fault strikes in a relatively north-south orientation across Panel 1126 but appears to turn more into a northwest-southeast direction across panels 1105 and 1107. The rest of the fault properties, such as the throw, dip and dip direction, were unfortunately not well documented during the development of these old panels, most likely due to it having a negligible effect on mining. The fault is nonetheless expected to have behaved as a stress concentrator during stooping which would have enhanced goafing of the roof in the area near it. It is assumed that the fault resulted in a cantilever effect of the roof, which would have increased the tensile stresses, especially as the pillar support underneath the roof was largely removed during stooping operations.

Cross-section C'-D' represents the subsidence measurements taken across the panel in north-south orientation. It extends across Panel 1126 and the adjacent stooped panels, namely Panels 1124, 1122, 1105 and 1107. These cross-sections show that the subsidence resulted in a depression formed on the surface of which the Survey Department measured the maximum subsidence to be approximately 300 mm (Salima, 2023).

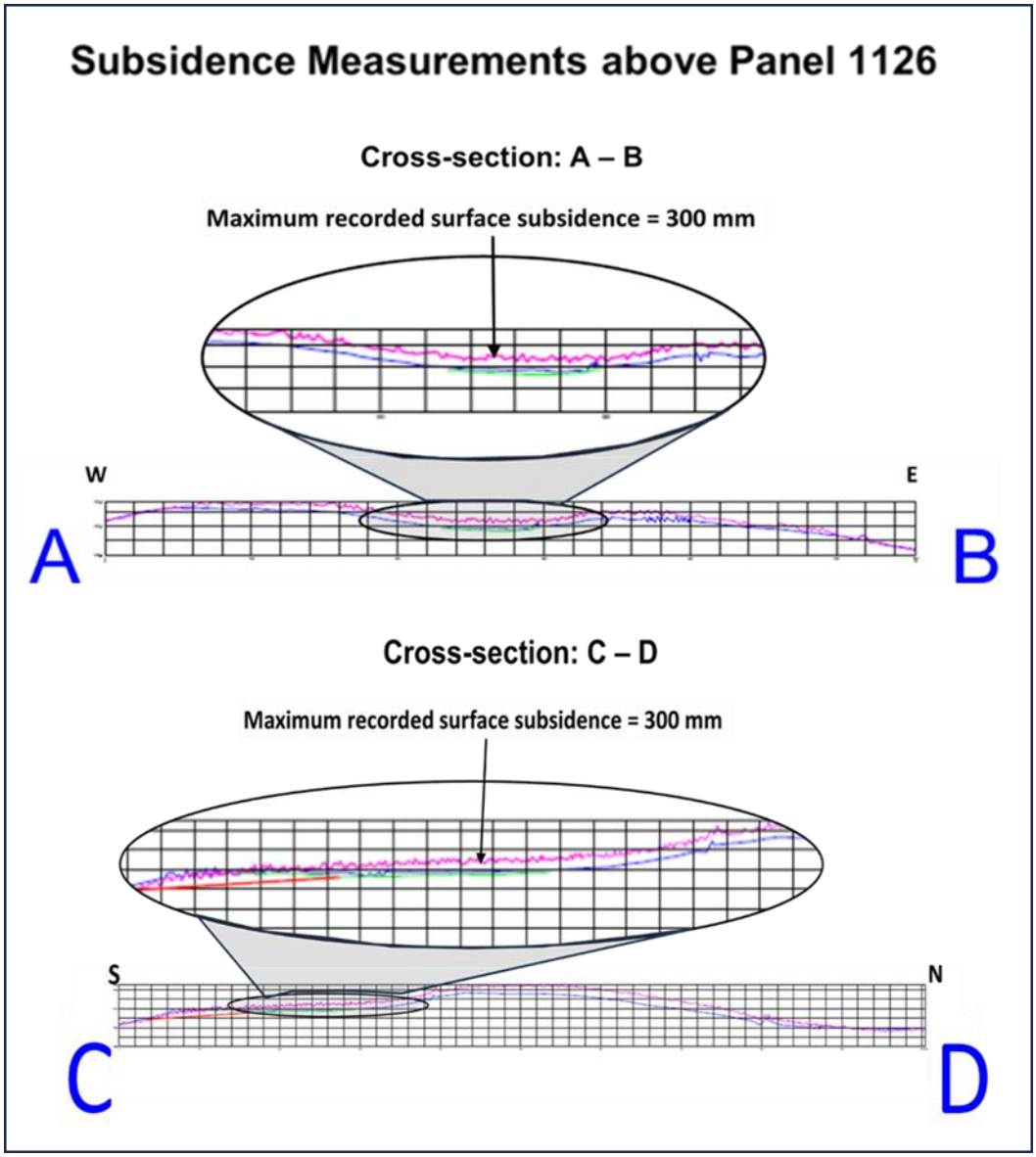


Figure 6-2: Subsidence measurements above Panel 1126.

Considering that subsidence was recorded, it indicates that goafing resulted in the failure of the sill. It is suspected that failure of the sill occurred because the fault extended through it. The fact that the subsidence was only reported in 2023, four years after the panel was stooped in 2019, also confirms that goafing, especially up to the surface, can be a time-dependent process.

Panel 135

The first reported goaf while stooping occurred in Panel 135 of the Shosholoza block (Figure 4-5). It occurred after several panels were already stooped in the 1100 block without any goafing being recorded. It was unexpected due to the fact that the effective span of Panel 135 was only 122 m, being significantly less than the critical span as indicated in Table 6-3. Joints were intersected and mapped during development; however, at that stage, it was uncertain whether these would have contributed to goafing (Table 6-4). Interestingly, their positions and the splits in which the goafing was reported did not correlate with each other. The ground conditions in Panel 135, apart from the joints, consisted of a competent sandstone layer forming the immediate roof. The joints are orientated perpendicular to the regional major horizontal stress direction as indicated by the Rose diagram (Figure 4-5; Table 6-4). It is suspected that this may have contributed to any horizontal stress induced by the joints. No subsidence above Panel 135 has been reported.

Panels 040 and 042

Goafing was shortly thereafter also reported in panels 040 and 042 (Figure 4-8), which were developed and stooped by Simunye Section. These goafs occurred sporadically and in isolated areas. They were mostly confined to the centre of the panels occurring predominantly in the intersections from L2 to R2 roadways. The roof of these panels consisted of the same competent sandstone material that is found across the majority of

the NDC lease area. There were also no geological discontinuities or poor roof conditions mapped during the development (Table 6-4). It was therefore thought at that stage that the goafing occurred in response to the enlarged intersections formed after taking the fourth fender-reducing cuts. Contrary to Panel 135, these panels are orientated perpendicular to the major horizontal stress direction. No subsidence has been reported above these panels.

Panel 179b

More consistent goafing was later reported in Panel 179b stooped by Eyethu Section at Okhozini Shaft. This was the first panel to be stooped outside of the Central Shaft area. It was in this specific panel where NDC had its first and only, stooping-related incident with a CM being partially buried by a goaf in the active intersection as seen in Figure 6-3. The CM was fortunately retrieved within three days without serious damage to the machine. No personnel were injured during this incident due to the goaf being arrested by the breaker lines.

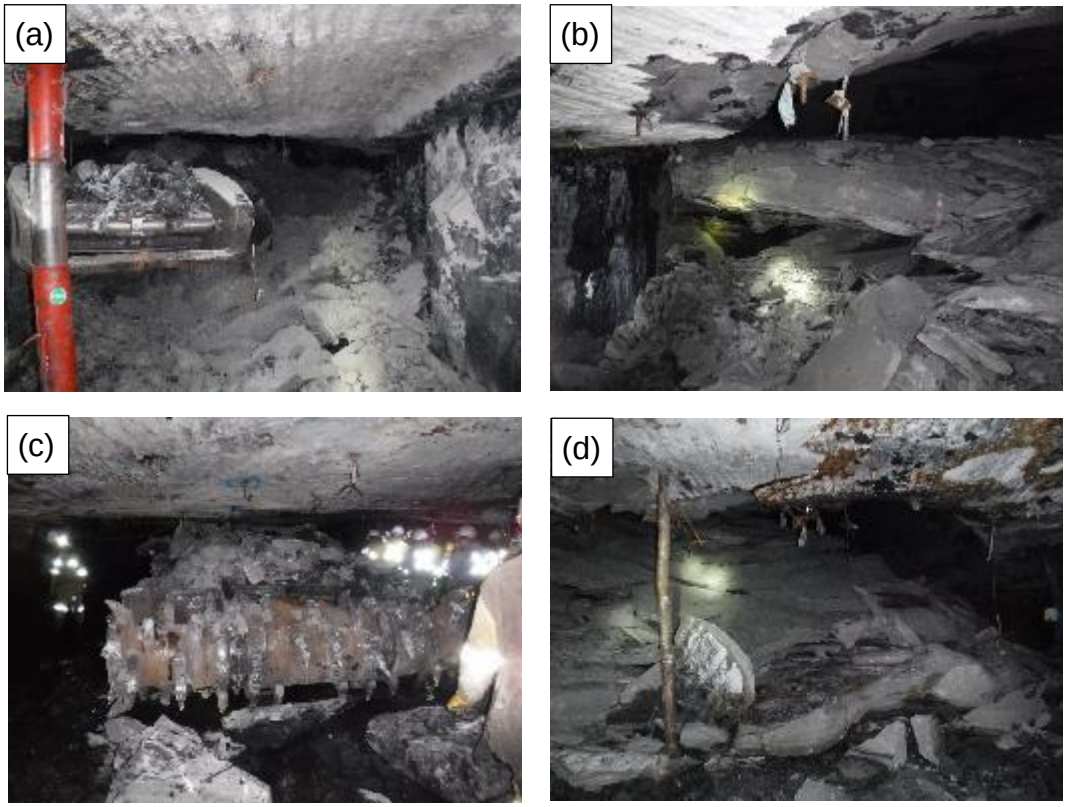


Figure 6-3: Eyethu goaf incident; (a) CM partially buried with only its conveyor boom visible from underneath the goaf material; (b) thick layer of sandstone lying on top of the CM indicating that the goaf only extended about 1.5 m into the immediate roof; (c) CM successful retrieved from the goaf; (d) goaf arrested by the breaker lines with the intact policeman stick indicating stable ground on the safe side.

Goafing in Panel 179b occurred even though the effective panel span was less than the critical span of the immediate sandstone roof. The panel had an effective span of 139 m compared to the critical span of 153 m for the immediate roof (Table 6-3). The roof in Panel 179b consisted of a competent sandstone layer with no joints or poor roof conditions mapped during development. Excessive pillar scaling was however recorded on the left-

hand side of the panel, which was closest to the dyke. Goafing in this panel was therefore attributed to the nearby dyke on the south side of the panel as shown in Figure 6-4. The orientation of the panel relative to the major horizontal stress direction was also considered a contributing factor in this instance. This is due to the regional major horizontal stress corresponding to the direction of the induced stress from the dyke (Table 6-4). No subsidence has been reported or measured above the panel since it has been stooped.

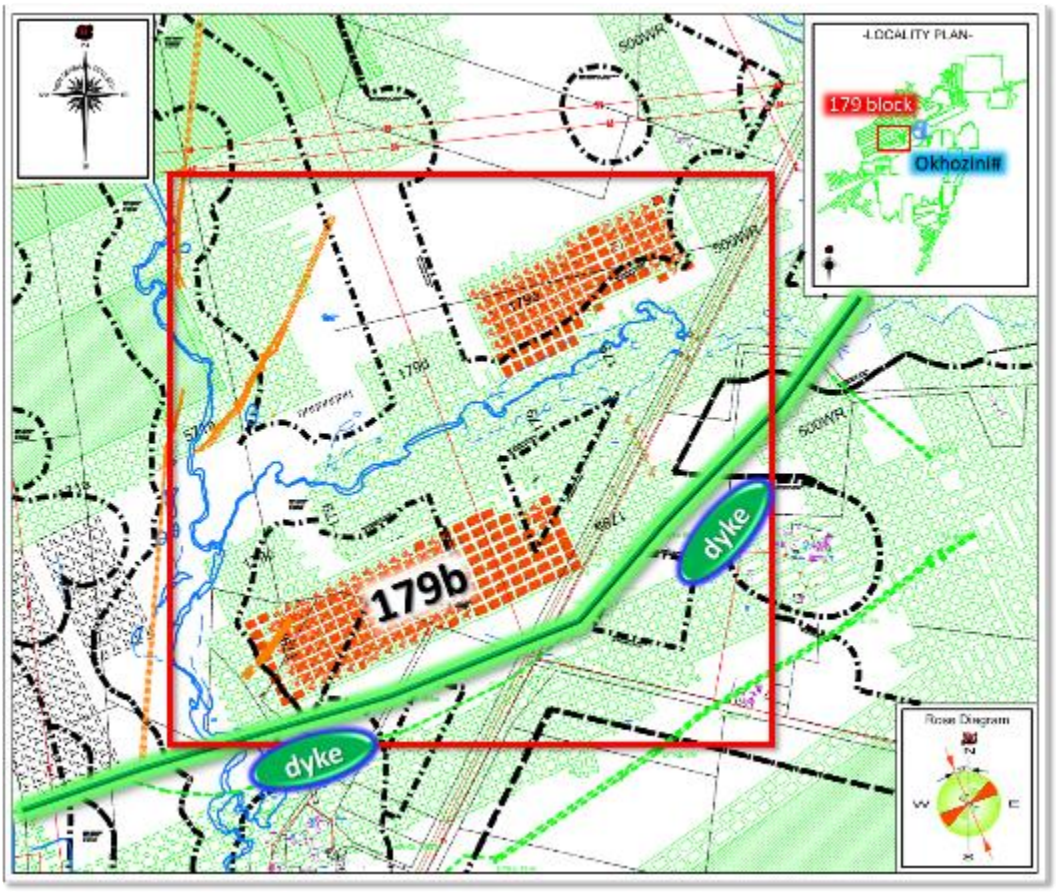


Figure 6-4: Eyethu Panel 179b with a nearby dyke to the south of it.

Panel 888

Goafing at North Shaft also occurred more consistently in some panels, even where their panel span was reduced by surface restrictions to well below the sub-critical span. One such example is Panel 888 which was developed and stooped by Lesedi Section. The first goaf occurred after only a couple of splits were stooped in an area where the effective panel span was reduced to 103 m (Table 6-3). The critical spans for goafing of the immediate sandstone roof and sill were calculated to be 171 m and 273 m respectively.

Similar to Panel 179b, goafing was attributed to the nearby dykes, as well as previously mined longwall panels as shown in Figure 6-5. The orientation of the panel relative to the major horizontal stress direction was again considered a contributing factor. The major horizontal stress corresponded to the direction of the induced stress from the dyke, despite the panel itself being orientated at a favourable, oblique angle (Table 6-4).

Increased stress was noticed during development as the section approached the dyke. This was seen in the form of increased pillar scaling. Good, stable roof conditions, however, remained prevalent towards the end of the panel. No surface subsidence has been reported above the panel since it goafed. It is worth mentioning that the frequency of goafing decreased the further the section stooped away from the dykes at the end of the panel.

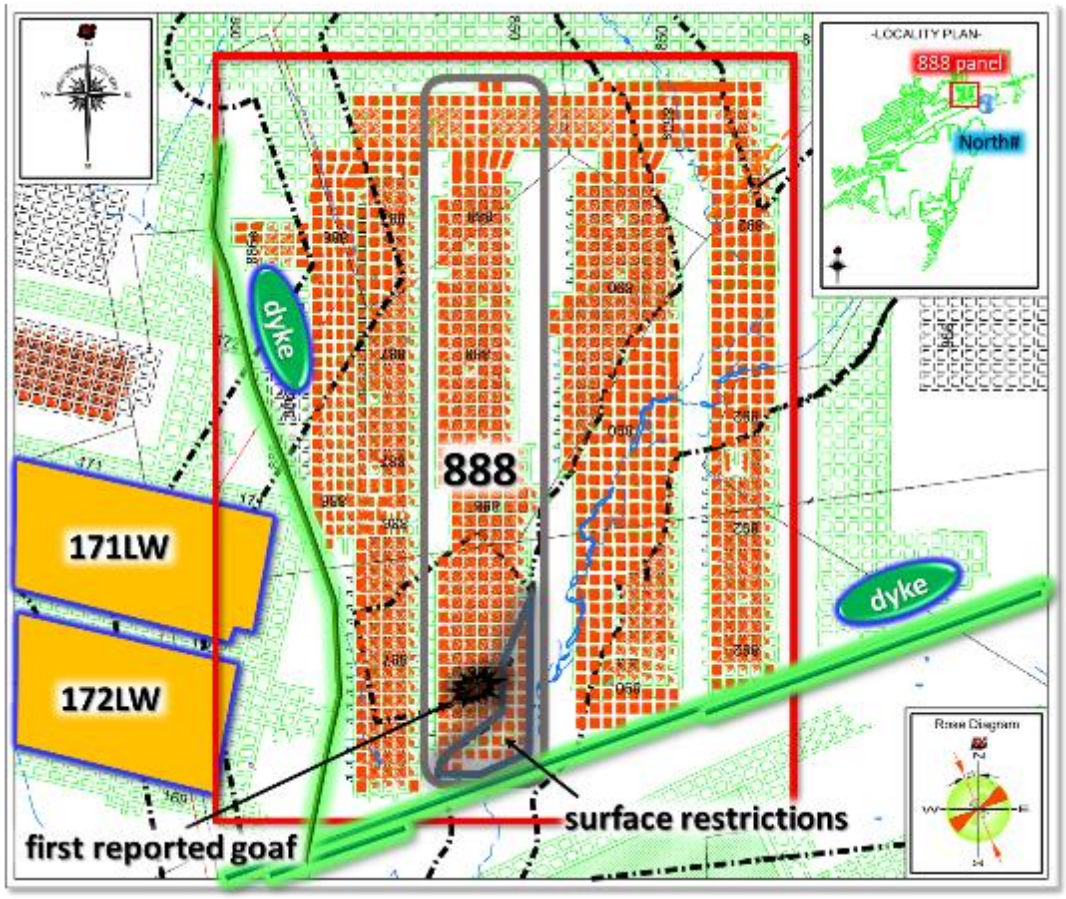


Figure 6-5: Panel 888 with nearby dyke and old longwall panels.

Panels 882c and 882d

Goafing also occurred in Panels 882c and 882d, which were developed and stooped by Inyanda Section. Again, these panels' effective spans were less than the critical spans calculated for each of them (Table 6-3). Panel 882c had an effective span of 127 m and Panel 882d an effective span of 152 m. Both of these were below the sub-critical spans to induce goafing of the immediate roof and the sill. Goafing was attributed to a nearby dyke and previously stooped panels as shown in Figure 6-6. Similar to Panels 179b and 888, the Rose diagram indicates that the regional major horizontal

stress corresponded to the direction of the induced stress from the dyke. It was therefore considered as a contributing factor to goafing in these panels.

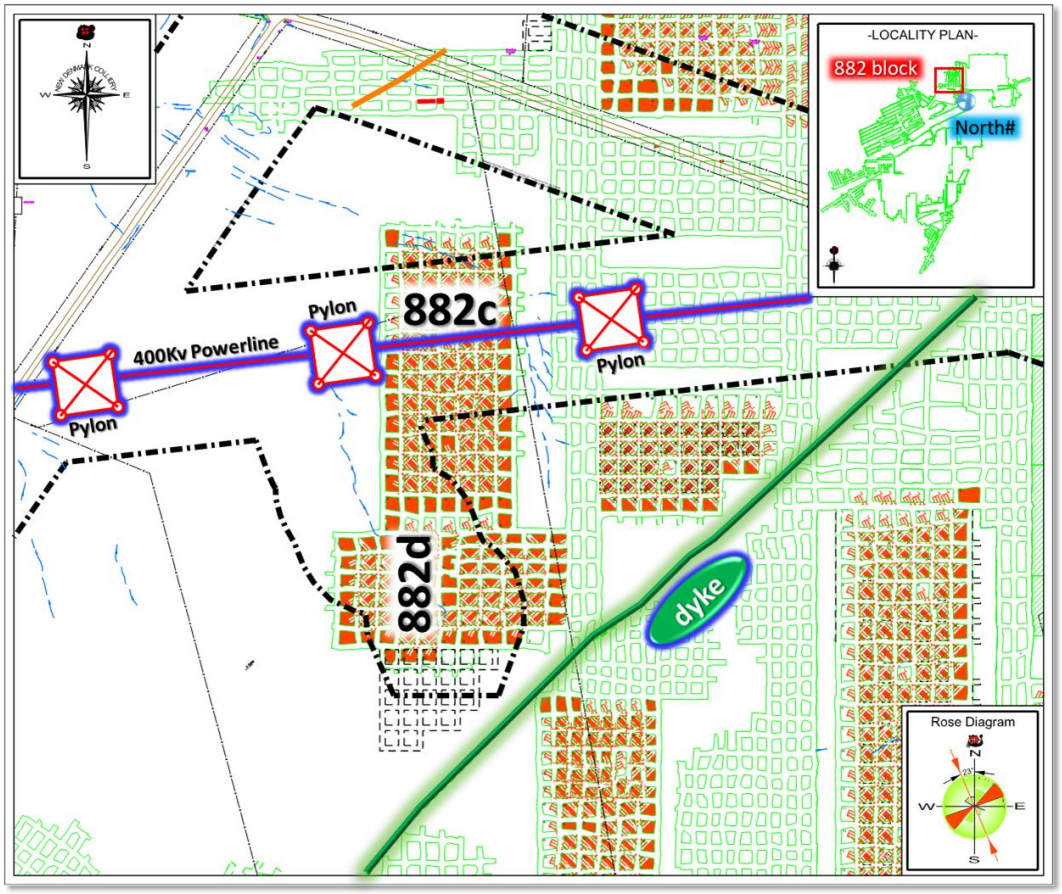


Figure 6-6: Panels 882c and 882d with nearby dyke and previously stooped panels.

Panels 1001B and 1001C

Goafing also occurred in Panels 1001B and 1001C at Central Shaft, which were developed and stooped by Simunye Section (Figure 6-7). Both panels had an effective span of 152 m which was on par with the critical span calculations for the immediate roof. Although this would have likely contributed, goafing in both panels only occurred right at the end of the

panels after stooping past a zone affected by multiple joints. Panel 1001C was developed and stooped after Panel 1001B, so it is expected that it would also have experienced increased stress from the adjacent stooped panel.

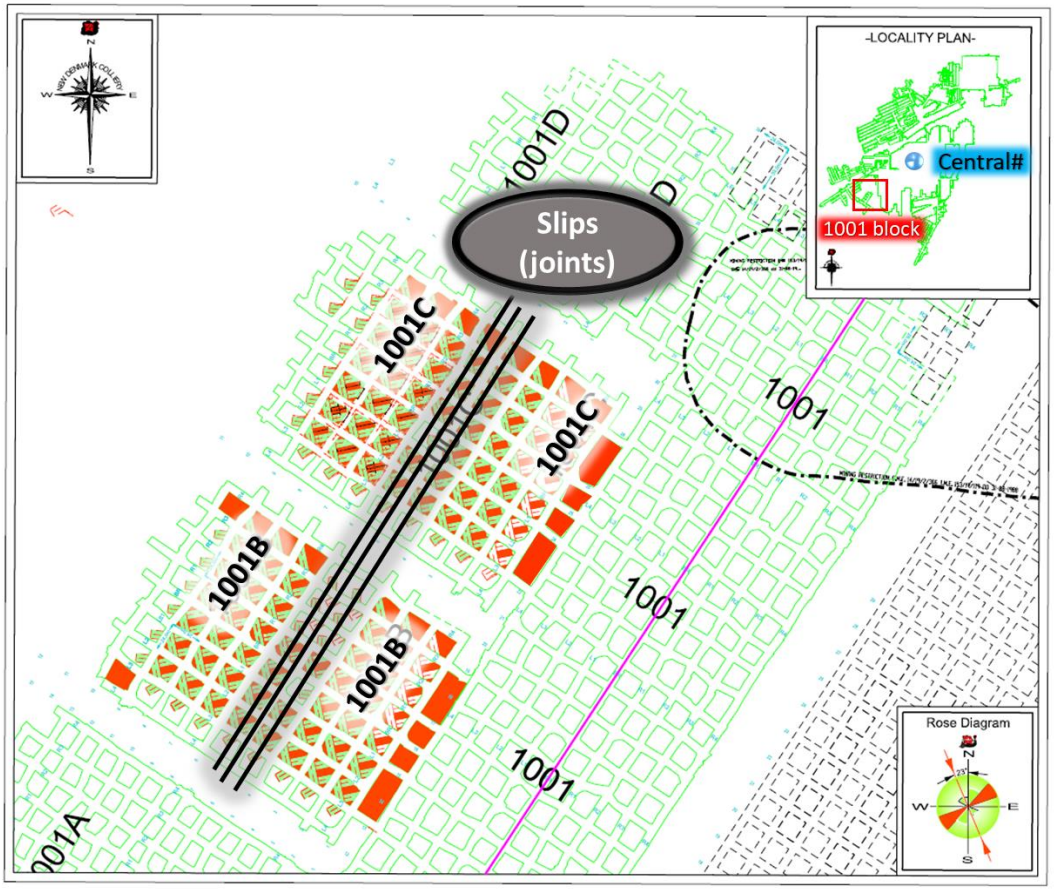


Figure 6-7: Panels 1001B and 1001C with multiple joints striking across them.

Panels 177/5 and 177/6

Panels 177/5 and 177/6 were the last two panels to have been developed and stooped. It was done by Thubelisha Section at Okhozini Shaft. Both panels goafed soon after stooping commenced. The goafing occurred

despite limited stooping ground and their effective panel spans being less than their critical spans (Table 6-3). The effective panel spans for Panels 177/5 and 177/6 were 80 m and 104 m, respectively. This was well below the sub-critical span of 134 m for each of the panels.

During development, a noticeable increase in stress was observed in these panels, which was evident in the form of increased pillar scaling. The stress appeared to increase towards the end of the panels as the sections approached the faults shown in Figure 6-8. Panel 177/5 was designed to fall outside of the fault and its affected zone, which runs at an oblique angle past the panel on the northeastern side. Panel 177/6 on the other hand was initially planned to develop through the fault and then stoop back. However, the maximum displacement of 1.5 m along the fault plane proved to be too challenging. Consequently, the panel was stopped short and stooping operations commenced sooner than planned.

Goafing in these panels were attributed to the presence of the two faults at the end of Panels 177/5 and 177/6. The initial goafing occurred near the faults, after which it became less frequent the further away the the stooping face was from them. Goafing was mostly confined to the centre of the panels between L1 and R1 roadways and was preceded by telltale signs, such as bent policeman sticks and cracking noises. Analysis of the Rose diagram shows that the faults were orientated at an oblique angle to the regional major horizontal stress direction (Table 6-4). However, it is uncertain whether it assisted with goafing.

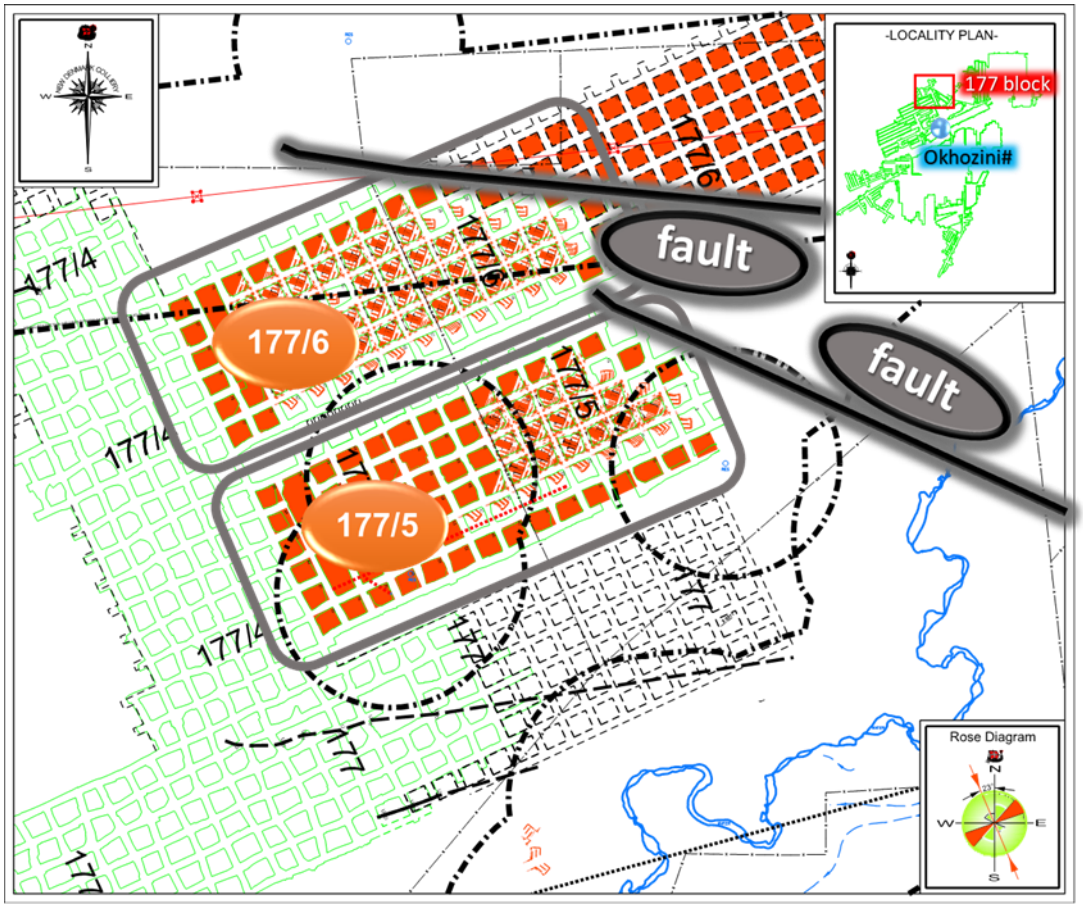


Figure 6-8: Panel 177/5 with limited stooping ground and a fault at the end of the panel.

6.3 Analysis of the Numerical Modelling

6.3.1 1100 Block

Model setup

The model for the 1100 block was set up according to the geological borehole logs and surveyed mining parameters of the area. Analysis of these logs indicated that the No. 4 coal seam has an average thickness of 2.3 m with the depth to the floor ranging from 175 m on the southern side to

more than 200 m on the northern side. The full seam was mined due to its relatively low seam height.

The immediate roof consists of a thick competent unit of sandstone which has a minimum thickness of about 20 m. It is furthermore overlain by a series of competent sandstone units, of which some are interbedded with siltstone. A significantly thick dolerite sill occurs close to the surface. It has an average thickness of 54 m and occurs roughly 130 m above the No. 4 coal seam. The overburden thus consists of multiple thick units of competent rock material, which has the potential to span over extensive mining voids, as shown in Table 6-1.

Panel 1120 (Figure 1-7) formed the focus point of the numerical modelling done for the 1100 block. The panel was divided into two blocks due to its length, namely a northern and a southern portion. The model consisted of 990 x 990 grids with a grid size of 0.5 m, which represents an actual area of 495 m x 495 m. The modelling area and corresponding virgin overburden load are shown in Figure 6-9.

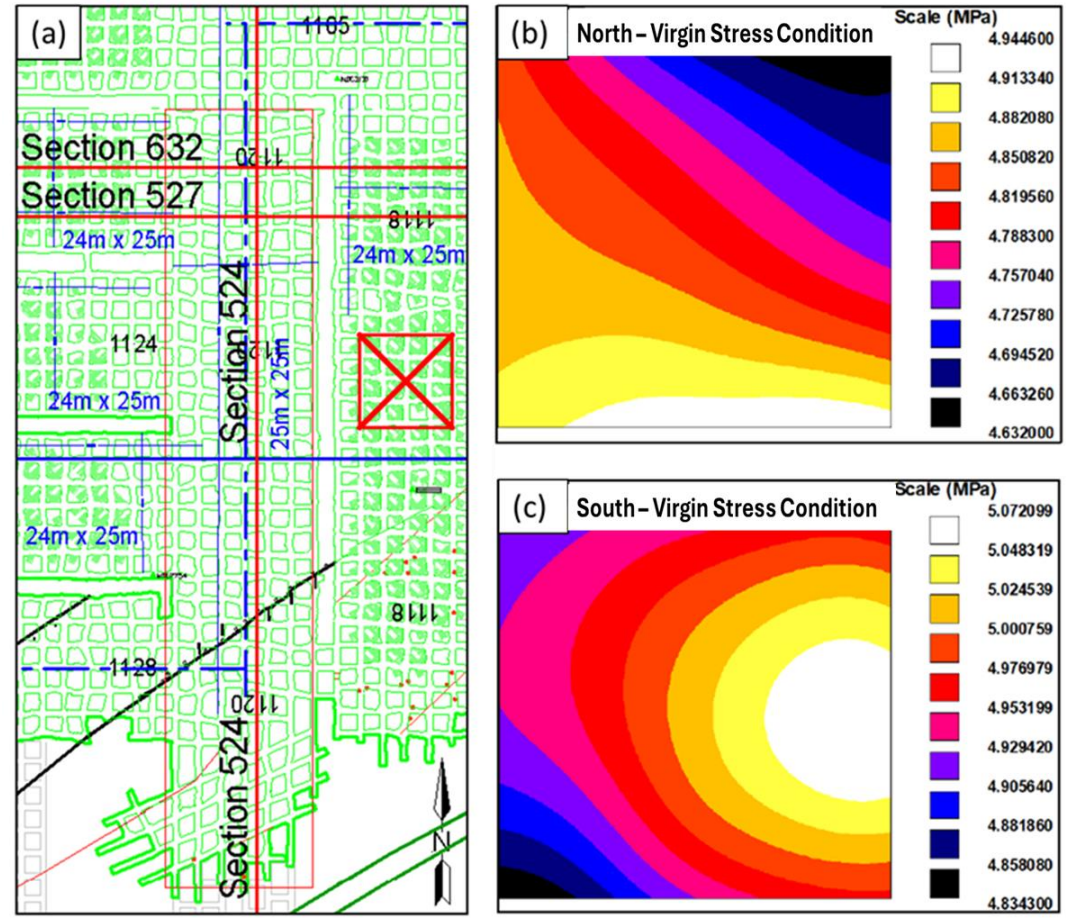


Figure 6-9: 1120 Modelling area; (a) Plan view of Panel 1120 indicating the various locations of the models; (b) northern portion virgin overburden stress model; (c) southern portion virgin overburden stress model (Jansen van Vuuren & De Beer, 2022a).

The modelled virgin overburden load was simply a check to ensure that the model was correctly set up. It simulates the vertical virgin stress, in other words, the overburden load down to the No. 4 coal seam before any mining activities. It ranges between 4.6 MPa and 5.1 MPa across the area, indicating a slight increase in vertical stress from north to south. This can either be attributed to variations in surface topography or a dipping coal

seam. It nonetheless correlates well with the average virgin stress of 4.65 MPa expected for a 190 m thick overburden load.

North to south

Panel 1120 was initially simulated with its neighbouring panels and all their pillars intact. The pillars were drawn up according to their actual mining dimensions to simulate their stress conditions before and after stooping and to compare them to the expected tributary load (stress). Figure 6-10 shows the stress contour plots for the northern and southern portions of Panel 1120 before any stooping activities. The green line indicates the north-south direction through the centre of Panel 1120.

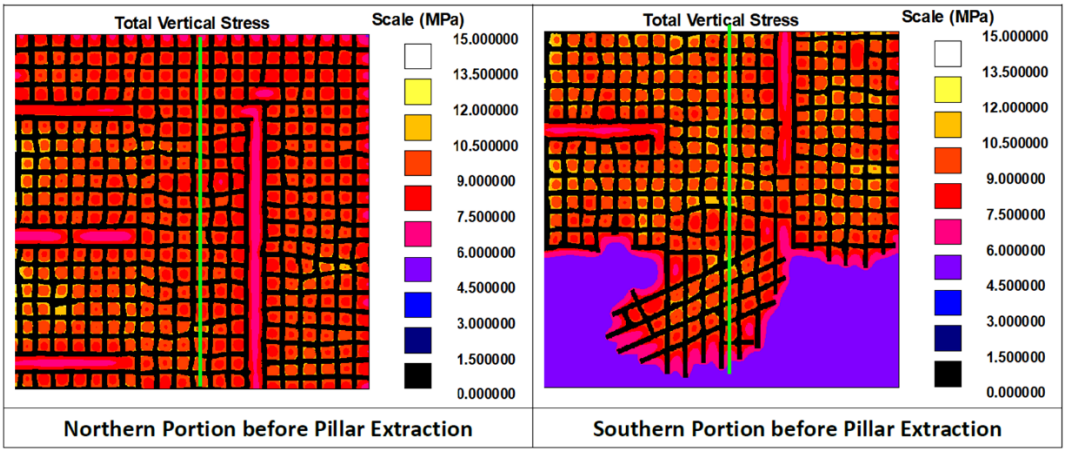


Figure 6-10: Stress contour plots for Panel 1120 before stooping – north to south (Jansen van Vuuren & De Beer, 2022a).

Figure 6-11 shows the stress contour plots for the northern and southern portions of Panel 1120 after its neighbouring panels have been stooped. It represents the current condition underground and as indicated on the

mining plans. The figure also shows the effects of offline mining by indicating a large and small pillar and the total vertical stress experienced by each. They also served as reference points when the data was plotted.

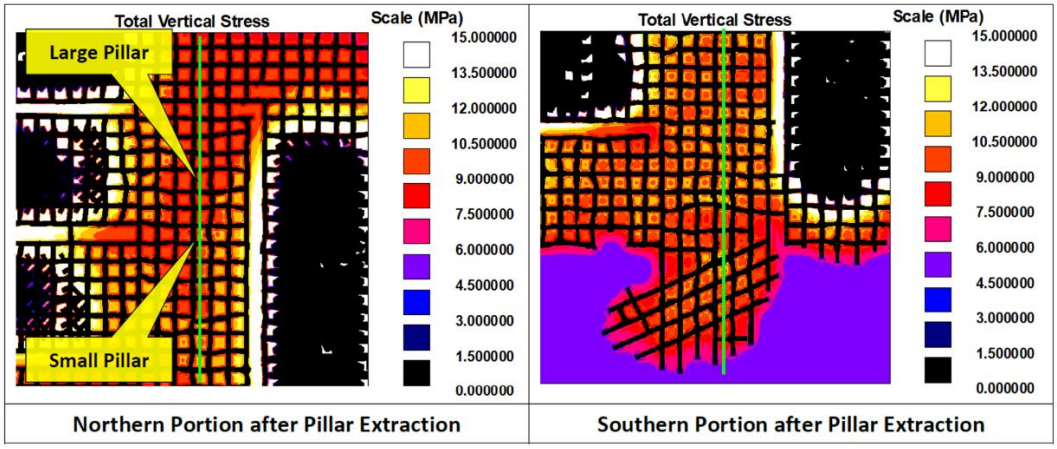


Figure 6-11: Stress contour plots for Panel 1120 after stooping of adjacent panels – north to south (Jansen van Vuuren & De Beer, 2022a).

The numerical modelling results obtained for Panel 1120 before and after the stooping of adjacent panels, specifically those along Section 524, were plotted in Figures 6-12 and 6-13. These graphs assisted in clarifying the data and improved the assessment of changes in vertical stress. Figure 6-12 indicates the results for the northern portion of Panel 1120, while Figure 6-13 indicates those for the southern portion.

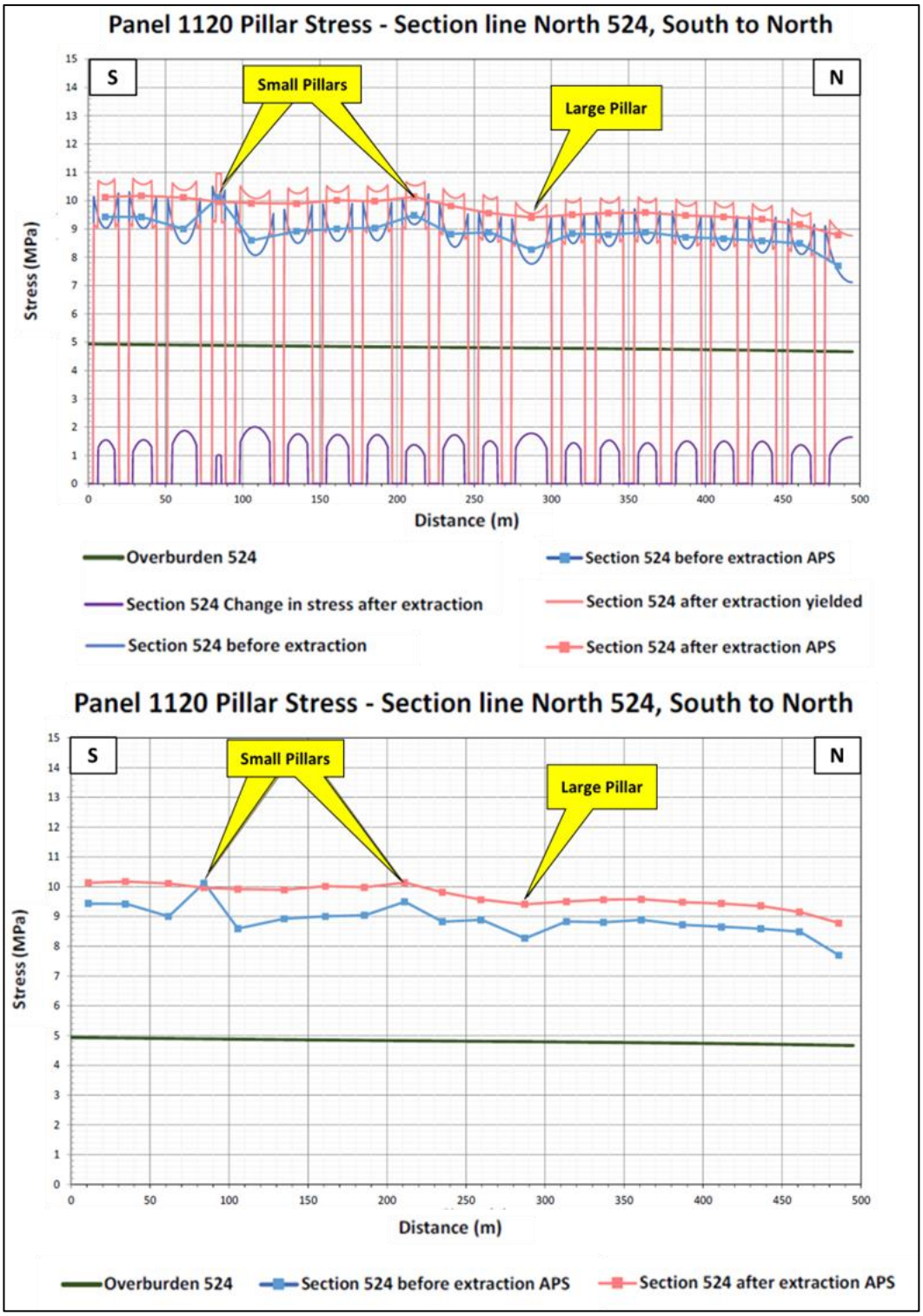


Figure 6-12: Panel 1120 pillar stress along Section 524 – northern portion (Jansen van Vuuren & De Beer, 2022a).

The following information is derived from the graphs indicated in Figure 6-12:

- The virgin vertical stress for the northern portion of Panel 1120 ranged from 4.7 MPa to 4.9 MPa.
- The Average Pillar Stress (APS) after pillar development was approximately 8.9 MPa. This was about 5% less than the tributary stress (load), which was calculated to be 9.4 MPa for each pillar.
- The APS increased to 9.7 MPa after stooping in the adjacent panels, with individual pillars being as high as 10.2 MPa. This was an increase of about 10% in the stress carried by the pillars along the centre of Panel 1120 after the stooping of the adjacent panels.
- The increased stress on the pillars reduced the SF from 1.9 to about 1.82 assuming a calculated pillar strength of 17.7 MPa.

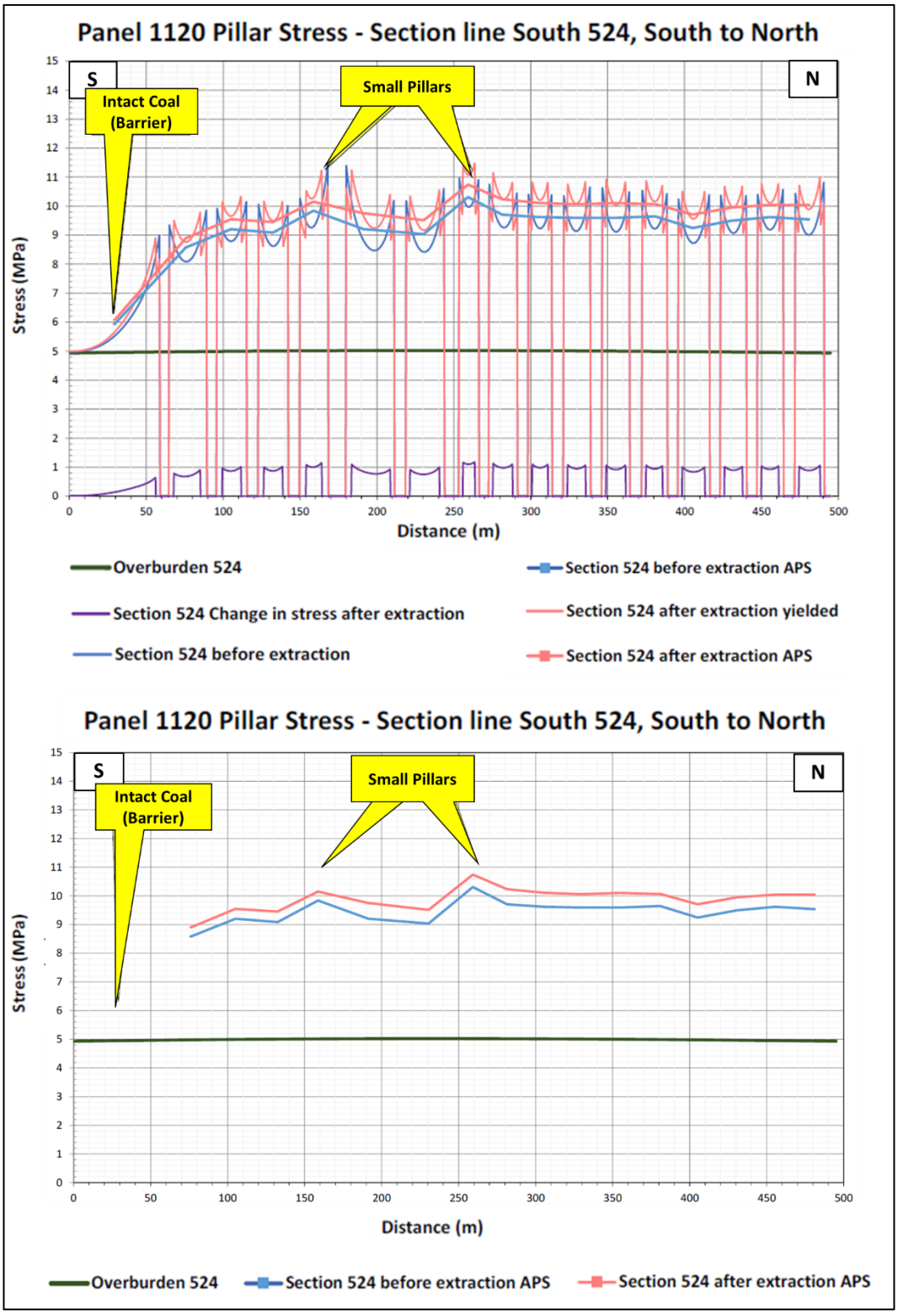


Figure 6-13: Panel 1120 pillar stress along Section 524 – southern portion (Jansen van Vuuren & De Beer, 2022a).

In the southern portion (Figure 6-13):

- The virgin vertical stress ranged from 4.9 MPa to 5.0 MPa.
- The APS after development was roughly 9.5 MPa, which was similar to the tributary stress for each pillar calculated at 9.4 MPa.
- The simulated APS increased to 9.9 MPa after stooping in the adjacent panels, ignoring the substantial intact coal on the southern side of the panel. Individual pillars were as high as 10.7 MPa with the peak stress in the small pillars' ribsides reaching a high of 11.5 MPa.
- The APS along the centre of Panel 1120 increased by about 4.7% after stooping of the neighbouring panels.

East to west

An east-to-west analysis was also done across Panel 1120 similar to the one along Section 524 from north to south. Figure 6-14 shows the stress contour plots for the northern portion of Panel 1120 where the green line represents the east-west section through Section 527. The northern portion was selected for analysis due to a 10% increase in pillar stress after stooping compared to the 4.7% across the southern portion.

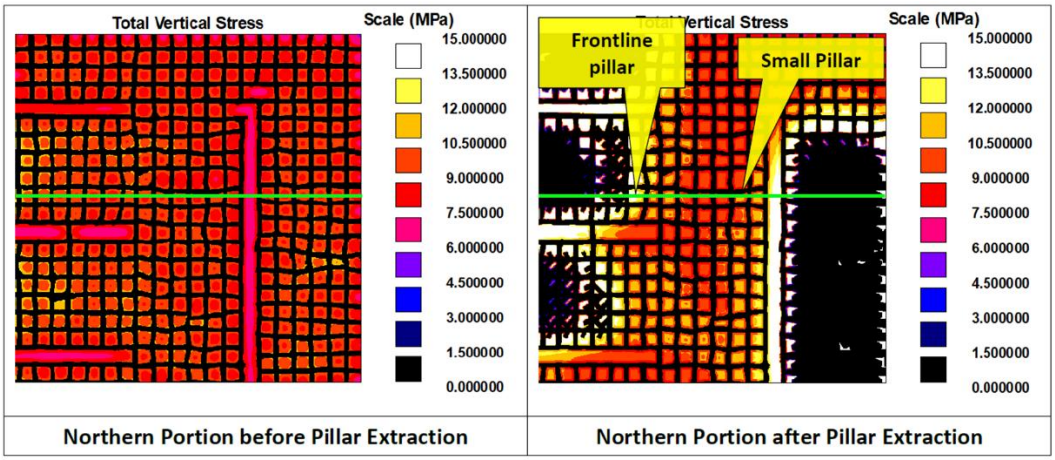


Figure 6-14: Stress contour plot for Panel 1120 before and after stooping – east to west (Jansen van Vuuren & De Beer, 2022a).

The numerical modelling results plotted in Figure 6-15 suggest the following:

- The virgin vertical stress along Section 527 was approximately 4.8 MPa.
- The simulated APS after development was roughly 9.0 MPa, which increased to about 11.0 MPa after stooping.
- The overall increase in APS due to stooping was 2.0 MPa, which was a 22.3% increase. This included the increased APS experienced by the frontline stopper pillars on the west and the barrier pillar on the eastern side. However, when these were excluded, the increased pillar load was 1.2 MPa, which accounted for a 13.4% increase.
- Apart from the pillar stress values, the graph visually demonstrates how the frontline and barrier pillars carried the highest induced stress from the adjacent stooping panels, after

which the pillar stress slightly dissipated towards the centre of Panel 1120. It highlighted the importance of these pillars and their mitigating effects on the increased pillar stress from the surrounding stooped panels.

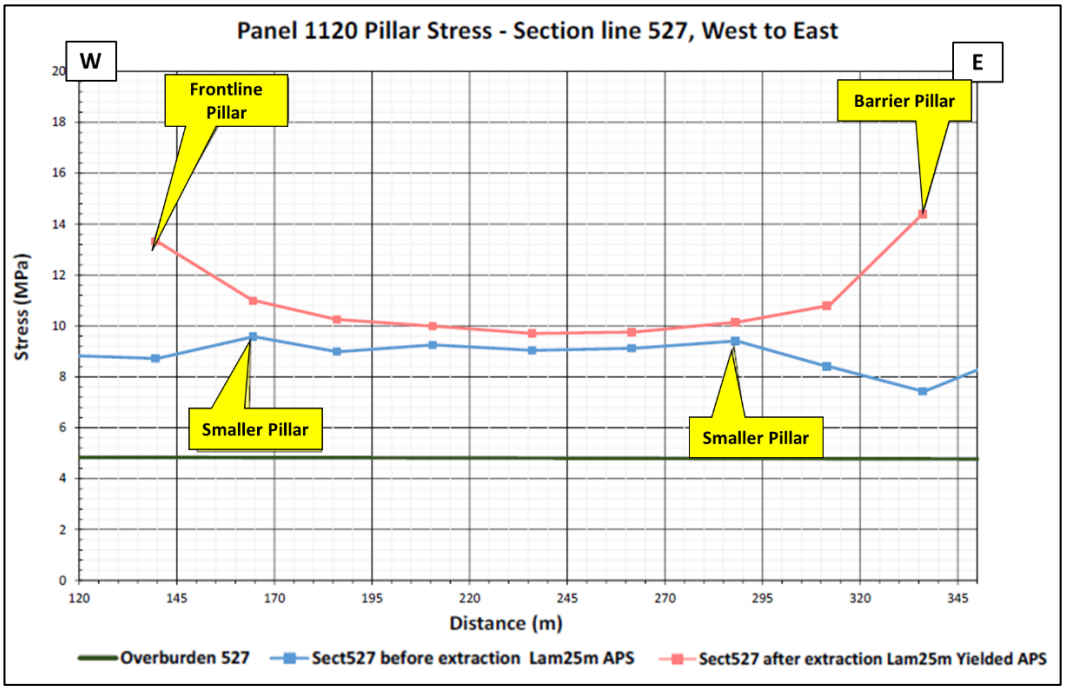


Figure 6-15: Panel 1120 pillar stress across Section 527 (Jansen van Vuuren & De Beer, 2022a).

Effect of barrier pillar width

Numerical modelling of Panel 1120 and the surrounding stooped panels was further used to analyse the effect of a barrier pillar on mitigating the increased vertical stress from an adjacent stooping panel, especially if it did not goaf. The strength of the pillar and its ability to mitigate the increased stress was largely dependent on its width. The objective was thus to determine the minimum required barrier pillar width between a main

development and stooping panel, as well as between two adjacent stooping panels. This was achieved by simulating different scenarios in which the barrier pillar's width varied from 75% - 300% of its original width. This specific exercise focused on the barrier pillar to the east of Panel 1120, separating it from the adjacent stooped panel, Panel 1118. Figure 6-16 shows the stress contour plots for these analyses along the northern portion of Panel 1120 and its surrounding stooped panels.

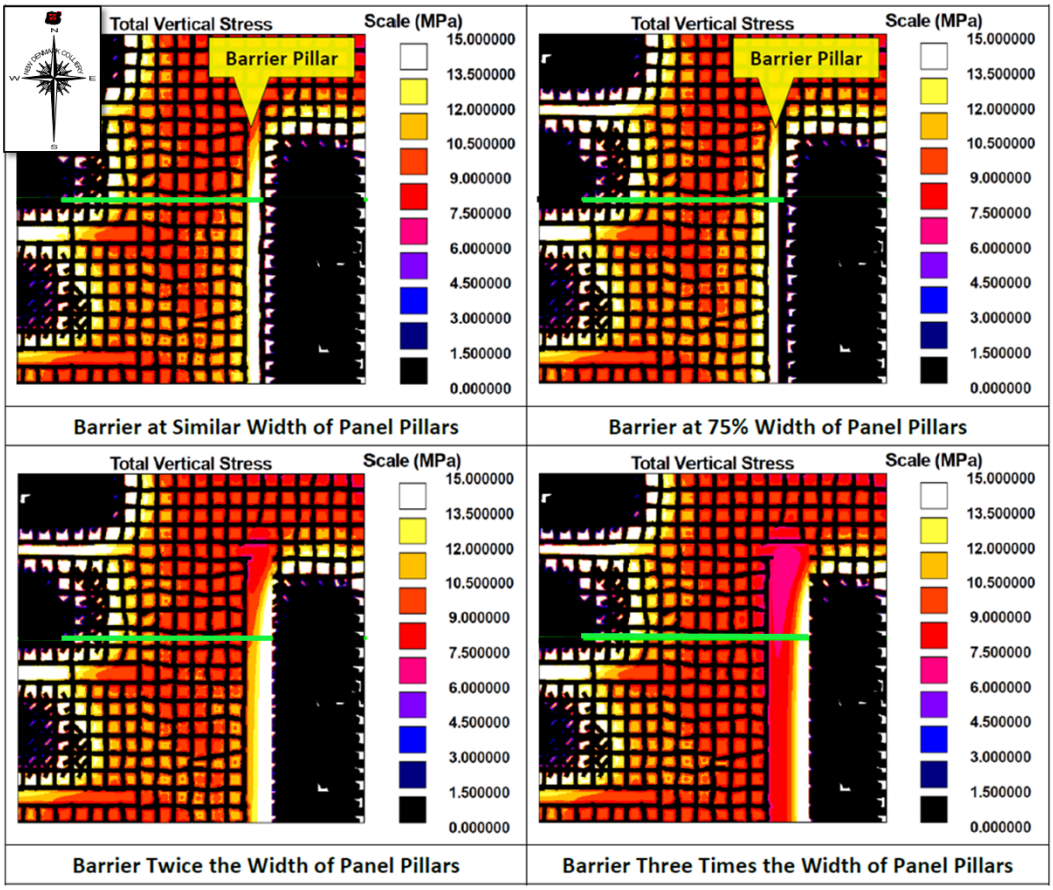


Figure 6-16: Stress contour plots for Panel 1120 simulating various barrier pillar widths (Jansen van Vuuren & De Beer, 2022a).

The baseline was to simulate the barrier at its original width, which is equal to that of the adjacent in-panel pillars in Panels 1118 and 1120. A second simulation was done with the barrier pillar width reduced to 75% of its original width, after which it was increased to 200% and 300%. The results for each of these simulations were plotted in a trendline graph, as provided in Figure 6-17. It allowed for easy comparison between the effects of the various pillar widths. The barrier pillar on the eastern side of Panel 1120, and consequently on the graph, was further made the reference point with the x-axis indicating the distance that it would take for the increased pillar stress after stooping to dissipate to that before stooping. Each value point represents the APS experienced by the in-panel pillars of Panel 1120. This information also assisted in determining the stand-off distances between stooped panels and sensitive underground infrastructure, such as belt and travelling roads, underground workshops and even shafts.

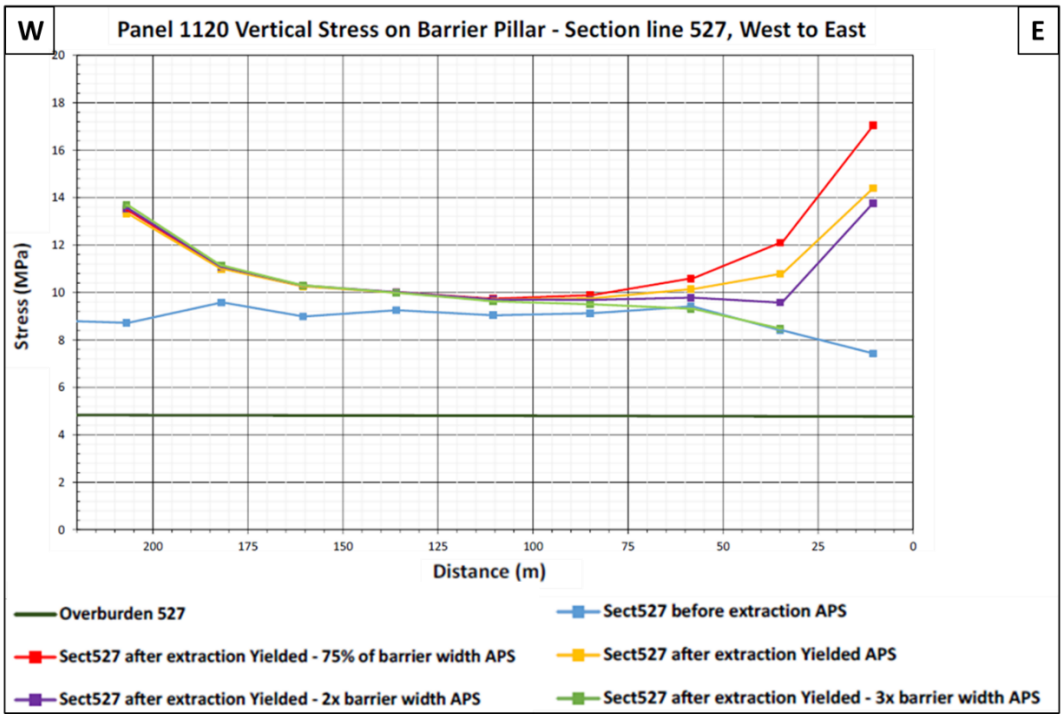


Figure 6-17: Panel 1120 vertical stress conditions across barrier pillars of various widths (Jansen van Vuuren & De Beer, 2022a).

The following information was drawn from Figure 6-17:

- For a barrier pillar width equal to the in-panel pillar width, i.e. 100% of width:
    - There was a 7 MPa or 94% increase in the APS across the barrier after Panel 1118 was stooped. It represents the distance 0 m – 25 m from the centre of the barrier, towards the western side.
    - The first in-panel pillar of Panel 1120, thus immediately west of the barrier, experienced a 2.4 MPa or 28% increase in the APS between 25 m – 50 m from the barrier.

- For the next four pillars, the APS was less than 1 MPa or 7% - 8%. This was the centre of the panel and represents the distance 50 m to 150 m from the barrier.
- Thereafter the APS increased again to the west, due to the stooped panel on the western side of Panel 1120.

- For a barrier pillar width at ±75% of the in-panel pillar width:
  - It experienced a 9.6 MPa or 129% increase in the APS across the barrier, which represents the distance 0 m – 25 m from the barrier towards the western side. This was 2.65 MPa or 38% higher compared to the full-width (100%) barrier.
  - The first in-panel pillar of Panel 1120 experienced a 3.7 MPa or 44% increase in the APS, 25 m – 50 m from the barrier. It was 1.3 MPa or 55% higher, compared to the full-width (100%) barrier.
  - The vertical stress decreased for the next pillar as there was only 1.2 MPa or 13% increase in the APS, 50 m – 75 m from the barrier.
  - For the next three pillars, the APS was less than 1 MPa, or 8%. This is the centre of the panel and represents the distance 75 m – 125 m from the barrier. It was only 0.1 MPa higher, compared to the full-width (100%) barrier.
  - The APS thereafter increased again to the western side.

- For a barrier pillar width at ±200% of the in-panel pillar width:
    - There was a 6.35 MPa or 85% increase in the APS across the barrier, representing the distance 0 m – 25 m from the barrier centre towards the western side. This was 0.6 MPa or 9% less compared to the full-width (100%) barrier.
    - The first in-panel pillar experienced a 1.2 MPa or 14% increase in the APS, 25 m – 50 m from the barrier. It was 1.2 MPa or 51% less compared to the full-width (100%) barrier.

      The next four pillars experienced less than 7% to 8% in APS, which was similar to the full-width (100%) barrier.

- For a barrier pillar at ±300% of the in-panel pillar width:
    - The APS across the barrier was very similar to the originally developed barrier before stooping.
    - There was a marginal increase in the APS on the first in-panel pillar immediately west of the barrier.
    - Most of the Panel 1120 pillars were completely shielded by the wide barrier pillar and the effect of stooping in the adjacent Panel 1118 was marginal.
    - The pillars on the western side of Panel 1120 were more affected by the stooped panels on the opposite side.

A summary of the results is provided in Appendix D.

6.3.2 Shosholoza Block

Model setup

The model for the Shosholoza block was set up similarly to the 1100 block, using the geological borehole logs and surveyed mining parameters of that area. It focused on the main development, Panel 1134, and the three side panels, which were developed and stooped at that time, namely Panels 134, 135 and 136. Special focus was placed on where these side panels extended from Panel 1134. Panel 133 and its respective side panels 133a and 133b were not stooped at the time of the modelling. Figure 6-18 shows this study area with its various cross-section locations.

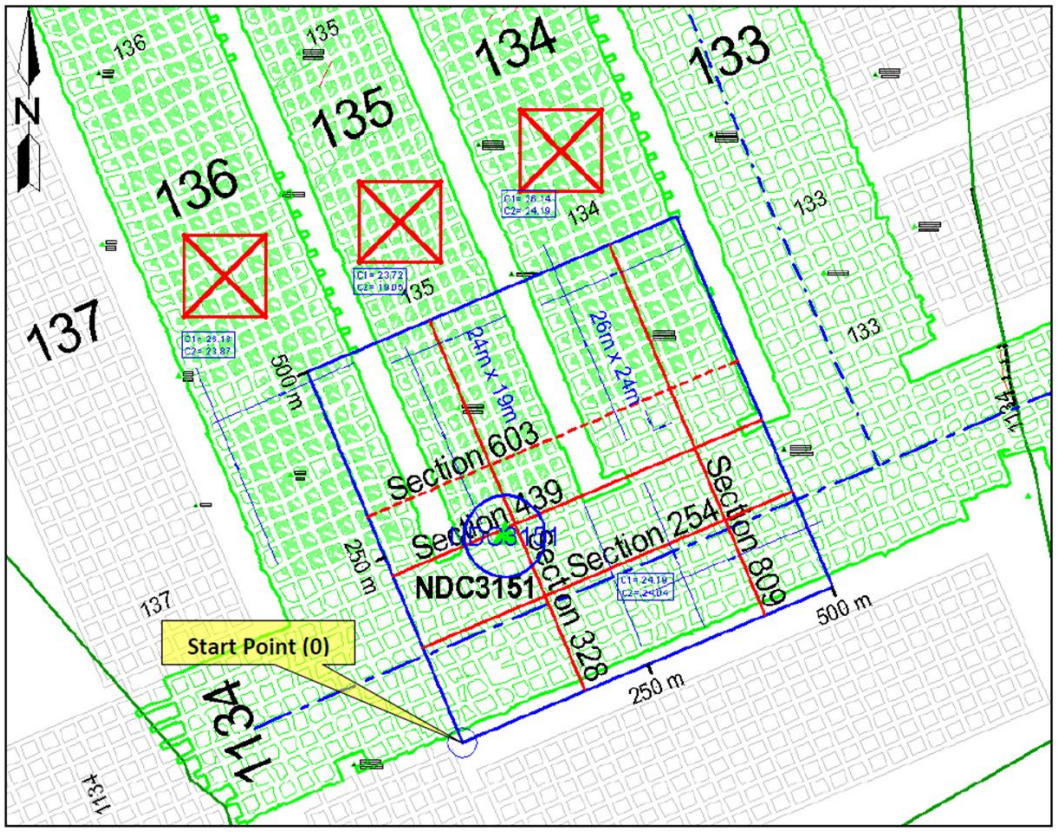


Figure 6-18: Shosholoza modelling area with its various cross-section locations (Jansen van Vuuren & De Beer, 2022b).

The geological borehole logs indicate that the No. 4 coal seam for this specific area occurs at an average depth of 162 m below the surface. The seam has an average thickness of 1.8 m and was therefore mined to its full height. It is overlain by a competent layer of gritstone-sandstone, which has an average thickness of 9 m. The dolerite sill above this area has an average thickness of 16 m and occurs approximately 98 m above the coal seam. Similar to the 1100 block, the overburden consists of multiple thick, competent units, which are stiff and have the potential to span over extensive mining voids.

Panel 1134 / 135

Panel 135, as previously mentioned, was not originally planned for stooping, hence its smaller pillar dimensions compared to the two neighbouring Panels 134 and 136. The pillars were rectangular with pillar centres of 24.0 m (length) x 19.0 m (width). Two rows of stopper pillars were left at the end of the stooping to separate the stooped-out Panel 135 from the main development, Panel 1134. This was done according to what is considered as good practice by Van der Merwe & Madden (2010). Figure 6-19 indicates the stress contour plots for Panel 1134 / 135 before and after stooping. The green line represents Section 328, which extends along the centre of Panel 135 to the southern side of Panel 1134.

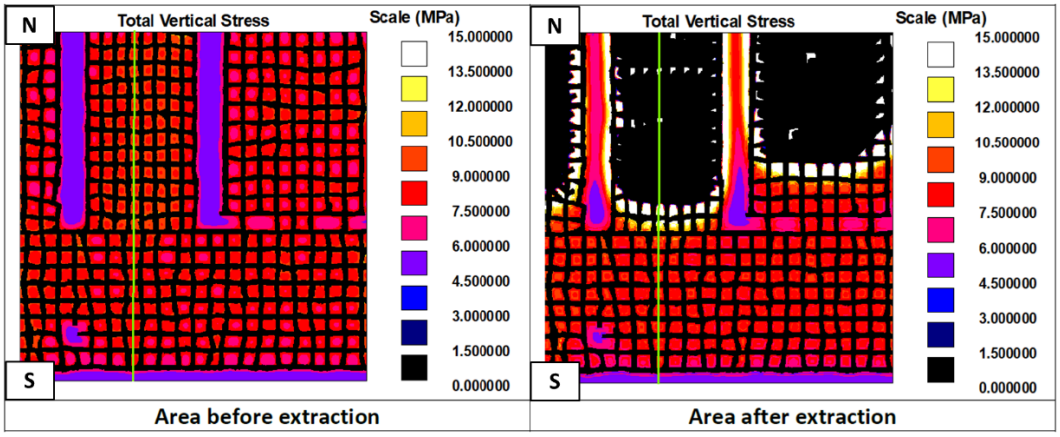


Figure 6-19: Stress contour plots for Panel 1134 / 135 before and after stooping (Jansen van Vuuren & De Beer, 2022b).

The results obtained from the stress contour plots, specifically those along Section 328, are plotted in Figure 6-20. It demonstrates the variation in vertical stress experienced by these pillars from before to after stooping.

The numbers on the graph equate to the pillar numbers, which start at Pillar #1 on the southern side of the panel, adjacent to the barrier pillar. Pillars #1 to #8 falls within Panel 1134 while Pillars #9 and #10 form the two rows of stopper pillars at the end of stooping Panel 135. Pillar #9 is referred to as the panel-entry pillars and Pillar #10 as the frontline pillars.

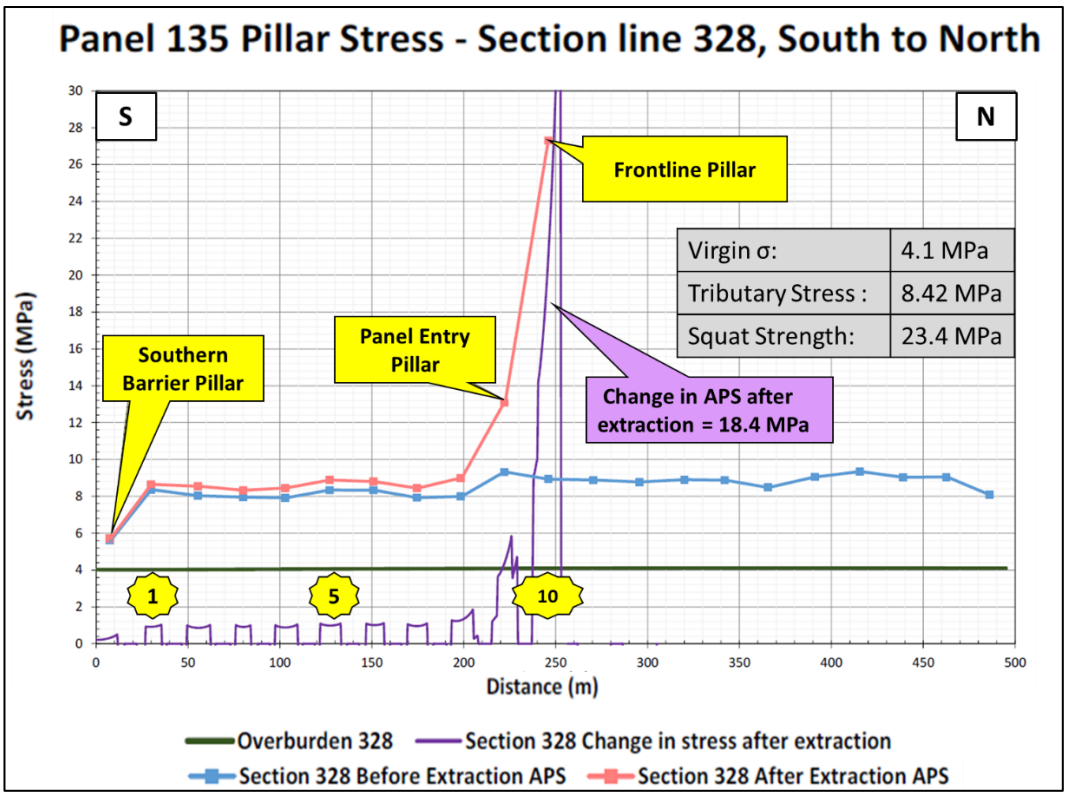


Figure 6-20: Panel 1134 / 135 pillar stress along Section 328 (Jansen van Vuuren & De Beer, 2022b).

Figure 6-20 indicates the following:

- The virgin vertical stress along Section 328 was approximately 4.1 MPa.

- The average pillar strength calculated using the squat-pillar formula (*Equation 2-2*) was 23.4 MPa, while the tributary stress (*Equation 2-3*) was calculated to be 8.42 MPa. This provided a SF (*Equation 2-4*) of approximately 2.7 during development.
- The numerical modelling results indicated that APS after development was 8.3 MPa. It correlated relatively well to the 8.42 MPa calculated using the empirical tributary stress formula. The APS of 8.3 MPa excluded the pillar stress of 5.6 MPa experienced by the southern barrier pillar of Panel 1134.
- The frontline pillars (Pillar #10) were subjected to the highest stress after stooping, which was 27.3 MPa according to the numerical modelling results. This was a significant increase of 18.4 MPa from before to after stooping. The APS of 27.3 MPa exceeded the pillars' calculated strength of 23.4 MPa and provided for a SF of approximately 0.85. Although it was expected that the pillars would fail, they remained stable despite excessive scaling. This was attributed to the ability of the overburden to span across the panel and lighten the stress on the frontline pillars. The support from the barrier pillars and to a lesser extent the remaining fenders in the stooped-out area also assisted in maintaining the stability of the pillars.
- The purple trendline, which represents the change in stress after pillar extraction, also indicates the variation in stress experienced by the frontline pillars. The ribsides of the pillars facing the

stooped-out area experienced the highest vertical stress ranging between 30 MPa and 32 MPa. These ribsides experienced excessive pillar scaling because of the high vertical stress. However, the stress decreased rather quickly along the length of the pillar where it reached an average of 18.4 MPa in the centre of the pillar. These results represent the difference between the APS before and after stooping. The stress continued to decrease towards the ribside facing south, in the direction of Panel 1134.

- The panel-entry pillars (Pillar #9) experienced an APS of 13.1 MPa after stooping, which was a substantial decrease in stress from the frontline pillars. This corresponded well to Van der Merwe and Madden's (2010) recommendation of leaving only two rows of stopper pillars at the end of a stooping panel.
- The APS further decreased to 9.0 MPa for Pillar #8, which is also described as the northern abutment for Panel 1134. This was a 1 MPa or 12.5% increase from before to after stooping.
- The APS for Pillars #1 to #8 after stooping was 8.6 MPa, which was approximately a 6.6% increase from development. This was an average increase of about 0.5 MPa after stooping. It indicates that the pillars in Panel 1134 were largely unaffected by the stooping of Panel 135. The average SF for these pillars remained above 2.5.

Panel 1134 / 134

Panel 134 was developed and stooped after panels 135 and 136. This was also after excessive pillar scaling observed in Panel 1120, which was caused by the increased stress from the surrounding stooped panels. It caused concern about the stability of the main development, Panel 1134. Consequently, the stooping layout was changed to leave four rows of stopper pillars at the end of Panel 134, with the first row including two larger panel-entry pillars. Figure 6-21 shows the stress contour plots for Panel 1134 / 134 before and after stooping. The green line represents Section 809, which extends along the centre of Panel 134 to the southern side of Panel 1134.

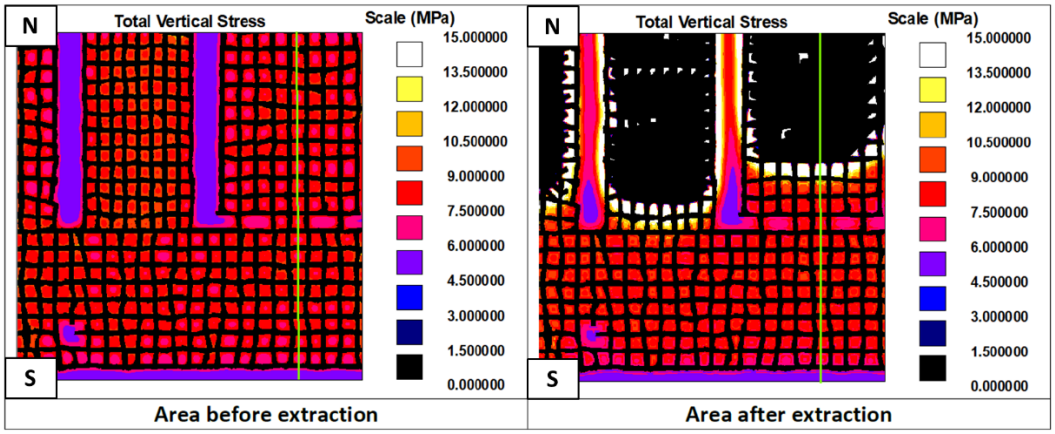


Figure 6-21: Stress contour plots for Panel 1134 / 134 before and after stooping (Jansen van Vuuren & De Beer, 2022b).

The variation in APS experienced by the pillars along Section 809 from before to after stooping is plotted in Figure 6-22. The numbers in the graph are similar to those in Figure 6-20. It starts with Pillar #1 on the southern

side of Panel 1134, adjacent to the barrier pillar. Pillars #1 to #8 fall within Panel 1134 while Pillars #9 to #12 form the four rows of stopper pillars at the end of stooping Panel 134. Pillar #9 is referred to as the panel-entry pillars and Pillar #12 as the frontline pillars.

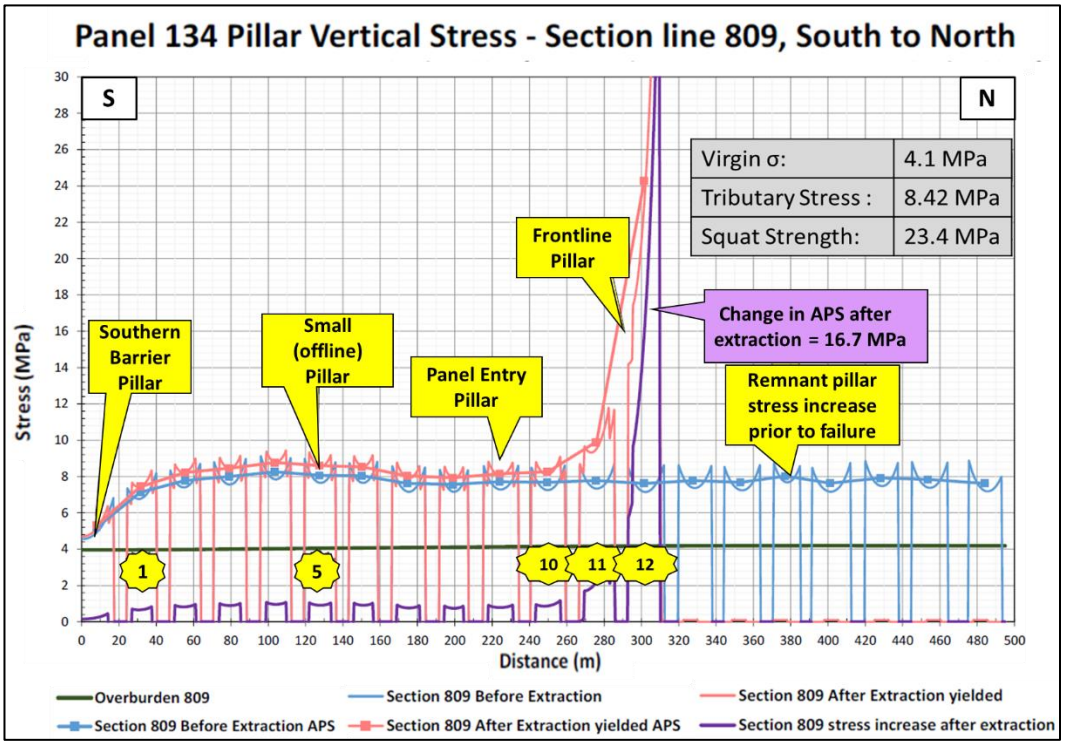


Figure 6-22: Panel 1134 / 134 pillar stress along Section 809 (Jansen van Vuuren & De Beer, 2022b).

Figure 6-22 indicates the following:

- The virgin vertical stress along Section 809 was approximately 4.1 MPa, which was the same as Section 328.
- Similar to the SF calculations for the pillars along Section 328, the average pillar strength calculated using the squat-pillar formula (*Equation 2-2*) was 23.4 MPa. The tributary stress (*Equation 2-3*)

was calculated to be 8.42 MPa. This provided a SF (*Equation 2-4*) of approximately 2.7 during development.

- The APS after development was 7.8 MPa. It excluded the APS of 5.2 MPa experienced by the southern barrier pillar of Panel 1134.
- The frontline pillars (Pillar #12) were subjected to the highest stress after stooping, which was 24.3 MPa according to the numerical modelling results. This was a significant increase of 16.7 MPa from before to after stooping. The APS for these frontline pillars were slightly less than those of Panel 135 (Section 328) due to the larger pillar dimensions. The pillar centres for Panel 1134 were 26 m (length) x 24 m (width) compared to Panel 135's smaller pillars with centres of 24.0 m (length) x 19.0 m (width). The APS on the frontline pillars of 24.3 MPa exceeded these pillars' strength of 23.4 MPa and reduced the SF to 0.96. The pillars nevertheless remained stable although affected by excessive scaling of their ribsides.
- The purple trendline shows the change in stress experienced by the frontline pillars after stooping. The ribsides of the pillars facing the stooped-out area experienced the highest vertical stress ranging between 30 MPa and 32 MPa. The stress however decreased rather quickly along the length of the pillar where it reached an average of 16.7 MPa in the centre of the pillar. This result shows the difference between the APS before and after

stooping. The stress continued to decrease towards the ribside facing south, in the direction of Panel 1134.

- The next two rows of stopper pillars (Pillar #11 and #10) only experienced a stress increase of 2.1 MPa and 0.6 MPa, respectively. This showed that the APS decreased substantially from the frontline pillars to the next two rows of stopper pillars.
- The panel-entry pillars (Pillars #9) experienced an APS of 8.2 MPa after stooping, which was merely an increase of 0.5 MPa from before to after stooping. This was attributed to the two rows of stopper pillars left between them and the frontline pillars, as well as the larger panel-entry pillars.
- The APS then further decreased to 7.9 MPa for Pillar #8, which was described as the northern abutment for Panel 1134. This was a 0.3 MPa or 4.8% increase from before to after stooping.
- The APS after stooping remained stable at a slightly higher stress of 0.45 MPa for the in-panel pillars (Pillars #1 to #8) of Panel 1134. This was a slight increase of 5.6%, which confirmed that the pillars in Panel 1134 were largely unaffected by the stooping of Panel 134. The average SF for these pillars remained above 2.5.

Effect of panel-entry layout

The most essential comparison made was the extent of the vertical stress zone from the stooped panels 134 and 135. It was done by comparing the

abutment pillars on the northern side of Panel 1134 at the location of the entries of the two stooped panels. The variation in pillar stress from before to after stooping for both Sections 809 and 328, thus north to south, are displayed on one graph, as seen in Figure 6-23. The table of results can also be seen in Appendix E for ease of comparison.

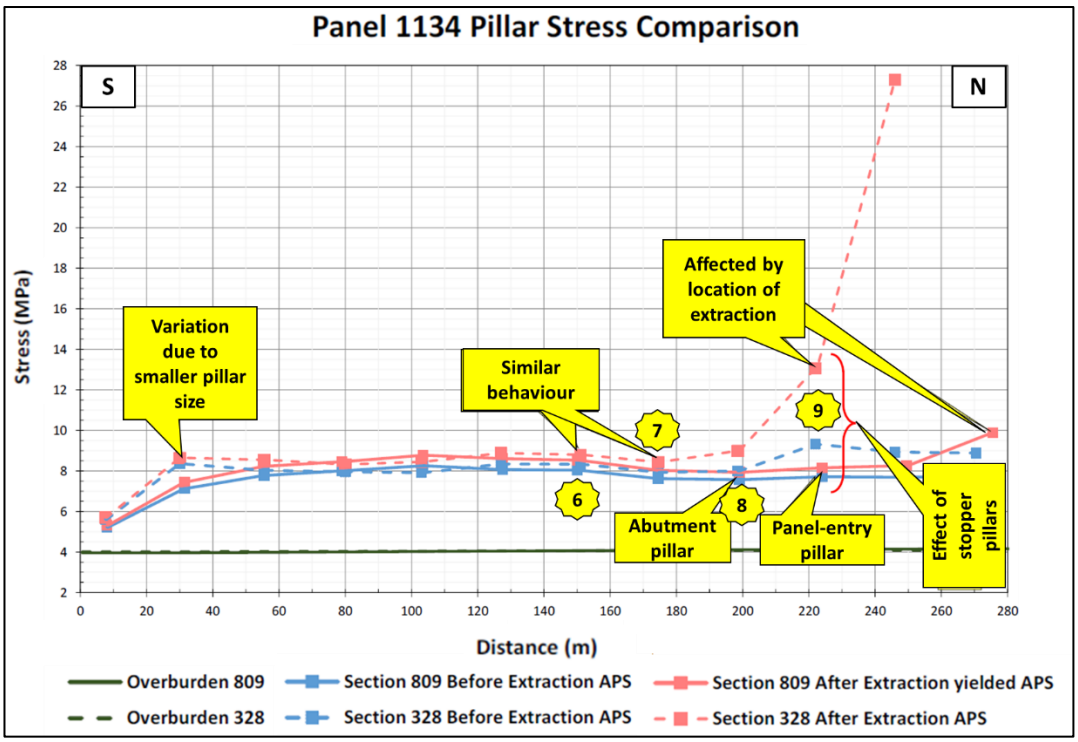


Figure 6-23: Panel 1134 abutment pillar – comparison of vertical stress (Jansen van Vuuren & De Beer, 2022b).

The effect of different panel-entry layouts is furthermore demonstrated by Figure 6-24, which shows the variation in pillar stress along Section 439. This section was drawn from west to east across the first row of stopper pillars (panel-entry pillars) of the stooped panels 135 and 134. It confirmed that the panel-entry pillars of Panel 135 experienced a higher

APS after stooping compared to those of Panel 134. This is due to only two rows of stopper pillars left at the end of Panel 135, while four rows of stopper pillars were left at the end of Panel 134. The buffering effect of the larger panel-entry pillars (Pillars #9) of Panel 134 could therefore not be truly reflected in the numerical modelling results due to the additional two rows of stopper pillars left between them and the frontline pillars. The APS induced by the stooping of Panel 134 had already decreased substantially after the first two rows of stopper pillars. This was a very conservative design in response to the pillar stability issues of Panel 1120. The panel-entry layout for Panel 134 was therefore amended to consist of three rows of stopper pillars at most, especially when stooping back to a main development.

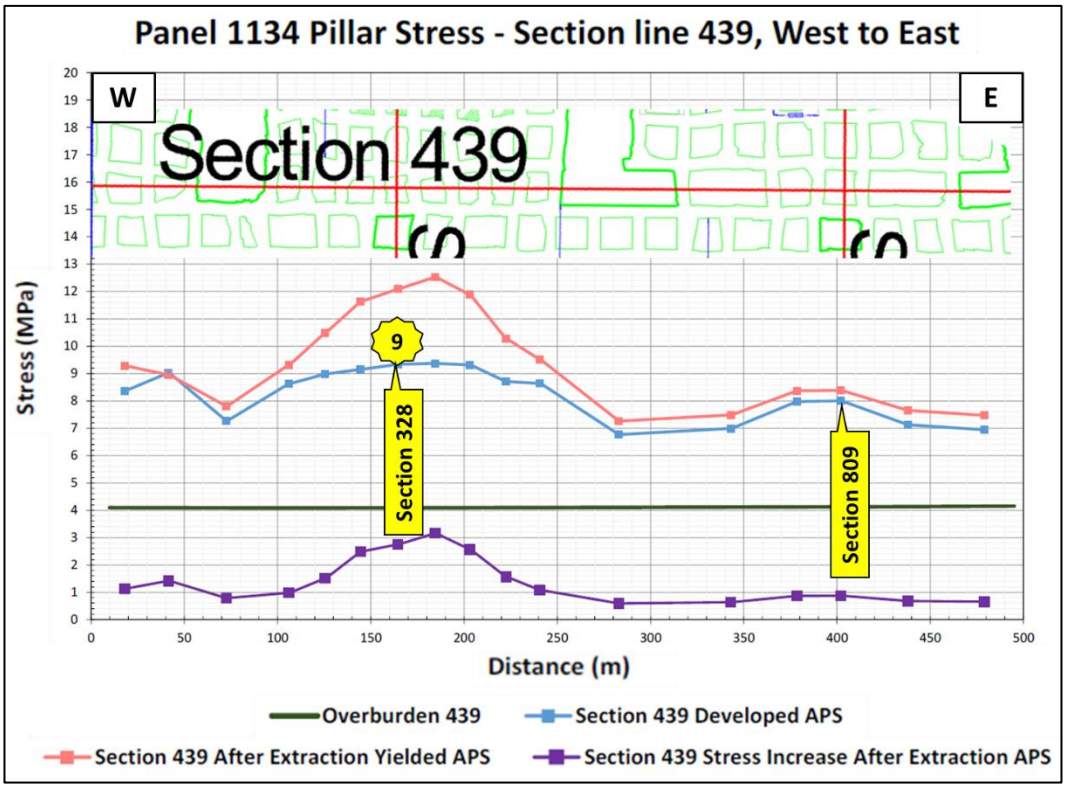


Figure 6-24: Pillar stress along Section 439 for panel-entry pillars of panels 135 and 134 – west to east (Jansen van Vuuren & De Beer, 2022b).

Panel 1134 Belt Road Pillars

Section 254 was drawn along the row of pillars next to the BR in Panel 1134, extending over a distance of 450 m from west to east. Figure 6-25 shows the variation in APS along this section from before to after stooping. These pillars remained largely unaffected by the stooping of Panels 135 (Section 328) and 134 (Section 809) as they only experienced a slight increase in APS of 1 MPa.

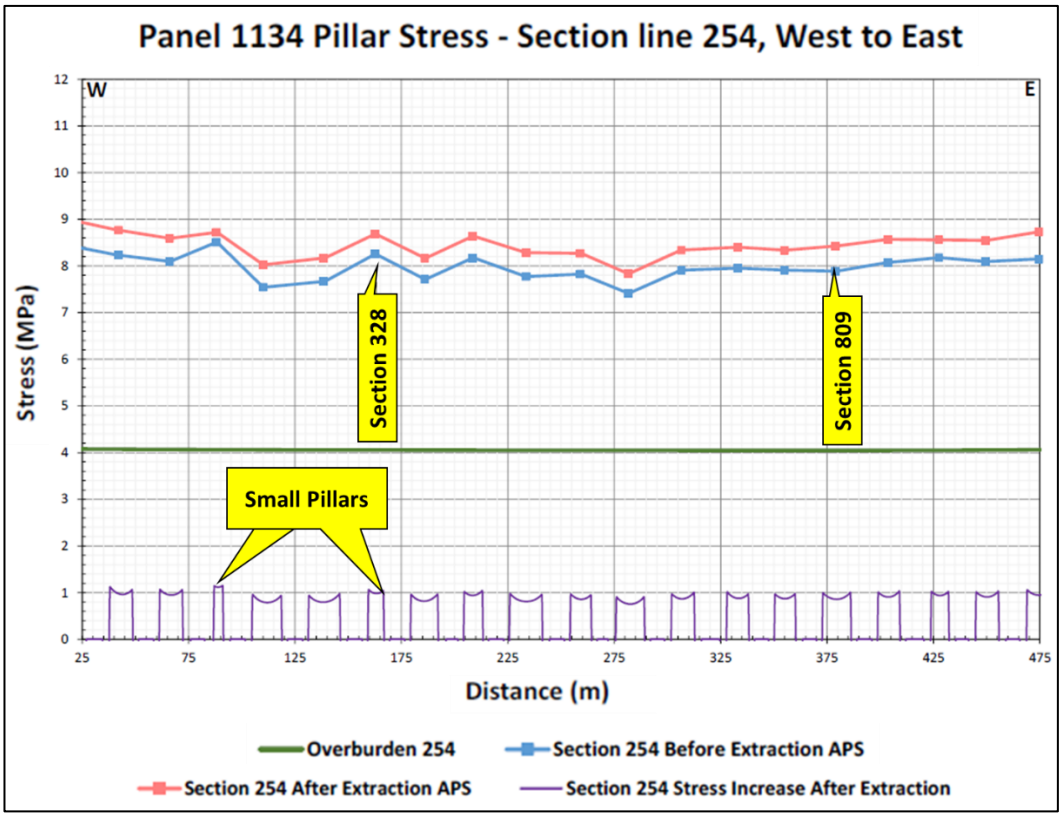


Figure 6-25: Pillar stress along Section 254 for Panel 1134 pillars – west to east (Jansen van Vuuren & De Beer, 2022b).

7 DISCUSSION OF RESULTS

7.1 Critical Span Calculations

Not all panels at NDC were initially designed for stooping, as is the case with many other mines (Livingstone-Blevins & Watson, 1982; Willis & Hardman, 1997). The mining parameters of these panels had to be optimised to extract the coal that remained locked up in the pillars left during development. The two most important parameters, namely the panel span and pillar dimensions, had to be managed to ensure the safe extraction of the pillars. An example of this can be seen in the 1100 panels and Panel 1135 of the Shosholoza block, where the pillar dimensions and specifically the panel span were less than those panels that were designed for stooping.

7.1.1 1100 Panels critical span calculations

The sill above the 1100 block has an average thickness of 54 m and occurs approximately 130 m above the No. 4 seam. To have induced complete goafing, i.e. goafing that would break the sill, the panels required a span of about 300 m each (Table 6-1). The sandstone layer forming the immediate roof itself has an average thickness of 40 m. This would have required the panels to be at least 200 m wide (Table 6-1) to exceed the super-critical span and ensure the goafing of just the immediate sandstone roof. Considering that the average panel span at this trial site was only 160 m and the stopper pillars along the periphery reduced this to an effective panel span of about 112 m, it is clear why no goafing was observed during stooping operations. Goaf initiation was attempted several times by blasting

in the roof but proved to be unsuccessful and too hazardous to continue. The only way that goafing could have been induced by exceeding the critical span was to join two panels together. The barrier pillar between two adjacent panels would need to have been mined out to achieve this.

7.1.2 Critical span calculations for planned stooping panels

Most panels after the 1100 block and Panel 135, especially at Central Shaft, were planned for stooping. These panels consisted of nine roadways with pillar centres of 26.0 m (length) x 24.0 m (width). The layout resulted in a panel span of approximately 200 m, which exceeded even the super-critical span for depths ranging from 160 m to 200 m (Table 6-2). Consistent goafing of at least the immediate sandstone roof was therefore expected according to Van der Merwe's critical span calculations (Van der Merwe, 1995). Goafing nonetheless occurred infrequently and was predominantly confined to the intersections (between the fenders) in the centre of the panels.

It became clear, especially during the stooping of these planned panels that the effect of the stopper pillars along the periphery of the panel, was underestimated. These pillars, although subjected to high abutment stresses, mostly remained intact and reduced the actual panel span of approximately 200 m to a lower effective span of roughly 150 m. It fell predominantly between the sub-critical and critical span making goafing unpredictable and inconsistent. The critical span theory is more suited to full extraction as it assumes that no form of support is left behind. The reality

with partial extraction, especially at NDC with its competent overburden, is that the strength of the remaining fenders and stopper pillars added to the stability of the roof, thus limiting goafing even further.

Figure 7-1 shows Panel 134 in the Shosholoza block as an example of where the actual panel span was reduced to an effective span of 152 m. In this specific instance, the effective panel span was slightly higher than the critical span required to induce failure of the immediate sandstone roof. The panel span was further reduced between splits 30 to 35 to a minimum of 80 m due to stopper pillars left intact to protect surface structures.

Panel 134 Critical Span Calculations		
Panel width (m)		**Comments**
Actual/Average	200	Measured from barrier pillar to barrier pillar.
Effective panel	152	Excluding the two pillars along the barrier.
Minimum	80	Panel width reduced even further by surface restrictions. (Applicable from splits 30 - 35).
Thick of dolerite sill	15.5	Occurs 96 m above the No. 4 seam.
Vd Merwe 1995 L- crit span (Eq 2-7)	142	Span required to induce failure of the sill and
Thick of immediate sandstone layer	16.8	Overlain by multiple, thick units of sandstone.
No sill; L- crit span (Eq 2-10)	150	Span required to induce failure of the immediate roof.
Sub-critical span	135	10% of the critical span. Effective panel width must be less to prevent goafing.
Super-critical span	165	10% of the critical span. Effective panel width must be more to ensure goafing.

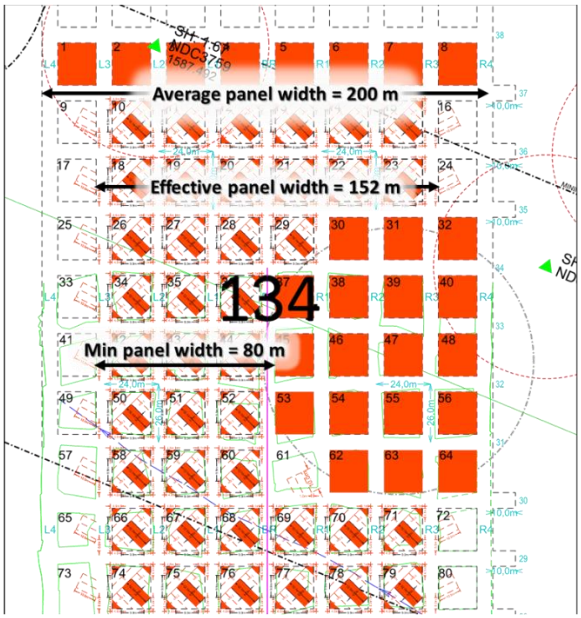


Figure 7-1: The actual panel span of Panel 134 is reduced by stopper pillars.

7.1.3 Challenges with increasing the panel span

Attempting to induce goafing by increasing either the effective or the actual panel span was impractical. The function of the stopper pillars left along the periphery of the panel was to protect the bleeder road. This ensured that ventilation could flow along the panel and across the goaf area. It was therefore not an option to mine these stopper pillars out as the bleeder road was a ventilation requirement for safe stooping.

Increasing the actual panel span to more than 200 m by adding roadways or increasing the pillar width would have introduced additional production challenges. These include a decrease in production rate, which can in turn be attributed to increased away-time of the shuttle cars from the CM. The shuttle cars would have to travel longer distances between the CM and feeder breaker, especially when the CM is cutting along the flanks of the panel (Malebana, 2023; Mandivheyi, 2023). Cable management can also become an issue as it would be difficult for the machines to reach the flanks of the panel. More cables would need to be used, which would have increased the risk of cable damage (Malebana, 2023; Mandivheyi, 2023).

7.2 Goafing in NDC Stooping Sections

It was concluded from the information above that goafing in NDC stooping sections was unlikely to be induced by exceeding the super-critical, or even the critical spans of the immediate sandstone roof or that of the sill higher up in the stratigraphy (Tables 6-1 and 6-2). Instead, goafing most frequently occurred in panels where their effective spans were well below the sub-

critical spans (Table 6-3). Analysis of these panels indicated that goafing was most likely caused by geological structures occurring either within the panels or near them (Table 6-4). Although the effects of these have not yet been quantified, it is suspected that they altered the stress regime, especially the horizontal stress, in and around the panels and therefore played a more significant role than the panel spans.

The goafing in these panels was observed to occur more towards the centre of the panel and predominantly in the intersections, between the fenders. It was estimated to extend between 1.5 m and 2.0 m into the immediate sandstone roof with goaf angles of approximately 25° from the vertical (Table 6-5). The immediate roof broke into slabs of sandstone with thicknesses estimated to vary between 100 mm and 300 mm. These slabs also had relatively sharp edges as they thinned out towards the edges (Table 6-5). The goafing was therefore described as low-angle shear failures caused by high horizontal stress.

The following theories have been derived on how the presence of geological structures have increased the horizontal stress and either directly caused goafing or contributed to it in certain panels:

- Dykes are known to cause high horizontal compressive stresses in the surrounding strata. It is due to the high magnitude of force that was required to displace the surrounding rock and allow the dyke to intrude (Van der Merwe & Madden, 2010). The effects of these high

horizontal compressive stresses can often be seen when mining towards a dyke. The immediate sandstone roof will break out in slabs reaching a maximum thickness of up to 300 mm. These sandstone slabs have similar characteristics as the broken-up goaf material described in Table 6-5.

The panels that have goafed due to the presence of a nearby dyke are the following: Panel 179b (Figure 6-4), Panel 888 (Figure 6-5), Panels 882c and 882d (Figure 6-6). It is worth mentioning that for all these panels, the regional major horizontal stress as indicated by the Rose diagram, was aligned with the direction of the induced horizontal stress from the dykes (Table 6-4). It is thus suspected that in these cases the regional major horizontal stress also contributed to the increased horizontal stress in the panels.

- Faults, joints and to a certain extent dykes, form discontinuities within the strata and change the behaviour of the overlying strata from that of a clamped, self-supporting beam to a cantilever beam (Wagner & Schümann, 1991; Van der Merwe & Madden, 2010). The strata used to be continuous and span over the underlying panels, thus limiting the magnitude of the vertical stress that the pillars were subjected to. In the case of a cantilever beam, the free end of the strata will now deflect and sag, and as a result exert more stress onto the pillars. The effect of this was increased pillar scaling, which was most noticeable in the following panels:

- On the south side (left-hand side) of Panel 179b, which was closest to the dyke (Figure 6-4).
- At the end of Panels 887 and 888 (Figure 6-5) as mining developed towards the dyke; and
- At the end of Panels 117/5 and 177/6 as mining developed towards the faults (Figure 6-8).

The weight of the cantilever beam will increase the pillar scaling during stooping as only fenders are left behind in the panel. The reduced load-bearing capacity of the fenders will result in even more sag and deflection of the overlying beam. It will in turn increase the horizontal compressive stresses along the bottom of the beam and tensile stresses along the top of the beam, which is suspected to induce goafing.

Panels that have goafed due to the presence of faults are the following: Panel 1126 (Figure 6-1), Panel 135 (Figure 4-5), Panels 1001B and 1001C (Figure 6-7); and Panels 177/5 and 177/6 (Figure 6-8). It was noticed during the underground inspections in each of these panels that goafing occurred near the geological structures and became less frequent further away, as the stooping face advanced away from them.

- The fact that goafing occurred more towards the centre of the panel can be attributed to the behaviour of the overlying strata, as well as the support offered by the abutments and adjacent stopper pillars.

Regardless of whether the overlying strata behaved as a clamped or cantilever beam, the most deflection and sag would still occur towards the centre of the panel. The goaf would also only occur in the intersections as the fenders continued to provide support even though they were subjected to excessive scaling.

- Other factors, such as nearby previously mined longwall, or even stooped panels, smaller fenders, the orientation of the major horizontal stress and fourth fender-reducing cuts, may also have contributed to goafing.

After goafing, the broken material filled up the intersections quickly due to the relatively low seam height, bulking factor (Table 2-1) and confinement offered by the intact fenders. From the underground observations, it was expected that the goaf material extended up to the roof at which point it choked and arrested further goafing, thus resulting in partial goafing. This is a typical feature of competent roof composition, compared to a weak roof. In weak roof conditions the goaf is expected to extend much deeper into the overburden as illustrated in Figure 7-2. These observations were made in 92% of NDC stooping panels where goafing was recorded.

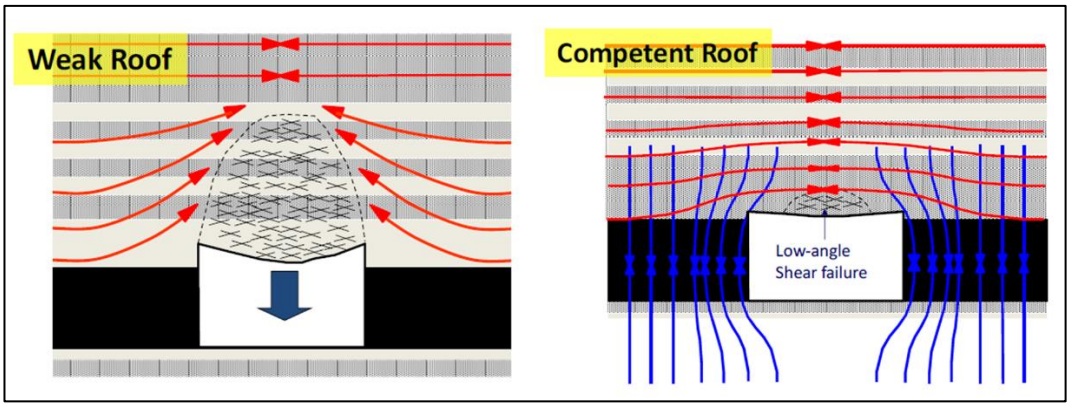


Figure 7-2: Goafing in areas with weak overburden compared to areas with competent overburden (Jansen van Vuuren & De Beer, 2022a).

Measured subsidence above Panel 1126 has however proved the opposite in that goafing can extend up to the surface, due to progressive caving over an extensive period. Although this can be described as complete goafing due to the sill being broken, it was merely a small, localised area affected by subsidence (Figures 6-1 and 6-2). Complete goafing, in its true sense, is only achieved through consistent and extensive goafing across the entire stooped panel. It is only then that there will be a complete relief of the abutment stresses. It is expected in the case of Panel 1126 that the abutments along most of the panel are still subjected to high vertical stress.

To put this in context, 50 panels have been stooped at NDC of which goafing was recorded in only 13 of them. This means that goafing occurred in only 26% of all panels stooped at NDC. Only one panel (2%) has goafed to the surface and resulted in minimal subsidence in agricultural land. This is considered an acceptable risk, since stopper pillars were in any case left

underneath sensitive surface structures, such as powerline pylons, surface streams and dams (Figure 4-12).

NDC stooping sections have and will at very most only experience partial goafing, which means that the abutments will remain under high vertical stress. Considering that it is impractical to further increase panel spans to induce goafing, high abutment stresses need to be managed. This became the primary objective of the project to ensure safe stooping operations and long-term stability of the mine. It can be achieved by increasing the width of the barrier pillars between panels and leaving a sufficient number of stopper pillars at the end of a stooped panel.

7.3 Analysis of the Numerical Modelling

7.3.1 1100 Block

The numerical modelling results obtained for the 1100 block indicate the variation in stress based on the size of the barrier pillar and distance away from it. The excessive APS across a panel appears to dissipate within 50 m to 75 m from the barrier pillar. The APS for pillars is only marginally higher beyond 75 m from the barrier pillar regardless of its width. The width of the barrier pillar proportionally increases or decreases this critical distance. However, the overlapping stress field for extracted panels on either side of the intact panel, or main development, must be considered, especially if there is no continuous barrier pillar or panel-entry pillars in place, on the opposite side of the panel. It also directly affects or describes the distance

that must be maintained from sensitive underground structures, on coal seam level.

The numerical modelling results confirm NDC's current design strategy. Production panels, which are planned for stooping, are separated with barrier pillars that have a minimum width equal to those of the in-panel pillars. It means that a barrier pillar will have a minimum width of 17 m. This may be increased to a width of approximately 24 m, which is roughly 140% of the minimum required width. It is more than sufficient for production panels as they are only required to be stable for a short-term period, typically between 3 to 12 months.

A barrier pillar that separates a main development from a production panel, which is orientated parallel to it, will have a minimum width of 50 m (Figure 4-11). This is nearly 300% of the normal barrier pillar width. Such a barrier pillar is deemed stable and expected to ensure long-term stability of the main development, which is typically required for more than five years, or even the life of mine (LOM).

Stooping may also not be done within 75 m of any sensitive underground structures, such as shafts, workshops, substations, belt- or travelling roads. This distance may be further increased by the responsible rock engineer if deemed necessary. There will also be no further stooping on both sides of a main development, as was done along Panel 1120, unless sufficiently sized barrier pillars and panel-entry pillars are in place.

7.3.2 Shosholoza Block

The pillar stress results differ between panels 134 (Figure 4-6) and 135 due to their different panel-entry layouts (Figures 6-21, 6-22 and 6-23). As mentioned above, the pillars in Panel 135 were stooped to within a much closer proximity of Panel 1134 leaving only two rows of stopper pillars. This was done according to what is considered as good practice by Van der Merwe & Madden (2010). A much more conservative approach was followed with Panel 134 with four rows of stopper pillars being left between the stooped ground and Panel 1134. It also had a more prominent panel-entry pillar configuration with the two larger panel-entry pillars. This change was made in response to the pillar stability issues of Panel 1120 after stooping on both sides of it.

The numerical modelling results for both Panels 135 and 134 showed that the frontline pillars experienced a significant increase in stress after stooping. The APS on the frontline pillars reached a maximum of 27.3 MPa in Panel 135 and 24.3 MPa in Panel 134. In both panels, the strength of the pillars was exceeded resulting in the pillars' SF being reduced to 0.85 and 0.96, respectively. The pillars did not fail although their ribsides, especially those facing the stooped-out panels, scaled excessively in response to the increased stress. The stability of the pillars was attributed to the ability of the overburden to span across the panel and lighten the load on the frontline pillars. The support from the barrier pillars and to a lesser extent the remaining fenders in the stooped-out area also assisted in maintaining

stability. The numerical modelling also indicated that the increased APS after stooping decreased substantially from the frontline pillars to the next row of stopper pillars. In the case of Panel 135, the APS decreased from 27.3 MPa on the frontline pillars to 13.1 MPa on the panel-entry pillars. For Panel 134, the APS decreased from 24.3 MPa on the frontline pillars to 9.9 MPa for the next row of stopper pillars. This corresponded well to Van der Merwe and Madden's (2010) recommendation of leaving only two rows of stopper pillars at the end of a stooping panel.

Considering that the research was done after Panel 134 was already stooped, the results indicate that the panel-entry configuration was indeed very conservative. It would have been safe to reduce the rows of stopper pillars to a minimum of two with the first row containing the two larger panel-entry pillars.

A decision has nonetheless been made that three rows of stopper pillars will be left at the end of a secondary panel being stooped back to a main development. The first row of stopper pillars (panel-entry pillars) will still include the two larger panel-entry pillars as shown in Figure 7-3. It will provide a 75 m stand-off distance between the secondary stooping panel and the main development which requires long-term stability.

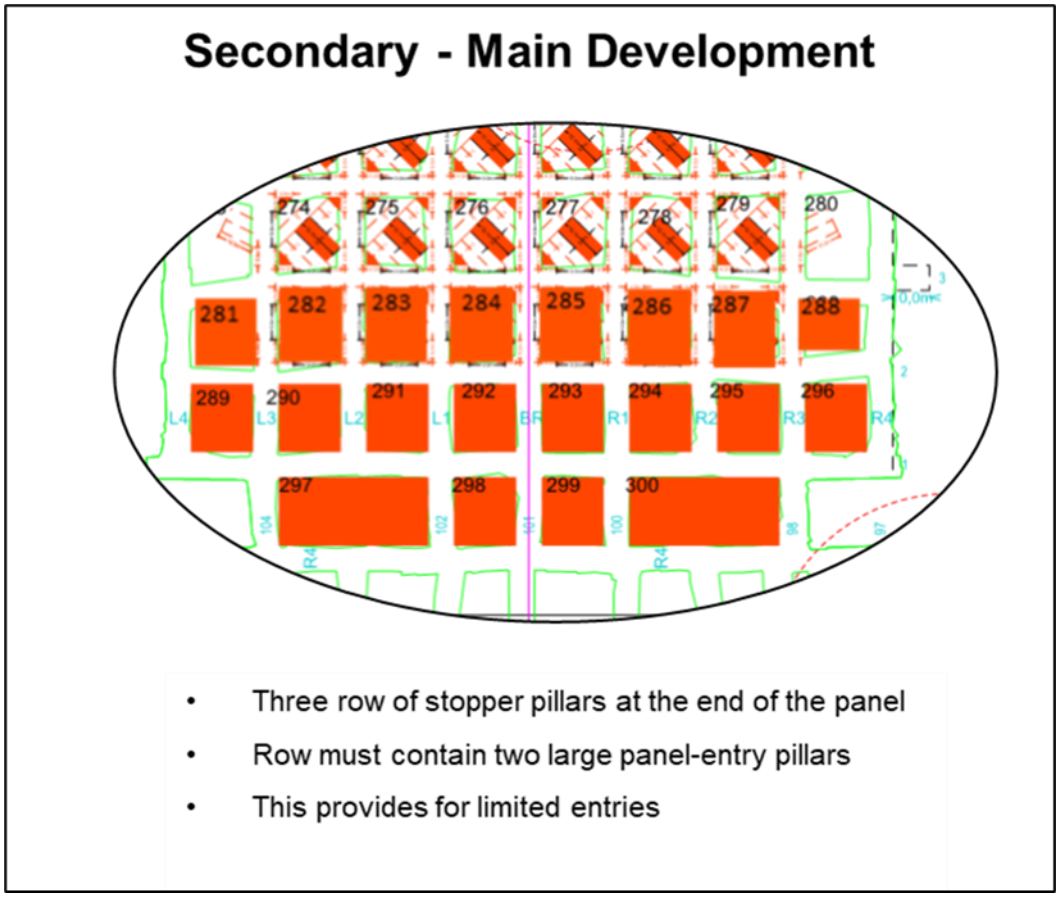


Figure 7-3: Ideal panel-entry configuration for a secondary panel being stooped towards a main development.

In the event of a tertiary panel being stooped towards a secondary panel, the rows of stopper pillars can be reduced to only one if it contains two large panel-entry pillars (Figure 7-4). However, this may be increased to two rows of stopper pillars, with the first row containing the two large panel-entry pillars, should longer-term stability be required. NDC's stooping strategy has been revised accordingly and has proven effective in the panels stooped since the 1100 block.

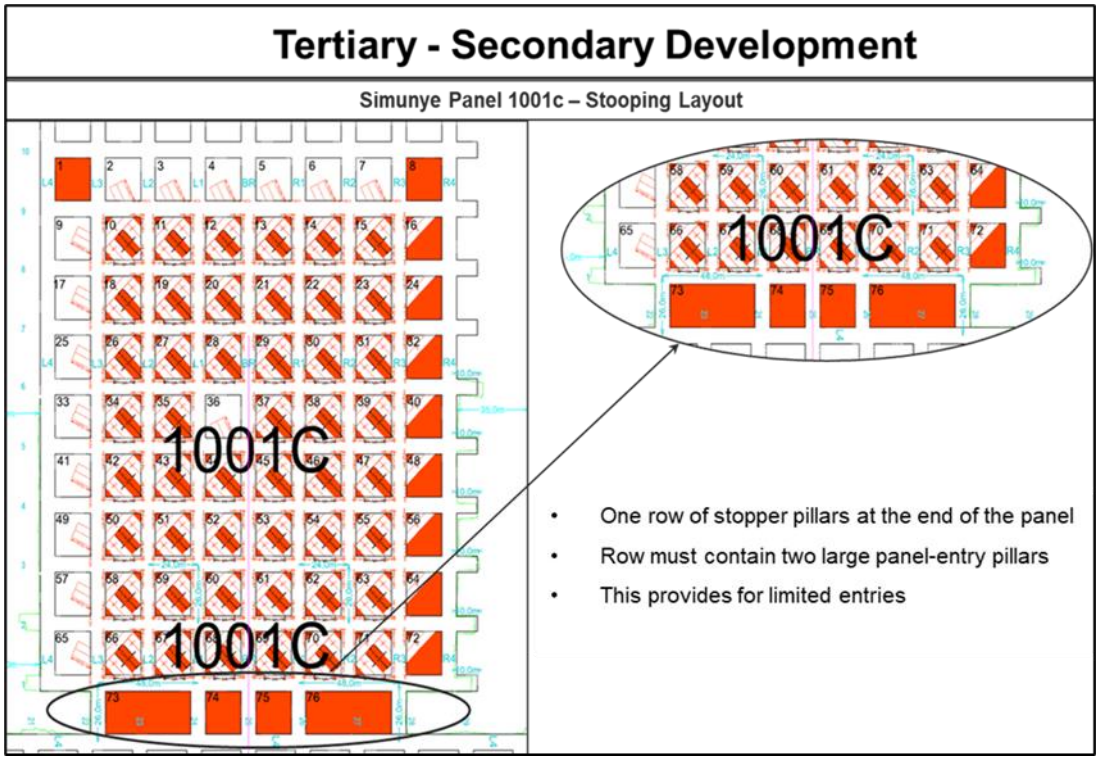


Figure 7-4: Ideal panel-entry pillar configuration for a tertiary panel being stooped towards a secondary panel.

7.4 Additional Risk

It has been proven that the high abutment stresses caused by partial goafing can be managed to ensure safe stooping operations at NDC. This will be achieved by increasing the barrier pillar width between strategic panels, leaving sufficient rows of stopper pillars at the end of a stooped panel and maintaining safe stand-off distances from sensitive infrastructure.

An additional risk was however identified, which was the potential build-up of methane in the cavities formed by the goaf. Plaistowe *et al*. (1989) warns that the accumulation of methane in such cavities may not necessarily be cleared by the normal ventilation current along the bleeder road. Rocks

falling during the progressive goafing process can ignite the methane through frictional heating and cause a methane explosion.

The Ventilation Department managed this risk by drilling methane drainage boreholes from the surface at regular intervals along the length of the stooping panels. These boreholes were drilled before stooping operations. Other boreholes drilled into the stooping panels, such as geological exploration boreholes, also assisted in draining any methane that may have accumulated in the goaf area. These boreholes did not take away from the bleeder road, but rather added to the arsenal of controls that ensured safe stooping operations at NDC.

8 CONCLUSION

Stooping has been well entrenched as a secondary mining method at NDC with a total of 50 panels safely stooped since the first panel in November 2018. It played an essential part in the mine's annual coal production as it contributed approximately 30%. It furthermore helped to minimise the impact of the longwall that was decommissioned in April 2021.

The first panels, especially those in the 1100 block, were not planned for stooping. Hence, the mine's stooping strategy had to be adjusted to optimise the prevailing conditions and mining parameters of these panels, for example, taking only two cuts per pillar on the smaller pillars. This is unfortunately a reality for several coal mines across South Africa. Most panels thereafter were designed for stooping, especially at the Central Shaft. They comprised of nine roadways with pillar centres of 26.0 m (length) x 24.0 m (width). This design allowed for the three cuts per pillar to be taken as per the conventional NEVID method. A fourth fender-reducing cut was later added to not only increase production, but also assist with goafing as it reduced the size of the fender by approximately 5 m.

Several lessons were learned from the stooping operations in the 1100 block, some of which were immediately and successfully applied to the Shosholoza panels. The stooping of these panels started soon after the first 1100 panels were stooped. These two areas therefore formed the main study areas for this research project. Observations in and around the

stooping panels were also modelled to gain a better understanding of the mechanisms of the observed behaviour.

Critical span calculations have shown that NDC's current panel spans are mostly insufficient to induce both failures (goafing) of the immediate sandstone roof, as well as the sill higher up in the stratigraphy. Although the actual panel span does exceed the super-critical span in many instances, intact pillars need to be left along the perimeter of the panel for protection of the bleeder road. These reduce the unsupported span to what has been referred to as an 'effective span', which is mostly less than the sub-critical span. Leaving the bleeder road pillars out of the design is not an option. Designing the panels to be wider to ensure goafing would also be impractical as this would bring with several production challenges, such as longer tramming times for the shuttle cars and poor cable management. Goafing in the stooping panels has therefore been limited and inconsistent, whether from one stooping panel to another or within a stooping panel itself. Goafing has only been recorded in 13 of the 50 stooped panels. Evidence suggested that these goafs may have been enhanced by horizontal stress concentrators, such as those produced by nearby geological structures. Previously mined longwall or stooped panels also influenced goafing in adjacent panels. The effect of these matters has not been quantified, but it appears that they may play a more significant role in whether goafing takes place than the panel spans.

Goafing, where it has occurred and could be inspected, has been described as low-angle shear failures, which were estimated to extend to a height of not more than 2 m above the immediate roof. This is referred to as partial goafing and consequently results in high abutment stresses.

Measured subsidence above the centre of Panel 1126 proved the opposite in that goafing can be time-dependent and indeed extend up to the surface. The subsidence-affected area was however small and confined to the position of a fault striking across the panel. Although the sill has been broken, complete goafing in its true sense should occur across the entire panel. It is therefore suspected that the abutments along the rest of the panel remained under high vertical stress.

Complete goafing in stooping panels, and the subsequent relief of high abutment stresses is unlikely. It is therefore essential that this be managed by leaving a safe stand-off distance between stooped panels and sensitive underground infrastructure. It includes leaving sufficient-sized barrier pillars between panels and an adequate number of stopper pillars at the end of a stooped panel.

Numerical modelling confirmed NDC's current design strategy for stooping sections. Barrier pillars between two short-term production panels will have a minimum width equal to those of the in-panel pillars. The barrier pillar width will be increased to at least 50 m in the case of a stooping panel being orientated parallel to a main development. Stooping panels will be further

compartmentalised by a panel-entry configuration, which consists of two large pillars. The rows of stopper pillars at the end of a stooped panel will vary from two to three depending on whether the panel is stooped towards a secondary or main development.

The research further showed that stooping may not be done within 75 m (approximately three rows of pillars) of any sensitive underground structures, such as shafts, workshops, substations, belts- or travelling roads. Stooping on both sides of a main development should also be avoided as much as practically possible. However, should it be required or planned for, sufficiently sized barrier pillars and panel-entry pillars must be left in place to minimise the risk of overlapping stress fields.

9 RECOMMENDATIONS

There is still much to be learned about goafing, and why it occurred in some panels and not in others. More work needs to be done in this area to improve understanding of goafing and enable proper design. In addition, underground stress and strain measurements need to be made around the barrier pillars to determine whether they are carrying the overburden as shown by the numerical models.

The following exercises and measurements are recommended to improve the understanding of the goafing process and verify the numerical modelling results:

- Drilling boreholes from the surface into the previously stooped panels. This will determine whether the panel has goafed; and if so, how deep the goaf extended into the roof. The information will either support the expected goafing depth of only 2 m into the immediate overburden or indicate that the goafing extended much deeper into the overburden. The extent of the goaf in terms of area is also an important factor to investigate. An intrinsically safe camera can furthermore be lowered down a borehole into the stooping panel to obtain a visual of what the goaf area looks like. Several questions need clarification:
    - do the fenders remain intact like it was initially observed, or do they fail over time?
    - does goafing only occur in intersections or is it continuous?

- Strain cells should be installed above pillar fenders before stooping. The research will determine how the stress increases for a specific pillar as the stooping operations approach it and determine its final stress levels as a fender.

As rock engineers, mining engineers and managers, it is important to realise that we can never know enough about the ground conditions in which we mine and the effect of the mining methods we apply. There is always more knowledge to be gained, which can be used to improve our mining method in terms of safety and productivity.

REFERENCE LIST

Arch Coal. (no date). *Figure 8.3.1 A section in a room and pillar mine.* Module 8.3.1 Room and Pillar Method. Lecture notes distributed in Mining Engineering at the John A. Dutton Institute for Teaching and Learning Excelllence

Beukes, J.S. (1989). *Stooping practices in South African collieries, Part 1: Rib pillar extraction.* Chamber of Mines of South Africa, Report No. 3/89.

Fauconnier, C.J. & Kersten, R.W.O. (1982). Increased Underground Extraction of Coal. The Journal of the Southern African Institute of Mining and Metallurgy (SAIMM). Monograph Series No. 4.

Galvin, J.M. (1983). *The Development of the Theory of Dolerite Sill Behaviour. Fifth Congress of the International Society for Rock Mechanics.* Melbourne, Australia, 10-15 April 1985. Paper Number: ISRM-5 Congress-1983-177.

Galvin, J.M. (2015). Pillar extraction. In: J.M. Galvin, ed. 2015. *Ground Engineering – Principles and Practices for Underground Coal Mining.* Springer International Publishing, Switzerland. Ch8:309-358.

Gonsalves, R., Sibiya, T., Salima, A. & Malebana, M. (2021). *Mandatory Code of Practice to Combat Roof Fall Accidents in Underground*

Coal Mines. *New Denmark – Rock Engineering*. Seriti. New Denmark. Doc. ND_MIN_COP_011703. Issued 22 Nov. 2021. Confidential to NDC.

Gonsalves, R. (2021). *New Denmark Stooping Standard*. Seriti. New Denmark. Doc. ND_MIN_STD_028437. Effective date: 20 Sep. 2021. Confidential to NDC.

Gonsalves, R. (2023). *Rock Engineering Underground Technical Standards and Procedures*. New Denmark – Rock Engineering. Doc. ND_RE_SOP_028448. Issued 17 Feb. 2023. Confidential to NDC.

Jansen van Vuuren, J. & De Beer, D. (2022)a. *New Denmark Colliery: Geomechanical Risks Associated with Pillar Extraction – 1100 Area.* Final Project Report No. STC 2109-995. Saxum Mining, Johannesburg.

Jansen van Vuuren, J. & De Beer, D. (2022)b. *New Denmark Colliery: Geomechanical Risks Associated with Pillar Extraction – Shosholoza Area.* Final Project Report No. STC 2109-995. Saxum Mining, Johannesburg.

Kgengwe, N. (2021)a. *Section Roadway Standard.* New Denmark – Mining. Doc. ND_MIN_STD_019893. Issued 9 Dec. 2021. Confidential to NDC.

Kgengwe, N. (2021)b. *Cutting Sequence Procedure*. New Denmark – Mining. Doc. ND_MIN_SOP_SR018602. Issued 24 Nov. 2021. Confidential to NDC.

Lind, G.H. (2002)a. Key success elements of *coal pillar extraction experiences in New South Wales*. *The Journal of The South African Institute of Mining and Metallurgy,* 102(04), pp.199-206. Available at: http://saimm.org.za/Journal/v102n04p199.pdf

Lind, G.H. (2002)b. Coal pillar extraction experiences in New South Wales. *Journal of The South African Institute of Mining and Metallurgy*, 102(04), pp.207-215. Available at: https://www.saimm.co.za/Journal/v102n04p207.pdf

Livingstone-Blevins, G. & Watson, S. (Eds) (1982). *Pillar Extraction.* Chamber of Mines of South Africa, Report No. NS 469, Johannesburg.

Malebana, M. (2023) Personal Communication.

Mandivheyi, S. (2023) Personal Communication.

Mark, C., McCall, F.E., & Pappas, D.M. (1997). A statistical overview of retreat mining of coal pillars in the United States. *Paper presented at the Seminar on New Technology for Ground Control in Retreat Mining*. NIOSH, pp.2-16.

Mark, C., Chase, F. & Pappas, D. (2003). Reducing the risk of ground falls during pillar recovery. *Proceedings of the Society for Mining, Metallurgy, and Exploration (US). Annual Meeting.* Feb 24-26, Cincinnati, Ohio. 314, pp.153-160. Available at: https://stacks.cdc.gov/view/cdc/9460/cdc_9460_DS1.pdf

Moolman, C. & Canbulat, I. (2003). Task 2.5.2. *Economic and safe extraction of pillars and associated reserves using underground mining methods.* Coaltech 2020. September. Available at: https://coaltech.co.za/wp-content/uploads/2019/10/Task-2.5.2-Economic-and-safe-extraction-of-pillars-and-associated-reserves-using-underground-mining-methods-2003.pdf

Nayak, R.C. & Dalai, S.K. (2010). *Evaluation of bord and pillar mining systems in MCL coal mines.* BTech. Department of Mining Engineering, National Institute of Technology. Rourkela-769008. Available at: http://ethesis.nitrkl.ac.in/1692/1/final.pdf

Pankaj, D., Sunil, D., Vishal, K. & Siddharth, S. (2018). Coal Pillar Extraction by Continuous Miner using Fish and Tail Method – A Case Study. *International Journal of Mechanical and Production Engineering*, 6(2), pp.45-49. Available at: http://www.iraj.in/journal/journal_file/journal_pdf/2-448-152361270245-49.pdf

Plaistowe, R.H.A., Poultney, M.O., Van Schalkwyk, B, Hichens, R.L. & Bradbury, T.J. (1989). Decision-making considerations for pillar extraction. *The Journal of the South African Institute of Mining and Metallurgy:* The Total Utilisation of Coal Reserves, Vol. 1, Witbank.

Prinsloo, L. (2019). Personal Communication.

Ryder, J.A. & Jager, A.J. (2002*). A Textbook on Rock Mechanics for Tabular Hard Rock Mines.* The Safety in Mines Research Advisory Committee (SIMRAC). Johannesburg.

Salamon, M.D.G. (1967). A method of designing bord and pillar workings. *The Journal of the South African Institute of Mining and Metallurgy*, 68(2), pp.68-78. September. Available at: https://journals.co.za/doi/pdf/10.10520/AJA0038223X_3919

Salamon, M.D.G. & Munro, A.H. (1967). A study of the strength of coal pillars. *The Journal of the South African Institute of Mining and Metallurgy*, 68, pp.55-67. November. Available at: https://journals.co.za/doi/pdf/10.10520/AJA0038223X_4155

Salamon, M.D.G. & Oravecz, K.I. (1976). *Rock Mechanics in Coal Mining.* Johannesburg: Chamber of Mines of South Africa. Project Report No. CM/807/66. Series No. 198.

Salima, A. (2021)a. Personal Communication.

Salima, A. (2021)b. *Locality Map of New Denmark Colliery.* NDC Survey Department. Confidential to NDC.

Salima, A. (2023). Personal Communication.

Sasol Mining. (no date). Stooping Training Video. Sasol Mining Company.

Sibiya, T. (2019). Personal Communication.

Sibiya, T. (2021). *New Denmark Colliery General Stratigraphic Column*. NDC Geology Department. Confidential to NDC.

Sibiya, T. (2022). *NDC Geological Structures Plan.* NDC Geology Department. Confidential to NDC.

Van Der Merwe, J.N. (1991). *Subsidence caused by high extraction coal mining in the Sasolburg and Secunda areas: Prediction thereof and the mitigation of its effects.* Ph.D. University of the Witwatersrand, Johannesburg. Available at: https://hdl.handle.net/10539/27318

Van Der Merwe, J.N. (1995). *Prediction of dolerite sill failure.* 8th ISRM Congress. Tokyo, Japan, September 1995. Paper Number: ISRM-8 Congress-1995-251.

Van der Merwe, J.N. (2006). Beyond Coalbrook: what did we really learn? *The Journal of the South African Institute of Mining and Metallurgy*, 106(12), pp.857-868. Transaction paper. Available at: https://hdl.handle.net/10520/AJA0038223X_3128

Van Der Merwe, J.N. & Madden, B.J. (2010). *Rock Engineering of Underground Coal Mining.* 2nd ed. Johannesburg: The Southern African Institute of Mining and Metallurgy (SAIMM). Special Publications series 8 (SP8), Johannesburg.

Van der Merwe, J.N. & Mathey, M. (2013). Update of coal pillar database for South African coal mining. *The Journal of the South African Institute of Mining and Metallurgy*, 113(11), pp.825-840. Available at: https://www.researchgate.net/publication/262743180_Update_of_coal_pillar_database_for_South_African_coal_mining

Wagner, H. (1981). *An investigation of pillar extraction systems to improve percentage extraction in South African Collieries*. Coal Symposium, Pretoria, 11 May.

Wagner, H. & Schümann, E.H.R. (1991). Surface effects of total coal-seam extraction by underground mining methods. *The Journal of the South African Institute of Mining and Metallurgy*, 91(07), pp.221-231. Available at: https://www.saimm.co.za/Journal/v091n07p221.pdf

Willis, R.P.H. & Hardman, D.R. (1997). *Projections of likely changes in mining circumstances, conditions and technologies which may affect safety and health risks*. Final Project Report No. SIMRISK 401, SIMRAC, Johannesburg.

APPENDIX A

Table A-1: Critical span calculations for the 1100 panels.

Shaft	Area/ Block	Panels	Average Mining Depth (m)	Base of Dolerite Sill (m)	Thick of Dolerite Sill (m)	Base Lower sandstone (m)	Thick Lower sandstone (m)	Actual Panel span (m)	Effective Panel span (m)	Critical span for immediate roof (m) (Eq 6-1)	Sub-critical span for immediate roof (m)	Super-critical span for immediate roof (m)	Critical span for sill (m) (Eq 6-2)	Sub-critical span for sill (m)	Super-critical span for sill (m)
Central	1100 Block	1111	193.95	66.26	62.52	191.70	15.60	158.00	108.00	180.88	162.79	198.97	319.34	287.41	351.27
		1126	195.28	63.68	54.86	193.24	22.22	160.60	110.60	182.12	163.91	200.33	299.89	269.91	329.88
		1124	193.51	60.92	51.32	190.78	21.44	158.00	108.00	180.47	162.42	198.51	290.63	261.57	319.70
		1122	193.54	59.30	51.80	191.36	102.16	158.00	108.00	180.50	162.45	198.54	294.32	264.89	323.75
		1109	192.18	67.32	63.47	190.05	15.46	182.00	132.00	179.23	161.30	197.15	319.26	287.33	351.19
		1105	184.28	54.30	43.73	181.93	23.51	158.00	108.00	171.85	154.67	189.04	266.39	239.75	293.03
		1107	192.47	59.13	55.71	190.34	15.53	158.00	108.00	179.50	161.55	197.45	305.98	275.38	336.58
		1118	199.57	66.72	56.76	197.75	24.87	158.00	108.00	186.12	167.51	204.73	305.95	275.35	336.54
		1116	188.54	54.75	41.68	185.94	124.13	158.00	108.00	175.83	158.25	193.42	263.15	236.83	289.46
		1142	-	-	-	-	-	160.00	122.00	-	-	-	-	-	-
		Average	**192.59**	**61.37**	**53.54**	**190.34**	**40.54**	**160.86**	**112.06**	**179.61**	**161.65**	**197.57**	**296.10**	**266.49**	**325.71**
		Min	**184.28**	**54.30**	**41.68**	**181.93**	**15.46**	**158.00**	**108.00**	**171.85**	**154.67**	**189.04**	**263.15**	**236.83**	**289.46**
		Max	**199.57**	**67.32**	**63.47**	**197.75**	**124.13**	**182.00**	**132.00**	**186.12**	**167.51**	**204.73**	**319.34**	**287.41**	**351.27**

APPENDIX B

Table B-1: Critical span calculations for planned stooping panels.

Area/ Block	Panels	Average Mining Depth (m)	Base of Dolerite Sill (m)	Thick of Dolerite Sill (m)	Base Lower sandstone (m)	Thick Lower sandstone (m)	Actual Panel span (m)	Effective Panel span (m)	Critical span for immediate roof (m) (Eq 6-1)	Sub-critical span for immediate roof (m)	Super-critical span for immediate roof (m)	Critical span for sill (m) (Eq 6-2)	Sub-critical span for sill (m)	Super-critical span for sill (m)
1134/ Shosholoza Block	135	160.67	63.72	16.58	158.90	12.82	160.00	122.00	149.84	134.86	164.82	144.90	130.41	159.40
	136	163.57	64.32	16.41	161.75	11.50	200.00	152.00	152.54	137.29	167.79	146.40	131.76	161.04
	134	161.41	63.59	15.47	159.59	16.81	200.00	152.00	150.53	135.48	165.59	142.13	127.92	156.34
	133	164.13	61.48	11.95	162.47	3.96	200.00	152.00	153.07	137.76	168.38	135.31	121.78	148.84
	133A	159.17	57.70	13.89	157.10	3.90	200.00	152.00	148.44	133.60	163.29	141.10	126.99	155.21
	133B	164.21	62.01	23.70	162.46	4.72	200.00	152.00	153.14	137.83	168.46	173.25	155.93	190.58
1130/ Mmabatho Block	1130	167.70	-	-	166.02	13.67	200.00	152.00	156.40	140.76	172.04	-	-	-
	1130B	171.57	45.82	5.26	169.88	8.36	200.00	152.00	160.01	144.01	176.01	135.76	122.19	149.34
	1130C	170.58	27.37	16.53	168.91	16.06	200.00	152.00	159.08	143.17	174.99	197.72	177.95	217.49
	1130D	168.11	34.86	12.66	166.36	18.67	200.00	72.00	156.77	141.10	172.45	171.05	153.94	188.15
	1130E	162.58	-	-	160.93	16.43	200.00	152.00	151.62	136.46	166.78	-	-	-
	1130F	167.28	-	-	165.62	7.68	200.00	152.00	156.01	140.40	171.61	-	-	-
1001/ Simunye Block	1001B	164.19	66.00	6.51	162.00	6.47	200.00	152.00	153.12	137.81	168.44	112.95	101.66	124.25
	1001C	164.00	67.52	7.04	161.60	7.48	200.00	152.00	152.95	137.65	168.24	113.01	101.71	124.31
Average		**164.94**	**55.85**	**13.27**	**163.11**	**10.61**	**197.14**	**144.14**	**153.82**	**138.44**	**169.21**	**146.69**	**132.02**	**161.36**
Min		**159.17**	**27.37**	**5.26**	**157.10**	**3.90**	**160.00**	**72.00**	**148.44**	**133.60**	**163.29**	**112.95**	**101.66**	**124.25**
Max		**171.57**	**67.52**	**23.70**	**169.88**	**18.67**	**200.00**	**152.00**	**160.01**	**144.01**	**176.01**	**197.72**	**177.95**	**217.49**

APPENDIX C

Table C-1: NDC stooping panels where goafing was recorded and their critical span calculations.

No.	Location			Panel Dimensions							Critical Span Calculations - No Sill			Critical Span Calculations - Sill		
	Panels	Shaft	Section	Average Mining Depth (m)	Base of Dolerite Sill (m)	Thick of Dolerite Sill (m)	Base Lower sandstone (m)	Thick Lower sandstone (m)	Actual Panel span (m)	Effective Panel span (m)	Critical span for immediate roof (m) (Eq 6-1)	Sub-critical span for immediate roof (m)	Super-critical span for immediate roof (m)	Critical span for sill (m) (Eq 6-2)	Sub-critical span for sill (m)	Super-critical span for sill (m)
1	1126	Central	Siyanqoba	195.28	63.68	54.86	193.24	22.22	160.60	110.60	182.12	163.91	200.33	299.89	269.91	329.88
2	135	Central	Shosholoza	160.67	63.72	16.58	158.90	12.82	160.00	122.00	149.84	134.86	164.82	144.90	130.41	159.40
3	040	Central	Simunye	162.99	66.97	11.92	160.59	12.57	160.00	122.00	152.00	136.80	167.20	128.51	115.66	141.36
4	042	Central	Simunye	164.53	69.71	9.30	162.35	10.91	183.00	140.00	153.44	138.10	168.79	118.67	106.81	130.54
5	179b	Okhozini	Eyethu	164.28	47.05	20.81	162.22	13.20	183.00	139.00	153.21	137.88	168.53	181.14	163.03	199.25
6	888	North	Lesedi	184.14	45.76	42.32	182.25	16.98	175.00	127.00	171.73	154.56	188.90	273.47	246.12	300.82
7	887	North	Lesedi	164.28	47.05	20.81	162.22	13.20	127.00	79.00	153.21	137.88	168.53	181.14	163.03	199.25
8	882c	North	Inyanda	186.12	48.72	41.06	184.42	22.45	175.00	127.00	173.58	156.22	190.93	266.98	240.28	293.67
9	882d	North	Inyanda	191.08	55.37	50.65	189.39	23.91	200.00	152.00	178.20	160.38	196.02	293.61	264.25	322.97
10	1001B	Central	Simunye	164.19	66.00	6.51	162.00	6.47	200.00	152.00	153.12	137.81	168.44	112.95	101.66	124.25
11	1001C	Central	Simunye	164.00	67.52	7.04	161.60	7.48	200.00	152.00	152.95	137.65	168.24	113.01	101.71	124.31
12	177/5	Okhozini	Thubelisha	159.24	40.90	18.59	157.29	14.42	152.00	80.00	148.50	133.65	163.35	176.37	158.73	194.01
13	177/6	Okhozini	Thubelisha	159.24	40.90	18.59	157.29	14.42	152.00	104.00	148.50	133.65	163.35	176.37	158.73	194.01
			Average	**170.77**	**55.64**	**24.54**	**168.75**	**14.69**	**171.35**	**123.58**	**159.26**	**143.33**	**175.19**	**189.77**	**170.79**	**208.75**
			Min	**159.24**	**40.90**	**6.51**	**157.29**	**6.47**	**127.00**	**79.00**	**148.50**	**133.65**	**163.35**	**112.95**	**101.66**	**124.25**
			Max	**195.28**	**69.71**	**54.86**	**193.24**	**23.91**	**200.00**	**152.00**	**182.12**	**163.91**	**200.33**	**299.89**	**269.91**	**329.88**

APPENDIX D

Table D-1: Variation in vertical stress for different barrier pillar widths (Jansen van Vuuren & De Beer, 2022a).

Stress (MPa)	0-25m	25-50m	50-75m	75-100m	100-125m	125-150m	150-175m	175-200m	200-225m
Developed	7.43	8.41	9.41	9.12	9.04	9.25	8.99	9.57	8.72
75% Barrier	17.04	12.10	10.59	9.89	9.74	10.01	10.28	11.04	13.46
100% Barrier	14.40	10.78	10.14	9.76	9.70	9.99	10.25	10.99	13.32
200% Barrier	13.77	9.58	9.78	9.69	9.70	10.01	10.29	11.08	13.54
300% Barrier	7.40	8.48	9.31	9.50	9.63	9.99	10.30	11.12	13.68
Stress Δ (MPa) Compared to Vertical Stress After Development									
75% Barrier	9.61	3.69	1.18	0.77	0.70	0.76	1.29	1.47	4.73
100% Barrier	6.97	2.38	0.73	0.64	0.66	0.74	1.26	1.42	4.60
200% Barrier	6.35	1.17	0.38	0.57	0.66	0.76	1.30	1.50	4.82
300% Barrier	-0.03	0.07	-0.09	0.38	0.59	0.73	1.31	1.55	4.96
Stress Δ %									
75% Barrier	129%	44%	13%	8%	8%	8%	14%	15%	54%
100% Barrier	94%	28%	8%	7%	7%	8%	14%	15%	53%
200% Barrier	85%	14%	4%	6%	7%	8%	14%	16%	55%
300% Barrier	0%	1%	-1%	4%	7%	8%	15%	16%	57%
Pillar to Pillar Stress Δ (MPa)									
75% Barrier	2.65	1.32	0.45	0.13	0.04	0.02	0.02	0.05	0.14
200% Barrier	-0.62	-1.21	-0.36	-0.07	0.00	0.02	0.04	0.09	0.22
300% Barrier	-7.00	-2.31	-0.83	-0.26	-0.07	-0.01	0.05	0.13	0.36
Pillar to Pillar Stress Δ %									
75% Barrier	38.0%	55.3%	61.7%	20.7%	5.9%	2.4%	1.9%	3.7%	3.0%
200% Barrier	-9.0%	-50.8%	-48.8%	-10.7%	0.2%	2.5%	3.1%	6.1%	4.8%
300% Barrier	-100.4%	-97.0%	-112.7%	-40.3%	-11.1%	-0.9%	3.7%	9.4%	7.8%

APPENDIX E

Table E-1: Panel 1134 average vertical pillar stress comparison (Jansen van Vuuren & De Beer, 2022b).

APS_v	Barrier Pillar	Pillar #1	Pillar #2	Pillar #3	Pillar #4	Pillar #5	Pillar #6	Pillar #7	Pillar #8	Pillar #9	Pillar #10	Pillar #11	Pillar #12	Ave.
	Large / wide	Abut. South		Small pillar effect / offline					Abut. North	Panel entry			Front Line	(MPa)
134 Development	5.2	7.1	7.8	8.0	8.3	8.1	8.0	7.6	7.6	7.7	7.7	7.8	7.6	7.8
134 Extracted	5.3	7.5	8.2	8.5	8.8	8.6	8.5	8.0	7.9	8.2	8.3	9.9	24.3	8.4
Δ Yield %	1.8%	4.4%	5.7%	5.6%	6.2%	6.7%	6.2%	5.4%	4.8%	5.7%	7.6%	27.2%	218.8%	25.3%
135 Development	5.6	8.4	8.0	8.0	7.9	8.3	8.3	7.9	8.0	9.3	8.9			8.3
135 Extracted	5.7	8.6	8.5	8.3	8.4	8.9	8.8	8.4	9.0	13.1	27.3			10.9
Δ Yield %	1.7%	3.5%	6.4%	4.7%	6.8%	6.6%	5.6%	6.5%	12.5%	40.3%	205.8%			29.9%